UQAR

Université du Québec
à Rimouski

INTERACTION ENTRE LA MATIÈRE ORGANIQUE ET LE FER DANS UN ESTUAIRE SOUTERRAIN

EXEMPLE DES PLAGES DE SÉDIMENTS PERMÉABLES

Mémoire présenté

dans le cadre du programme de maitrise en Océanographie

en vue de l'obtention du grade de maître ès sciences

PAR

MAUDE SIROIS

Janvier 2018

Composition du jury :

Huixiang Xie, président du jury, UQAR-ISMER

Gwénaëlle Chaillou, directeur de recherche, Université du Québec à Rimouski

Yves Gélinas, codirecteur de recherche, Université Concordia

Sue Ziegler, examinateur externe, Memorial University of Newfoundland

UNIVERSITÉ DU QUÉBEC À RIMOUSKI
Service de la bibliothèque

Avertissement

Rien ne se perd, rien ne se crée,
tout se transforme

- Lavoisier

RÉSUMÉ

Les plages sont des sources de carbone organique dissous (COD) à l'océan côtier. Lorsqu'elles sont connectées aux aquifères, elles agissent comme des estuaires souterrains (ES) dans lesquels le carbone organique (CO) dissous et particulaire est activement transformé. Le fer est un élément qui interagit avec le CO et pourrait contrôler la mobilité du COD dans les ES et son export aux eaux côtières. L'objectif général de ce projet de maitrise est de comprendre et caractériser le rôle des plages dans le transfert de CO du continent à l'océan. Plus spécifiquement, nous souhaitons 1) déterminer le devenir et les sources de COD en combinant l'analyse des concentrations et la signature isotopique du COD (δ^{13}C-COD) dans un ES et 2) quantifier et identifier le CO piégé par les oxydes de fer réactifs. La plage de la Martinique (Iles-de-la-Madeleine, QC), où les eaux souterraines rencontrent les eaux de mer dans un ES microtidale, fut prise comme laboratoire naturel. Aux printemps 2013 et 2015, des prélèvements d'eaux souterraines et de sédiments ont été effectués dans un transect perpendiculaire à la ligne de rivage dans l'ES. Les sources potentielles de COD, dissoutes et particulaires, ont été prélevées. Les résultats montrent que le COD provenait principalement de la dégradation du carbone organique particulaire (COP) présent localement. Le COD était de source terrigène (signature en C3) en 2013, due à la dégradation d'un ancien sol forestier présent dans la zone d'étude. En 2015, par contre, cette source était marine (plantes marine en C4), probablement due à la dégradation de macroalgues accumulées en surface de la zone intertidale. Dans l'ES, les oxydes de fer réactifs agissaient comme piège pour le CO, particulièrement celui de source terrigène. L'oxydo-réduction du fer et le dépôt de macroalgues ont favorisé la quantité de CO terrigène piégé avec les oxydes de fer réactifs. Dans un ES, les sources de COD seraient donc variées et changeraient rapidement du terrigène au marin en fonction des sources de COP présentes dans le milieu. En agissant comme piège transitoire à CO, les oxydes de fer contrôleraient l'export de CO terrigène à l'océan côtier.

Mots clés : Carbone organique dissous, Fer, Plage, Estuaire souterrain, Interface Continent-Océan

ABSTRACT

Sandy beaches are sources of dissolved organic carbon (DOC) to the coastal ocean. When they are connected to the aquifer, they act as subterranean estuary (STE) where DOC and particulate organic carbon (POC) are actively transformed. Iron (Fe) can interact with organic carbon (OC) and control the mobility of DOC in STE and its export to the coastal ocean. The general objective of this master's thesis was to understand and characterized the role of sandy beaches in the transfer of OC from the continent to the ocean. More specifically, we aimed to 1) determine the behavior and the source of DOC with the concentration of DOC and the isotopic signature of the δ^{13}C-DOC in a STE and 2) quantify and identify the OC trapped reactive Fe oxides. The Martinique Beach (Iles-de-la-Madeleine, QC), where groundwater mixes with recirculated seawater in a microtidal STE, is a natural laboratory. In spring 2013 and 2015, groundwater and sediments were sampled in the STE in a transect perpendicular to the shoreline. The potential particulate and dissolved sources of DOC were also sampled. The results show that DOC could be from the degradation of POC locally present in the STE. This POC could be from terrestrial sources (C3 plants) in 2013 due to the degradation of an old buried soil present in the study beach. However, in 2015, the DOC was from marine sources (C4 marine plants), probably due to the degradation of seaweeds accumulated at the surface of the intertidal zone. In the STE, reactive Fe oxides trap OC and especially terrestrial OC. With the redox oscillation of Fe, seaweed accumulation increased the quantity of terrestrial OC trapped by reactive Fe oxides. In STE, sources of DOC vary and change rapidly from terrestrial to marine sources according to the POC present in the system. Reactive Fe oxides acts as transitory trap for OC and control the export of terrestrial OC to coastal ocean.

Keywords: Dissolved Organic Carbon, Iron, Sandy Beach, Subterranean Estuary, Continent-Ocean Interface

TABLE DES MATIÈRES

LISTE DES TABLEAUX

LISTE DES FIGURES

INTRODUCTION GÉNÉRALE

Les liens entre le continent et l'océan sont encore mal compris dans le cycle du carbone (C). Avec ses 1750 PgC (1015 g) stockés dans les fonds marins, l'océan est le principal réservoir de surface de C (Ciais et al., 2013). Les fleuves et les rivières sont considérés comme des vecteurs de matière du continent à l'océan (matière organique et inorganique) (Cai, 2011; Cole et al., 2007). Cependant il existe une autre source importante d'apports : les décharges d'eaux souterraines (SGD pour *submarine groundwater discharge* en anglais) (Cai et al., 2003; Cole et al., 2007). Les SGD peuvent être plus importantes par endroits que les apports de surface et ainsi contrôler la chimie des eaux côtières (Maher et al., 2013; Santos et al., 2009). Certaines études affirment que ces systèmes sont une voie d'échange chimique importante entre le continent et l'océan (Boudreau et al., 2001; Huettel et al., 1996; Huettel et Rusch, 2000) pouvant, par exemple, augmenter l'eutrophisation, l'acidification, l'hypoxie ainsi que la productivité des milieux côtiers (Moore, 2010). Les SGD représentent 2 à 8 % des apports des rivières (Cho et Kim, 2016; Taniguchi et al., 2002). Dû au manque de connaissance sur les SGD ainsi qu'à leur importance dans les apports de matière au milieu marin à travers les environnements côtiers comme les plages, il est important d'améliorer nos connaissances sur les mécanismes agissant dans les eaux souterraines des plages. De plus, puisqu'une part importante du carbone total sur terre est organique et dans le contexte de changement global actuel, il est important de bien comprendre le cycle du C organique (CO) (Guenet et al., 2010).

LES PLAGES : DES RÉACTEURS BIOGÉOCHIMIQUES À L'INTERFACE CONTINENT-OCÉAN

Plus de 70 % des côtes mondiales sont des plages de sédiments perméables (Emery, 1968; McLachlan et Brown, 2006). Ces environnements agissent comme une porte d'entrée pour les échanges entre le milieu marin et le continent. Avec plus de 75 % de la population

mondiale vivant sur les côtes, il est donc pertinent d'étudier les environnements côtiers (Ward et al. 2017 et références associées). En plus d'être utiles pour la réduction des impacts lors des tempêtes, les plages aident également pour la purification de l'eau et sont une niche écologique pour plusieurs espèces comme les oiseaux marins (Nel et al., 2014). Cependant, elles sont aussi des écosystèmes vulnérables qui sont affectés par l'érosion due à la hausse du niveau marin en réponse au changement climatique (Defeo et al., 2009; Hinkel et al., 2013) ainsi qu'à la pression anthropique (Dugan et al., 2010). Les plages de sable ont longtemps été considérées comme des déserts biogéochimiques en raison de la faible teneur en matière organique (MO) et des autres substances réactives (ex. : nutriments et métaux) (Boudreau et al. 2001). Elles sont cependant de réels réacteurs biogéochimiques dans lesquels la MO est minéralisée, menant à la production de métabolites et de carbone inorganique dissous (CID) (Anschutz et al., 2009; Boudreau et al., 2001; Charbonnier et al., 2013; Moore et al., 2011). Les flux d'eau et de matière à travers ces environnements sableux sont connus pour être hétérogènes spatialement (ex. : entre les différentes plages et au sein d'une même plage) et temporellement (ex. : entre les différentes saisons) (Cai, 2011; Heiss et Michael, 2014; Huettel, 2017). Les plages demeurent des environnements peu représentés dans la littérature comparativement à d'autres systèmes côtiers comme les estuaires, les mangroves ou encore les barrières de corail (Nel et al., 2014).

ESTUAIRE SOUTERRAIN ET DÉCHARGES D'EAU SOUTERRAINE

Lorsque les plages sont connectées aux aquifères côtiers, on peut les caractériser comme des estuaires souterrains (ES). Moore (1999) est le premier à définir un ES comme « un aquifère côtier où les eaux souterraines du drainage des terres sont fortement diluées avec l'eau de mer qui a envahi l'aquifère à travers une connexion à la mer » (traduction libre). Bien que ce terme restreigne la circulation souterraine à une zone géographique particulière et limite les échanges verticaux et transversaux, il permet de conceptualiser les mécanismes physico-chimiques impliqués dans la dilution des eaux douces continentales par les eaux salées océaniques. Les ES sont donc des environnements clé à l'interface continent-océan (Fig. 1).

Les apports d'eaux souterraines jusqu'à l'océan côtier jouent un rôle majeur dans les cycles biogéochimiques des océans (Taniguchi et al., 2002), particulièrement à l'échelle locale ou régionale (Charette et al., 2005; Santos et al., 2009) où les décharges d'eau souterraine ou SGD sont une voie d'échange entre les ES et l'océan. Les SGD à l'océan côtier sont connues depuis longtemps, mais l'intérêt scientifique est devenu plus important seulement depuis les années 2000 en raison des complexités engendrées par l'échantillonnage. Comme les rivières, les SGD sont une source importante d'eau douce et de matière au milieu côtier (Taniguchi et al., 2002). D'après Burnett et al. (2006), ces décharges sont définies comme les écoulements d'eau à travers les sédiments, sans égard à leur origine marine (ou de recirculation) ou continentale (eau souterraine) et sont gouvernées par des processus physiques (convection, convection géothermale, pompe tidale et les vagues) (McCoy et Corbett, 2009) et chimiques (condition redox et réactions diagénétiques) (Roy et al., 2011). Une douzaine de forçages d'origine océanique et continentale contrôlent les flux de SGD à l'océan (Santos et al., 2012). Ces derniers peuvent varier dans le temps à fréquence quotidienne (p. ex. oscillations tidales, vagues), saisonnière (p. ex. recharge et variation du niveau piézométrique), annuelle ou pluriannuelle (p. ex. oscillation atmosphérique ; hausse du niveau marin) (Roy et al., 2013). L'écoulement d'eau dans les sédiments perméables (voir les flèches vertes dans la Fig. 1) s'effectue en suivant le gradient hydraulique. Une augmentation du niveau piézométrique a pour effet d'augmenter les écoulements et donc de diminuer le temps de résidence des masses d'eau dans les sédiments. Cela peut avoir pour effet de changer la composition chimique des décharges (Heiss et Michael, 2014). La pompe tidale quant à elle influence la recirculation de l'eau de mer dans les sédiments (voir les flèches bleues dans la Fig. 1). Les marées, dont les effets peuvent être perçus jusqu'à plusieurs mètres de profondeur, provoquent l'infiltration de l'eau de mer lors des marées hautes et l'exfiltration de l'eau de recirculation lors des marées basses (Robinson et al., 2007). Il y a ainsi un renouvellement de l'eau de mer dans les sédiments. La convection, quant à elle, est liée à la densité, donc au gradient vertical de salinité et de température des masses d'eau, peut aussi affecter les décharges (Webster et al., 1996). Par exemple, une arrivée brusque d'eau froide sur le

sédiment plus chaud peut mener à un échange rapide entre l'eau souterraine et l'eau de mer (Rocha et al., 2009). Les différents forçages agissent à des échelles spatio-temporelles différentes. Par exemple le gradient hydraulique varie avec les saisons, les vagues sur une échelle de quelques secondes et minutes et la pompe tidale varie de quelques heures à une journée. Les impacts de ces différents forçages, variant différemment selon les plages, font que les SGD sont différents d'une plage à l'autre et ont un impact local sur l'environnement côtier.
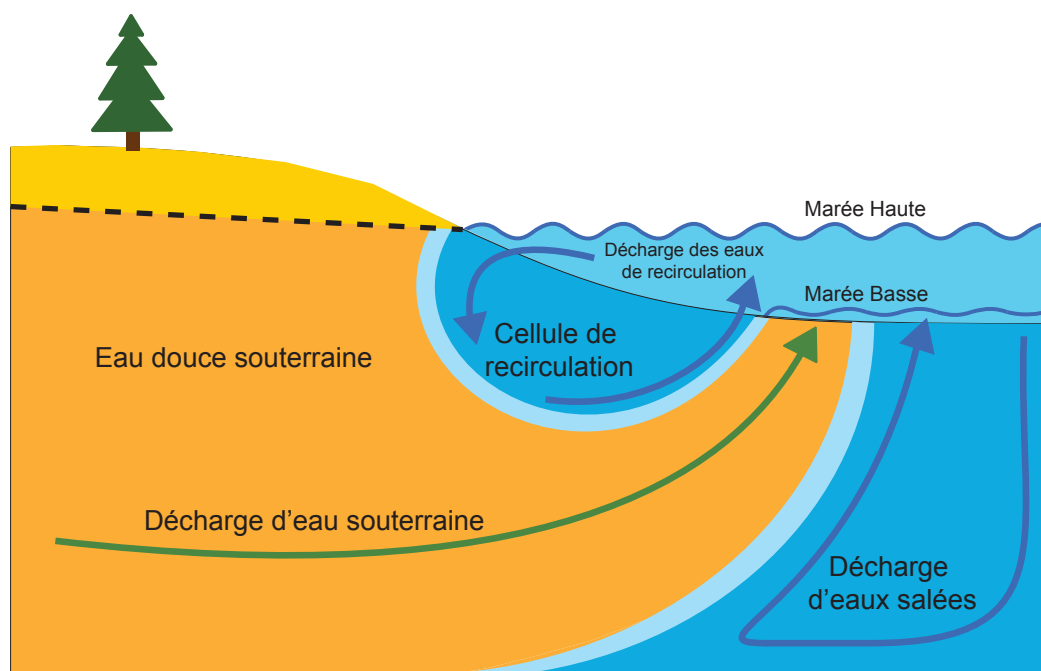
Figure 1 : Schématisation d'un ES et des SGD en milieu côtier. Le trait pointillé représente la hauteur de la nappe d'eau douce de l'aquifère et sa pente le gradient hydraulique. La flèche verte représente les décharges d'eau douce souterraine allant jusqu'au milieu marin. Les flèches bleues représentent l'infiltration et l'exfiltration de l'eau de mer dans les sédiments perméables des plages

TRANSPORT DU CARBONE ORGANIQUE DU CONTINENT À L'OCÉAN

Les décharges d'eau souterraine ont une forte hétérogénéité spatiale et temporelle ce qui rend leur quantification variable non seulement à l'échelle locale, mais aussi à l'échelle

globale (Burnett et al., 2006; Cho et Kim, 2016). Les plages de sable sont des zones actives qui participent au cycle du C en fournissant de la matière organique dissoute (MOD) aux eaux côtières (Avery et al., 2012; Chaillou et al., 2016; Goñi et Gardner, 2004; Kim et al., 2012). Ces flux de MOD, participant à l'eutrophisation, l'acidification et l'hypoxie des eaux côtières, devraient être considérés dans le bilan global du carbone (Moore, 2010). Quelques études se sont concentrées sur la mesure des flux de carbone organique dissous (COD) (Avery et al., 2012; Chaillou et al., 2016, 2014; Kim et al., 2012; Santos et al., 2009), mais aucune d'entre elles n'a pu faire de mesures directes de ces flux (c'est-à-dire de mesurer directement le C sortant par les SGD à l'interface plage-eau). Il est cependant difficile d'estimer la concentration moyenne de COD apporté à l'océan côtier en raison (1) des processus biogéochimiques qui modifient la concentration en COD lors du transit des eaux souterraines à la zone de décharge des plages et (2) de la dynamique des apports de COD (ex. : pompe tidale, saison, etc.).

Différents processus biogéochimiques affectent les concentrations de COD (Fig. 2). Ce dernier peut avoir un comportement conservatif, c'est-à-dire qu'il varie de manière linéaire avec la salinité. Ce comportement a déjà été observé dans certaines études en Corée du Sud (Kim et al., 2013) et aux États-Unis (Beck et al., 2007). À l'inverse, un comportement non conservatif, avec une consommation ou une production *in situ* de COD, a déjà été rapporté dans d'autres sites, comme dans le golfe du Mexique (Santos et al., 2009), aux États-Unis en Caroline du Sud (Goñi et Gardner, 2004) ou encore aux Îles-de-la-Madeleine dans le Golfe du St-Laurent (Chaillou et al., 2016; Couturier et al., 2016). La minéralisation de la MO dans les sédiments de la plage (Anschutz et al., 2009; Charbonnier et al., 2013) supporte une consommation complète ou incomplète du CO alors que la production peut être fournie, par exemple, par des algues benthiques (Kim et al., 2012). La minéralisation de la MO par les micro-organismes en condition aérobie ou anaérobie est au cœur de la diagenèse précoce. Il s'agit des réactions biogéochimiques d'oxydo-réduction contrôlées par la thermodynamique dans les sédiments marins. La MO agit comme donneur d'électrons et différentes substances sont utilisées comme accepteurs d'électrons dépendamment de leur énergie de réaction. Les oxydes de Fe peuvent être utilisés comme

oxydants. Celui qui fournira le plus d'énergie sera utilisé en premier. Avec la profondeur et la disponibilité des différents oxydants, plusieurs réactions biogéochimiques se produisent successivement dans cet ordre : réduction de l'oxygène, suivi de celles de nitrate, du manganèse, du fer, des sulfates puis du dioxyde de carbone par les processus de méthanogénèse (Fig. 2) (Froelich et al., 1979; Rullkötter, 2006). D'autres processus peuvent contrôler/réguler la disponibilité du COD disponible dans le milieu. Plusieurs de ces processus sont liés au cycle du fer (Fe) : la floculation (ou coagulation), l'adsorption et la coprécipitation du CO sur des matrices minérales avec les oxydes métalliques. Ces processus (qui seront détaillés plus loin, c.f. p.14) ont pour effet de piéger le CO à court terme (dans le cas de la floculation et de l'adsorption) ou à plus long terme (dans le cas de la coprécipitation). Ces mécanismes ont déjà été observés dans les sols (Guggenberger et Kaiser, 2003; Kaiser et Guggenberger, 2003, 2000) et dans les sédiments marins (Barber et al., 2017a; Hedges et Keil, 1995; R. G. Keil et al., 1994; Lalonde et al., 2012). Pour ce qui est des sédiments côtiers non cohésifs des plages, ce piégeage du CO n'a été que très peu étudié jusqu'à tout récemment (voir Linkhorst et al., 2016).
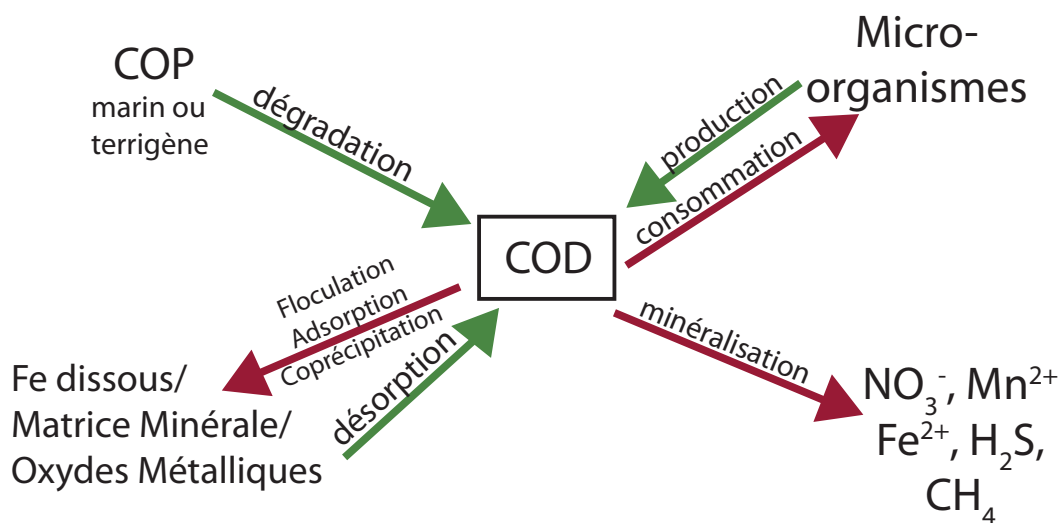
Figure 2 : Mécanismes biogéochimiques qui contrôlent le COD dans les eaux porales. Les flèches vertes représentent les mécanismes qui augmentent la concentration en COD alors que les flèches rouges représentent ce qui diminue les concentrations en COD (COP : Carbone organique particulaire)

De par la proximité avec l'eau de mer, le COD des plages est instinctivement considéré comme exclusivement d'origine marine, issu du phytoplancton et du phytobenthos (Heymans et McLachlan, 1996). Anschutz et al. (2009), en se basant sur des flux de silices et des prélèvements *in situ*, ont montré que la MO marine est apportée par la pompe tidale jusque dans les sédiments de la plage d'étude et qu'elle serait piégée suffisamment longtemps pour être minéralisée. Kim et al. (2012) ont eu la même conclusion en utilisant les indices optiques de la MOD colorée et les acides aminés totaux dissous hydrolysables (THAA). Cependant, Couturier et al. (2016) ont montré à l'aide des indices optiques de la MOD colorée que le COD produit serait de source terrigène dans un ES d'une plage.

Le devenir du carbone organique (CO) terrigène dans l'océan fait l'objet de nombreux débats (Bianchi, 2011; Burdige, 2005; Hedges et al., 1997; Tesi et al., 2014). Auparavant, on pensait que le CO d'origine terrigène qui arrivait dans l'océan était peu dégradé, car il est plus réfractaire que celui d'origine marine. Cependant des études ont montré que seulement 30 % du carbone enfoui dans les zones côtières était d'origine continentale (Burdige, 2005), laissant alors supposer que le CO délivré par les continents ne serait pas aussi récalcitrant que l'on pensait (Mayorga et al., 2005) puisque ce carbone serait minéralisé de façon importante. La notion de *Priming Effect* soutient que la dégradation de MOD réfractaire, comme la MOD terrigène, serait liée à celle de la MOD labile, comme la MOD marine. Dans le cas *d'un Priming Effect* positif, ce mélange de MOD réfractaire et de MOD labile aurait pour effet de stimuler l'activité enzymatique des communautés bactériennes et d'augmenter ainsi la minéralisation de la MO réfractaire (Bianchi, 2011). Le *Priming Effect* serait alors un des processus qui expliquerait la forte minéralisation de la MOD terrestre en milieu côtier. Bianchi (2011) insiste sur le fait qu'il faut élargir nos connaissances sur le *Priming Effect* en raison de son impact sur le cycle du C en milieu côtier. De savoir si les plages sont des sources de CO au milieu marin ainsi que l'origine du carbone qui est exporté permet de connaître la réactivité du CO dans le milieu marin.

La chimie des eaux côtières est donc intimement liée aux apports et au devenir du carbone terrigène jusqu'à l'océan. Il est donc important :

1) de connaître l'origine du CO présent ou produit dans les plages de sable afin d'évaluer la réactivité du CO qui se rend à l'océan côtier ;

2) de quantifier ces apports de CO liés aux SGD en tenant compte des transformations potentielles lors du transit

CARACTÉRISATION DE LA MOD ET DU COD : ÉTAT DES CONNAISSANCES

La MOD est un mélange complexe de molécules organiques, la mesure du COD permet d'estimer sa quantité dans le milieu. Toutes les eaux naturelles contiennent du COD qui peut être fraichement produit et réactif, donc labile. Certains composés du COD peuvent être peu réactifs ou alors récalcitrants, donc qui sont peu ou pas minéralisés. Cette minéralisation peut prendre jusqu'à 6000 ans (Druffel et Williams, 1992).

La MOD que l'on retrouve dans l'environnement peut être séparée selon son origine, soit terrigène (e.i. continentale) ou marine. La MOD provenant de différentes sources a des caractéristiques chimiques différentes associées à ces matériaux sources (Aiken, 2002). La MOD terrigène est souvent composée de substances humiques et fulviques et a un poids moléculaire moyen plus élevé que la MOD marine. Elle est issue de la biomasse continentale, des plantes, de la dégradation des sols, de l'érosion côtière ainsi que du ruissèlement des sols forestier et agricole (Benner et al., 2005; Hedges et al., 1997; Stedmon et al., 2003). La MOD marine, quant à elle, vient principalement de la production primaire marine. Ce carbone est principalement composé de molécules de faible poids moléculaire comme les protéines (acides aminés), carbohydrates (sucres) et lipides. Il est reconnu dans la littérature que la MO marine est plus réactive que la MO terrigène (Hedges et al. 1997 et références associées) dans les eaux côtières. Dans les eaux souterraines, selon Aiken (2002), il existe trois principales sources de MO. Il y a la MO enfouie, la MO des sols et des sédiments (Kalbitz et al., 2000) et la MO présente dans l'eau qui s'infiltre depuis

la surface des rivières, des lacs et des systèmes marins, qui peut dont être terrigène ou marine (Fig. 3).
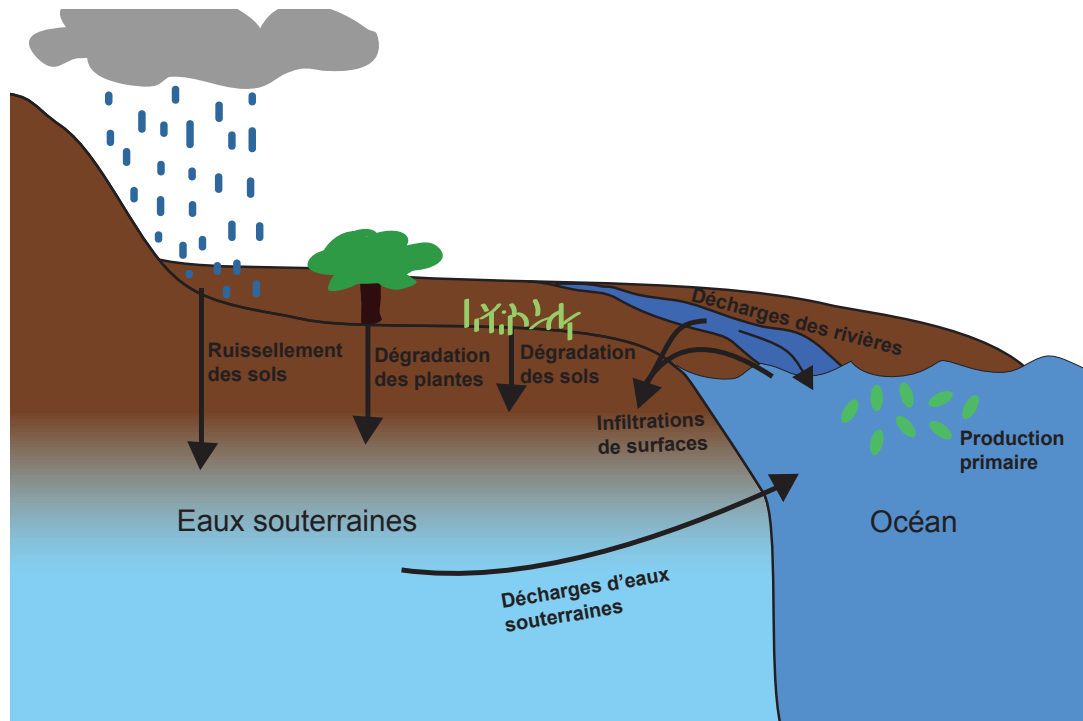
Figure 3 : Possibles sources de CO terrigène alimentant les eaux souterraines en MOD

Plusieurs méthodes peuvent être utilisées afin de déterminer l'origine du COD. Certaines se fient sur la caractérisation moléculaire du COD alors que d'autres utilisent des traceurs. Voici les principales méthodes utilisées dans la littérature :

- Indices optiques de la MOD colorée : Cette méthode se base sur les mesures d'absorbance et de fluorescence de la MOD retrouvée dans l'eau. Un indice optique, le $SUVA_{254}$, permet de montrer l'aromaticité des échantillons avec l'absorbance UV des échantillons mesuré à 254 nm. Le *slope ratio* permet une mesure indirecte des poids moléculaires en mesurant le rapport entre la pente de longueur d'onde plus courte (275-295 nm) avec la pente de longueur d'onde plus longue (350-400 nm) par la technique de régression non linéaire décrite par Stedmon et al. (2000). Il y a l'indice de fluorescence (FI) qui indique la

prédominance de matière autochtone donc de l'origine de la MOD par le ratio d'émission à 450 nm à 500nm avec une excitation à 370nm. Ensuite, l'indice BIX indique la productivité autotrophe de la fluorescence de la MOD colorée, donc si la matière est dégradée in situ (Couturier et al., 2016; Helms et al., 2008; Huguet et al., 2009; Mcknight et al., 2001; Weishaar et al., 2003). Par exemple, dans l'étude de Couturier et al. (2016), les auteurs ont montré que la MOD colorée retrouvée dans l'estuaire souterrain de la plage d'étude avait une forte présence de molécules de haut poids moléculaire, de forte aromaticité, de matière principalement autochtone et est produite *in situ* par l'activité microbienne.

- Mesure de la lignine : La ligne est utilisée comme traceur des molécules dérivées des plantes terrestres. Puisque la MOD marine ne contient pas de molécule lignine, il est possible de discriminer si la MOD provient du milieu marin ou terrestre. La mesure de la lignine se fait par oxydation avec l'oxyde de Cu (III) par micro-ondes. Les molécules issues de cette oxydation sont par la suite mesurées par chromatographie en phase gazeuse couplée à un spectromètre de masse. Les molécules issues de la lignine et du cutin mesurés par cette méthode sont les vanillyl phénols, syringyl phénol, cinnamyl ohénols et les acides dérivés du cutin. Dans les échantillons provenant de la MOD marine, on retrouvera plutôt des dérivés d'acides aminés, des p-hyroxyvenzènes et des acides benzoïques (Goñi et Hedges, 1995; Goñi et Montgomery, 2000; Hastings et al., 2012).

- Spectrométrie de masse à résonance cyclotronique ionique à transformation de Fourier (FT-ICR-MS) couplée à une ionisation de type « electrospray » (ESI-FT-ICR-MS) : Cette méthode permet d'identifier des milliers de molécules spécifiques dans la MOD où certaines d'entre elles sont majoritairement présentes dans la MOD terrigène, qui est de plus haut poids moléculaire et ayant des cycles aromatiques, alors que d'autres le sont principalement dans la MOD marine (Seidel et al. 2014; Linkhorst et al. 2016 et références associées). Cette

méthode nécessite cependant de retirer le sel dans les échantillons salés à l'aide de l'extraction sur phase solide.

- Ensuite, l'identification d'acides aminés spécifiques à l'aide de chromatographie liquide à haute performance (HPLC) permet de déterminer si le COD est composé de molécules terrigènes ou marines (Shen et al., 2015). Plus précisément, dans les eaux souterraines, les acides aminés peuvent indiquer l'étendue du processus diagénétique de la MOD. Par exemple, la concentration de glycine et d'énantiomère D des acides aminés augmente avec la dégradation de la MOD (Shen et al. 2015 et références associées).

Certaines des méthodes mentionnées ci-dessus prennent beaucoup de temps d'analyse dû aux multiples étapes en laboratoire et nécessitent des analyses rapides en laboratoire suite à l'échantillonnage en raison du temps de conservation. Certaines méthodes nécessitent également d'être couplée avec d'autres afin d'avoir une meilleure validation des résultats.

Une autre méthode intéressante pour déterminer les sources de COD est la signature isotopique du COD (δ^{13}C-COD). Le δ^{13}C-COD est utilisé depuis les années 60 dans le traçage de la dynamique du carbone dans les rivières, les estuaires, les systèmes côtiers et marins ainsi que pour les réseaux trophiques en écologie (Bauer, 2002; Williams et Gordon, 1970). Cependant, son utilisation afin de déterminer les sources de COD est plus compliquée en eau salée qu'en eau douce en raison de la salinité de l'eau. En effet, la présence de sel peut être jusqu'à 70 000 fois plus importante que le poids de COD dans des échantillons d'eau de mer (Lalonde et al., 2014a). Les anciennes méthodes analytiques devaient faire une étape supplémentaire afin de dessaler les échantillons avant la mesure du δ^{13}C-COD. Une méthode utilisée est l'extraction sur phase solide (SPE pour *solid phase extraction*) (Seidel et al., 2015). Cette méthode consiste à retenir les molécules de MOD sur une cartouche de SPE qui est par la suite extraite et analysée au spectromètre de masse à ratio isotopique (IRMS). Cependant, cette méthode a pour effet de retenir plus efficacement la MOD terrigène (75-90% d'efficacité) par rapport à la MOD marine (40-60% d'efficacité)

ce qui surestime la MOD terrigène par rapport à la MOD marine (Dittmar et al., 2008). Les méthodes prennent également beaucoup de temps d'analyse, allant jusqu'à trois heures par échantillon dus au nombre d'étapes (p. ex. : désalinisation, retrait du CO_2, etc.) (Williams et Gordon, 1970). Lalonde et collaborateurs. (2014a) ont donc développé une méthode qui mesure à la fois le δ^{13}C-COD et la concentration en COD à l'aide d'un analyseur à COD couplé à une trappe à CO_2 et à un IRMS à flux continu. Ce système analytique, qui peut autant analyser des échantillons d'eau douce que d'eau salée, nécessite moins d'étapes d'analyse que les anciennes méthodes et prend environ 20 min par échantillon. Cette méthode, très récente, est encore peu utilisée et ne s'effectue que par 5 laboratoires dans le monde donc utilisé par très peu de laboratoires dans le monde.

La composition en ^{13}C de chaque biomolécule dépend de plusieurs facteurs : 1) de la composition en ^{13}C de la source, 2) de la signature isotopique de l'assimilation du C, 3) du fractionnement isotopique associé au métabolisme et à la biosynthèse, puis 4) du carbone cellulaire disponible (Hayes, 1993). La principale différence entre le COD marin (la production primaire marine) et le COD terrigène (les plantes en C_3, les arbres) est la signature isotopique de la source, c'est-à-dire du CO_2 utilisé pour la photosynthèse. Le fractionnement chimique engendré lors de la fixation du CO_2 par l'enzyme Rubisco est d'environ -20 ‰ entre la source et la valeur finale. Les plantes terrigènes, qui incluent tous les arbres (C_3), ont donc une signature variant de -28 à -25 ‰ (Hedges et al., 1997; Peterson et Fry, 1987; Zeebe et Wolf-Gladrow, 2001) (Fig. 4). Il s'agit d'une signature très négative, dite « appauvrie », en raison de la signature du CO_2 atmosphérique utilisée, qui est autour de -8 à -9 ‰. La signature isotopique du COD marin est quant à elle plus « enrichie » que celle du COD terrigène. Le δ^{13}C-COD varie entre -19 et -24 ‰ puisque le CO_2 utilisé lors de la fixation du carbone est celui dissous dans l'océan produit par le phytoplancton marin qui a une signature initiale autour de 0 ‰ (Earth System Research Laboratory Global Monitoring Division of NOAA; https://www.esrl.noaa.gov/gmd/dv/iadv/) (Hoefs, 2009) (Fig. 4). Cependant, certaines exceptions s'appliquent : les plantes en C_4 et les cactus. Les plantes en C_4, comme le maïs, la canne à sucre ou les Zostères marines, ont une signature que l'on caractérisera de plus

« enrichie » et allant de -16 à -10 ‰ (Fig. 4). Cette différence est due au fractionnement chimique plus petit lors de la fixation du CO_2 engendré par l'enzyme phosphoénolpyruvate carboxylase (PEP) (Chmura et Aharon, 1995; Hedges et al., 1997; Peterson et Fry, 1987; Zeebe et Wolf-Gladrow, 2001). Pour ce qui est des cactus (ou CAM pour *crassulacean acid metabolism*), le fractionnement chimique engendré par la fixation du CO_2 est comme les plantes en C_3 durant le jour et comme les plantes en C_4 durant la nuit, donc leur signature isotopique peut être similaire à celle des plantes en C_3 et celle en C_4. Cependant, la signature se situe plus souvent entre les deux (Clark et Fritz, 1986).

À notre connaissance, il n'existe aujourd'hui aucune étude connue lors de la rédaction de ce mémoire sur l'utilisation du δ^{13}C-COD dans l'ES d'une plage afin de déterminer les sources du COD apporté au milieu côtier. Par contre, récemment, l'utilisation du δ^{13}C-COD avec un analyseur de COD couplé à un IRMS a récemment été utilisée dans la détermination des sources de COD dans les estuaires de surface (Barber et al. 2017b).
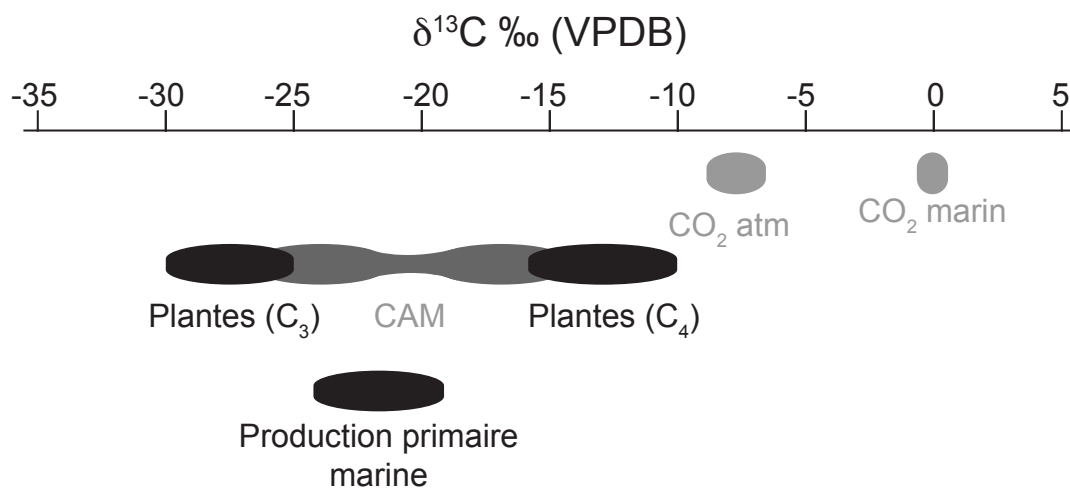
Figure 4 : Différentes gammes de δ^{13}C du CO_2 et du COD terrigène et marin. Les valeurs plus négatives sont dites plus « appauvries » alors que les valeurs moins négatives et plus proches de 0 sont dites plus « enrichies ». Le Vienna Pee Dee Belemnite (VPDB) est le standard utilisé comme référence dans le calcul de la signature isotopique du δ^{13}C (Clark et Fritz, 1986)

PIÉGEAGE DU CO PAR LE FE

Plusieurs mécanismes sont responsables de la mobilité et de la disponibilité du CO dans les eaux porales comme les interactions entre le Fe et le COD. Indépendamment de l'environnement, la réactivité chimique et la spéciation sont contrôlées par la thermodynamique et la cinétique des réactions (Aiken, 2002). La concentration et la nature du COD influencent cette mobilité et les différentes réactions qu'il peut y avoir avec le CO (Sholkovitz, 1976). Parmi les différentes interactions entre le CO et le Fe, le CO peut être associé à des particules ou associé à des constituants mobiles formant des agrégats de COD-Fe (floculation ou coagulation). La floculation du Fe avec le COD est un changement de la phase liquide à la phase solide (Sholkovitz, 1976) qui peut se produire lors d'un changement de salinité. Ce phénomène a tendance à former des agrégats très instables qui peuvent être dispersés rapidement dans les eaux côtières avec la turbulence et les courants (Sholkovitz, 1976). Ces liaisons entre le Fe et le CO sont réversibles, ce qui entraine un piégeage à court terme du CO (Barber et al., 2017a). L'interaction entre le CO et les oxydes de Fe réactifs est un autre processus pouvant réguler la disponibilité du COD dans la phase dissoute (eau porale ou souterraine). Les oxydes de Fe de taille nanométrique (oxydes de Fe réductible avec la dithionite : ferrihydrite, goethite et lépidocrocite ; Barber et al. 2017a) ont la plus grande interaction avec le COD. Ces mécanismes de piégeage peuvent se faire de deux façons, soit par l'adsorption avec les oxydes de Fe réactifs ou bien par la coprécipitation avec ces oxydes. L'adsorption est un mécanisme où le CO s'adsorbe à la surface d'oxydes de Fe déjà formés. Ce mécanisme entrainera alors un piégeage à court terme. Dans le cas de la coprécipitation, il s'agit de la formation d'oxyde de Fe en présence de CO où ils vont coprécipiter (Mikutta et al., 2014). Le CO adsorbé et coprécipité avec les oxydes de Fe réactifs auront des caractéristiques similaires. Cependant, le CO coprécipité sera plus difficile à désorber en raisons de liaisons plus fortes par rapport au CO adsorbé (Chen et al., 2014). En effet, la coprécipitation directe du Fe et du CO implique des liaisons covalente, ce qui peut amener à un piégeage à long terme du CO sous certaines conditions rédox (Barber et al., 2017a).

Ces différents mécanismes ont été démontrés dans les sols (Jones et Edwards, 1998; Kaiser et Guggenberger, 2003, 2000; Wagai et Mayer, 2007). Cette interaction entre le MOD et les phases minérales contribue à la préservation de la MO (Guggenberger et Kaiser, 2003) dans les sols ou la zone non-saturée des aquifères. L'interaction de la MO avec des matrices minérales est un des principaux facteurs qui contrôle la préservation de la MO sur la surface de la Terre (R. G. Keil et al., 1994). Le paradigme de la stabilisation par adsorption inclut qu'une fraction significative, et non toute la MO, soit passée à travers la phase dissoute avant l'adsorption ou la précipitation avec la matrice minérale. L'aire de surface minérale serait le facteur principal influençant la préservation de la MO (Hedges et Keil, 1995). En effet, une plus grande surface sur les grains, comme les sédiments cohésifs (argiles, silts), sera plus efficace pour piéger les MO (Burban et al., 1989; Edzwald et al., 1974).

Ces interactions ont été observées également dans toute une gamme de sédiments cohésifs marins (Barber et al., 2017a; R. G. Keil et al., 1994; Lalonde et al., 2012) qui sont comme les plus importants puits de CO sur terre (Hedges et Keil, 1995). La majorité du CO est « sorbé » sur la surface minérale des argiles et des oxydes métalliques (Hedges et Keil, 1995; R. G. Keil et al., 1994). Cependant certaines interactions Fe-CO sont pratiquement irréversibles en condition naturelle et comptent dans la préservation à long terme du CO réactif (Henrichs, 1995; Lalonde et al., 2012). Lalonde et al. (2012) montre que 20,5 ± 7,8 % du CO total dans les sédiments marins est associé avec le Fe. Les sédiments marins sont donc considérés comme un « rusty carbon sink » (Lalonde et al., 2012) qui protège la MO de la biodégradation.

Plus récemment, Linkhorst et al. (2017) se sont penchés sur la coagulation de la MOD sur le Fe dans l'estuaire souterrain d'une plage nordique sur l'île Spiekeroog en Allemagne. Cette étude montre à l'aide d'échantillons de la phase dissoute, d'expérience *in situ* et de l'utilisation de l'*ultra-high resolution electrospray ionization* FT-ICR-MS que le Fe pouvait provoquer la coagulation de molécules de haut poids moléculaire (>450 Da) de MOD aromatique terrigène et riche en oxygène. L'estuaire souterrain étudié pourrait donc

agir comme un site de stockage potentiel de MOD terrigène. Cependant, les auteurs laissent en suspend quelques questions : ces interactions CO-Fe se produisent-elles *in situ* ? S'agit-il d'un piégeage temporaire ou à long terme ? Quelle quantité de MO est piégée avec ce Fe ?

OBJECTIFS

Ce projet de maitrise porte sur l'étude de l'origine et du devenir du COD dans un estuaire souterrain d'une plage de sable. Cette étude vise à comprendre et caractériser le rôle des plages dans le transfert de matière du continent à l'océan. Plus spécifiquement, les objectifs étaient de :

1) déterminer le comportement et les sources de COD en combinant les concentrations et la signature isotopique du COD (δ^{13}C-COD) présent dans l'ES ;

2) quantifier et identifier le CO piégé / adsorbé par les oxydes de Fe.

Nous supposons que le transport par les SGD jusqu'à l'océan côtier serait de source terrigène provenant de la dégradation d'un ancien sol forestier telle que montrée par Couturier et al. (2016). Ensuite, lors de son transit vers l'océan, le COD devrait être piégé par le Fe présent dans l'aquifère ferrugineux modulant ainsi l'exportation de COD vers les écosystèmes côtiers (Chaillou et al., 2014; Couturier et al., 2016).

Les Îles-de-la-Madeleine sont un environnement idéal pour répondre à ces questions en raison de l'absence de rivière, de son hydrogéologie bien connue (Madelin'Eau, 2004), de la présence de nombreuses plages sur ses côtes et de sa formation géologique. Le site d'étude, la plage de la Martinique, est situé sur l'île de Cap-aux-Meules. Cette plage est composée principalement de sables moyens de 300 µm qui surmontent une couche de tourbe (ou paléosol) datée d'environ 900 ans BP (datation ^{14}C; Juneau, 2012) qui résulte d'un changement récent du niveau marin relatif aux Îles-de-la-Madeleine. Sous ce paléosol, on retrouve la formation géologique de grès rouge qui correspond à l'aquifère des Îles-de-la-Madeleine. Connectée à l'unique aquifère des îles, la plage est soumise à un régime

microtidal et à des décharges d'eaux souterraines allant jusqu'à 3,6 m^3/m/jour d'eau à l'océan. Plusieurs études se sont penchées sur la biogéochimie de cette plage (Chaillou et al., 2016, 2014, Couturier et al., 2017, 2016).

Ces études portent notamment sur la détermination des processus biogéochimiques dans la zone de mélange (Couturier et al., 2017, 2016), mais aussi sur la quantification des flux d'eau souterraine dans l'estuaire (Chaillou et al., 2016, 2014). Je propose ici un résumé de ces différentes études avec un intérêt particulier sur la caractérisation physico-chimique de la zone d'étude ainsi que sur les connaissances acquises sur le carbone dissous. L'article sur le devenir des espèces azotées dont je suis coauteure n'est pas présenté ici, mais se trouve en annexe de ce mémoire (voir annexe I).

Chaillou et al. (2016) présentent différentes techniques afin de mesurer les SGD dans la plage de la Martinique afin d'évaluer les flux de COD et de CID allant à l'océan avec des données hydrogéologiques et géochimiques. Il s'agit d'une première estimation des flux de carbone dans l'océan côtier canadien. Les calculs permettent de montrer que les flux souterrains apportent 147 kg DIC/j et de 27 kg DOC/jour dans la zone de décharge. Les auteurs observent que le CID et le COD ont des comportements non-conservatifs et sont produits au cours du transit de la plage à l'océan. Dû à ce comportement, il est difficile d'évaluer les flux de matière. Ensuite, Couturier et al. (2016) se sont concentrés sur la caractérisation et la distribution de la MOD en se basant sur les concentrations en COD ainsi que sur la mesure de différents indices optiques de la MOD colorée. L'utilisation d'indices optiques a permis de déterminer que la MOD présente dans le milieu serait produite *in situ*, que les composés seraient de haut poids moléculaire et qu'il y a une dominance de MOD d'origine terrigène dans ce système. Cette MOD terrigène proviendrait de la dégradation du paléosol dans la plage. Cette étude est la première à mettre en évidence le rôle des plages comme source de matière terrigène à l'océan côtier. Un point soulevé dans l'article est que les oxydes de métaux (oxydes de Fe) auraient un rôle important dans le piégeage de la MOD.

CONTRIBUTION DE L'AUTEUR ET PUBLICATION

Le chapitre de ce mémoire est présenté sous forme d'article scientifique en anglais intitulé « *Interaction between iron and organic carbon in a sandy beach subterranean estuary*». Cet article a été soumis le 30 septembre 2017 dans l'issue spéciale du *14th International Estuarine Biogeochemistry Symposium* (IEBS) ayant eu lieu à Rimouski en juin 2017 dans la revue *Marine Chemistry*. L'article a été accepté avec des corrections mineures et est en révision à la date du dépôt final de ce mémoire.

Toutes les données présentées dans ce mémoire sont issues de deux campagnes d'échantillonnage sur la plage de la Martinique en juin 2013 (18 mai au 8 juin 2013) et 2015 (30 mai au 14 juin 2015). J'ai organisé et participé au terrain de 2015. Les données de salinité, Fe dissous et de COD de l'échantillonnage de 2013 ont déjà été présentées dans l'article de Couturier et al. (2016), mais à titre de comparaison et étant donnée la différence significative entre les données de 2013 et 2015, elles ont été reprises dans l'article de ce mémoire. Les carottes de 2013 avaient également déjà été échantillonnées. J'ai analysé toutes les autres nouvelles données telles que la salinité, les concentrations en Fe dissous et en COD pour l'année 2015 ainsi que l'analyse des sédiments de 2013 et 2015. Les analyses de la signature isotopiques du δ^{13}C-COD de 2013 et 2015 ont été faites par moi-même avec l'aide de Andrew Barber et Yves Gélinas à l'Université Concordia. J'ai produit toutes les figures dans ce mémoire à l'exception de la carte du site d'étude qui a été produite par Marie-André Roy (géomaticienne, département Biologie, Chimie, Géographie, UQAR). J'ai également rédigé ce mémoire en très grande majorité. Tous les coauteurs de l'article (Mathilde Couturier, Andrew Barber, Yves Gélinas et Gwénaëlle Chaillou) ont participé à la révision et correction de l'article. Je suis également coauteure de deux articles publiés. Le premier, qui se retrouve en annexe, porte sur l'azote dans la plage de la Martinique aux Îles-de-la-Madeleine (Couturier, M., Tommi-Morin, G., **Sirois, M.**, Rao, A., Nozais, C., Chaillou, G., 2017. *Nitrogen transformations along a shallow subterranean estuary.* Biogeosciences. 14, 3321–3336. doi:10.5194/bg-2016-535; voir annexe I). Le second porte sur l'utilisation de la signature du δ^{13}C-COD dans l'estuaire, le Golfe du St-Laurent et la

mer du Labrador (Barber, A., **Sirois, M.**, Chaillou, G., Gélinas, Y., 2017. *Stable Isotope Analysis of Dissolved Organic Carbon in Canada's Eastern Coastal Waters*. Limnology and Oceanography. 00, 00-00. doi : 10.1002/lno.10666; voir annexe II). J'ai contribué à ces articles pour la collecte d'échantillons sur le terrain, l'analyse en laboratoire et j'ai aidé à leur révision. Je serai également coauteure d'un article en lien avec le δ^{13}C-COD et les bactéries dans la plage de la Martinique qui est actuellement en rédaction (en préparation).

CHAPITRE 1 : INTERACTION ENTRE LE FER ET LE CARBONE ORGANIQUE DANS L'ESTUAIRE SOUTERRAIN D'UNE PLAGE DE SÉDIMENT PERMÉABLE

1.1 RÉSUMÉ EN FRANÇAIS DU PREMIER ARTICLE

Comprendre le devenir du carbone organique dissous dérivé du milieu continental via les estuaires souterrains est essentiel pour calculer le budget de carbone des eaux côtières. Cependant peu d'étude existe sur l'interaction du carbone organique (OC) et du fer (Fe) dans ces systèmes dynamiques où l'eau douce se mélange à l'eau de recirculation de la mer. Dans cet article, nous nous sommes concentrés sur l'origine et le devenir du DOC et nous avons quantifié la proportion relative du OC piégé par les hydroxydes de Fe réactif le long de l'estuaire souterrain d'une plage sédiment perméable. Le signal du δ^{13}C-DOC de l'eau souterraine de la plage semblait rapidement répondre aux entrées de OC. Nos résultats montrent une empreinte terrigène de la matrice de l'aquifère résultant de la dégradation du POC de l'ancien sol forestier enfoui sous le sable de l'Holocène. Bien que le système soit sporadiquement affecté par les ajouts massifs de OC marin, cette empreinte marine semble, cependant, être rapidement évacuée de l'estuaire souterrain. Tel que reporté dans les sols et dans les sédiments marins, le piégeage Fe-OC se produit dans les sédiments sableux de l'estuaire souterrain. À l'interface entre l'eau souterraine et l'eau de mer, les hydroxydes de Fe réactifs nouvellement précipités interagissent et piègent le OC terrigène indépendamment de l'origine du DOC dans les eaux souterraines de la plage. Le fractionnement moléculaire du DOC le long de l'estuaire souterrain et le piégeage préférentiel des composés terrigènes favorisent la dégradation *in situ* et/ou l'export des molécules marines non stabilisées par le Fe jusqu'aux eaux côtières. Ces découvertes supportent l'idée que l'estuaire souterrain d'une plage de sable agit comme un puits pour le

OC terrigène à l'interface continent-océan et contrôle l'export de carbone marin vs terrigène dans les eaux côtières.

Cet article, intitulé «*Interaction between Iron and Organic Carbon in a Sandy Beach Subterranean Estuary*» a été soumis le 30 septembre 2017 dans l'issue spéciale du *14th International Estuarine Biogeochemistry Symposium* dans la revue *Marine Chemistry*. L'article est présentement en révision et a été accepté avec des corrections mineures à la date du dépôt final de ce mémoire. Je suis la première auteure de cet article suivi de Mathilde Couturier (Ph.D.), Andrew Barber (Ph.D.), Yves Gélinas (Pr.) et Gwénaëlle Chaillou (Pr.) qui ont tous contribué à l'échantillonnage, aux analyses en laboratoire et à la révision de cet article jusqu'à la version finale. Cet article sera encore révisé jusqu'à la soumission.

Les résultats de cette maitrise ont été présentés lors de différents congrès sous forme de présentation orale ou d'affiche énumérée ci-dessous :

Présentations orales :

Maude Sirois, Mathilde Couturier, Andrew Barber, Yves Gélinas, Gwénaëlle Chaillou, *Origin and behaviour of organic carbon along a subterranean estuary in Iles-de-la-Madeleine (Quebec, Canada)*, 14th International Estuarine Biogeochemistry Symposium, 4-7 juin 2017, Rimouski (Canada)

Maude Sirois, Andrew Barber, Mathilde Couturier, Yves Gélinas, Gwénaëlle Chaillou, *Are Fe-oxides interacting with OC along a Salinity gradient at the land-sea interface? Example of the Martinique beach (Iles-de-la-Madeleine, Quebec, Canada)*, 27 février au 3 mars 2017, ASLO 2017 Aquatic Science Meeting : Mountains to the Sea, Honolulu (Hawaï, USA)

Maude Sirois, Mathilde Couturier, Andrew Barber, Yves Gélinas, Gwénaëlle Chaillou, *Le carbone organique dissous : marin ou terrestre?*, 4-6 novembre 2016, Passé, Présent et Futur : Congrès Étudiant du Centre Eau Terre Environnement, Québec (Québec, Canada)

Présentations par affiches :

Maude Sirois, Mathilde Couturier, Andrew Barber, Yves Gélinas, Gwénaëlle Chaillou, *Le carbone organique dissous dans les plages : marin ou terrestre?*, 8-9 novembre 2016, AGA Québec-Océan 2016, Rimouski (Québec, Canada)

Maude Sirois, Gwénaëlle Chaillou, Yves Gélinas et Mathilde Couturier, *Les flux de carbone dans les plages, réduits par les oxydes de fer?,* 10-11 novembre 2015, AGA Québec-Océan 2015, Québec (Québec,Canada)

1.2 INTERACTIONS BETWEEN IRON AND ORGANIC CARBON IN A SANDY BEACH SUBTERRANEAN ESTUARY

Maude Sirois[1, 2], Mathilde Couturier[1], Andrew Barber[3], Yves Gélinas[3], Gwénaëlle Chaillou[1]

[1] Canadian Research Chair on Geochemistry of Coastal Hydrogeosystems, Département biologie, chimie, géographie, Université du Québec à Rimouski, 300 Allée des Ursulines, Rimouski, Québec, Canada, G5L 3A1.

[2] Institut des Sciences de la Mer de Rimouski, Université du Québec à Rimouski, 310 Allée des Ursulines, Rimouski, Québec, Canada, G5L 3A1.

[3] GEOTOP and the Department of Chemistry and Biochemistry, Concordia University, 7141 Sherbrooke St. West, Montréal, Quebec, Canada, H4B 1R6

1.3 INTRODUCTION

Sandy beaches are key ecosystems of the global land-sea continuum; they account for more than 70% of the world's ice free coastline (Emery, 1968; McLachlan and Brown, 2006). While sandy beaches have long been considered as biogeochemical deserts (Huettel et al., 1996), several recent studies highlighted their importance as biogeochemical reactors where carbon and nutrients are rapidly transformed (Anschutz et al., 2009; Beck et al., 2017; Chaillou et al., 2016, 2014; Charbonnier et al., 2013; Couturier et al., 2017, 2016, Santos et al., 2009, 2008). Their high permeability favors advective transport and the recirculation of seawater, which acts as an important carrier of dissolved carbon species from the coastal ocean into the beach groundwater. Moore (1999) proposed the term "subterranean estuary" (STE) for the coastal aquifer zone to emphasize the importance of freshwater and seawater mixing as well as water–particles interactions as water transits

toward the sea. As is the case in surface estuaries, concentration and nature of the dissolved species change greatly across the mixing zone of STEs and exhibit both production and removal processes, which often depend on redox conditions. Such behaviour along the groundwater flow path must be considered when determining accurate chemical fluxes and their impact on the coastal ocean (Beck et al., 2007; Chaillou et al., 2016, 2014; Couturier et al., 2016; Santos et al., 2009).

Several recent studies report investigations on the behavior of organic carbon (OC) from the aquifer to the coastal ocean. Transport of dissolved organic carbon (DOC) was found to be conservative in some STEs, such as the Hampyeong Bay's tidal flats (South Korea; Kim et al., 2013) and in West Neck Bay (NY, USA; Beck et al., 2007). In contrast, non-conservative behavior of DOC was reported during the transit of groundwater through the mixing zone of STE with an apparent production of DOC, as in the Gulf of Mexico (USA; Santos et al., 2009), in South Carolina (USA; Goñi and Gardner, 2004) and, more recently, on a beach of the Îles-de-la-Madeleine in the Gulf of St. Lawrence (Canada; Chaillou et al., 2016; Couturier et al., 2016). The origin and fate of this DOC pool is still not well defined. Marine-derived particles were identified as the main source of carbon in tidal sands (Anschutz et al., 2009; Kim et al., 2012; McLachlan and Brown, 2006). However, Couturier et al. (2016) have shown that DOC could also be of terrestrial origin based on optical properties of chromophoric dissolved organic matter (CDOM), which showed that lignin-, and more specifically humic-like dissolved organic matter dominated at the discharge zone. The submarine discharge of terrestrial OC could be a key controlling factor on the optical properties of coastal waters and associated ecosystems (Kim and Kim, 2017).

Several methods have been used to determine the origin of OC in aquatic systems: optical indices of CDOM (Couturier et al., 2016; Kim et al., 2012), lignin oxidation products (Shen et al., 2015), OC fingerprints and molecular composition by Fourier transform ion cyclotron resonance mass spectrometry (FT-ICR-MS) (Linkhorst et al., 2017; Seidel et al., 2014), as well as the relative contribution of specific amino acids (Shen et al.,

2015). The exploitation of the $\delta^{13}C$ signature of DOC ($\delta^{13}C$-DOC) has been used in soils (Kaiser et al., 2001; Palmer et al., 2011), stream waters (Bouillon et al., 2012; Palmer et al., 2011; Raymond and Bauer, 2001; Sanderman et al., 2009), groundwater from mangrove tidal creeks (Maher et al., 2013), fjords (Yamashita et al., 2015) and estuaries (Barber et al., 2017b; Osburn and Stedmon, 2011). Here, we present the first attempt to discriminate the origin of OC in beach groundwater by using the $\delta^{13}C$ signature of the DOC. These groundwater samples are particularly challenging to analyze for $\delta^{13}C$ owing to the generally low DOC concentrations combined with high salt and, under reducing conditions with high dissolved iron contents.

The difference in the $\delta^{13}C$ signature of marine and terrestrial DOC arises from the initial signature of the carbon source used for its fixation and from the different pathways for carbon fixation during photosynthesis (Guy et al., 1993; Hayes, 1993). Marine DOC is mainly derived from planktonic organisms that use marine dissolved inorganic carbon for carbon fixation during photosynthesis, which has a signature of about 0‰ (Earth System Research Laboratory Global Monitoring Division of NOAA; https://www.esrl.noaa.gov/gmd/dv/iadv/), whereas the ultimate building block for terrestrial DOC is the atmospheric CO_2, which has a signature of -8‰ to -9‰ (Earth System Research Laboratory Global Monitoring Division of NOAA; https://www.esrl.noaa.gov/gmd/dv/iadv/). The different photosynthetic fixation pathways used by C3 and C4 plants further induce a biochemical carbon fractionation of about -20‰ (C3) or about -12‰ (C4). Combined, the differences in the sources of carbon and in the carbon fixation pathways leads to signatures between about -24‰ and -19‰ for marine primary producers (and marine DOC), and to between about -28‰ and -25‰ for C3 plants-derived terrestrial DOC or between about -16‰ to -10‰ for C4 plants-derived DOC (Hedges et al., 1997; Peterson and Fry, 1987; Zeebe and Wolf-Gladrow, 2001).

Iron plays a pivotal role in the chemistry of STEs. The redox oscillations induced by tides, waves, seasonal water table levels and long-term sea level changes control the precipitation of ferric hydroxides at the redox interfaces within the STE (Charette and

Sholkovitz, 2002). This Fe curtain acts as an oxidative barrier for redox sensitive elements and elements with high affinity to Fe-hydroxides such as phosphate, barium, uranium and nitrogen species (Charette et al., 2005; Charette and Sholkovitz, 2006, 2002; Couturier et al., 2017; Sanders et al., 2017). Iron also interacts with OC and affects its mobility (Kaiser and Guggenberger, 2000) and its molecular properties (Poulin et al., 2014). Predominantly short-term, reversible interactions can occur through adsorption, flocculation or coagulation between Fe-hydroxides and OC, while the direct co-precipitation of Fe and OC, involving covalent bonding between the two elements, can lead to the long-term trapping of carbon under certain redox conditions (Barber et al., 2017a). The molecular composition of OC, and thus its origin, is an important control on the amount of OC trapped into Fe curtain, along with redox conditions and Fe concentrations. For example, Riedel et al. (2013) showed in peatlands that aromatic terrestrial OC was preferentially trapped compared to aliphatic compounds. Such Fe-OC interactions have been highlighted in marine sediments (Barber et al., 2017a; R. Keil et al., 1994; Lalonde et al., 2012), soils (Jones and Edwards, 1998; Kaiser and Guggenberger, 2003, 2000; Wagai and Mayer, 2007) and more recently beach groundwater samples (Linkhorst et al., 2017). In this latter study, the authors suggested that in STEs, Fe induced the flocculation of OC (mostly large, oxidized, and aromatic terrigenous molecules), acting as a potential inorganic regulator for the export of terrestrial OC to coastal waters. This "rusty carbon sink", as proposed by Lalonde et al. (2012), might control not only the submarine groundwater discharge OC fluxes but also the molecular properties of the exported OC (Linkhorst et al., 2017; Seidel et al., 2015, 2014). According to our knowledge, there is presently no direct quantification of this carbon sink within STE systems.

In the present work, we focused on the origin and behavior of OC along the STE of a sandy beach located on the Îles-de-la-Madeleine (Gulf of St. Lawrence, QC, Canada), where fresh groundwater flows seaward below a narrow intruding saline circulation cell located near the top of intertidal sediments. We determined both the horizontal and vertical distribution and origin of DOC based on its concentration and stable carbon isotope signature (δ^{13}C-DOC) in beach groundwater. In addition, we quantified the relative

proportion of OC trapped by reactive Fe-hydroxides along a cross-shore transect and determined the isotopic signature of the Fe-stabilized OC.

1.4 MATERIALS AND METHODS

1.4.1 Site Description

This study was conducted in the STE of the Martinique Beach on the Îles-de-la-Madeleine (Québec, Canada) (Fig. 5). This archipelago is located in the Maritimes Permo-carboniferous Shelf Basin (Brisebois, 1981). The main aquifer of the Archipelago is composed of sandstones from the Permian Inferior period (the Cap-aux-Meules formation; Brisebois, 1981). Groundwater flows through this unconfined aquifer and discharges into the ocean, both directly and through the overlying permeable tidal deposits. The Martinique Beach originates from a recent transgression sequence and is located at the seaward boundary of the Permian aquifer. The rapid rates of relative sea-level rise along the Atlantic Coast of Canada over the middle to late Holocene buried the unconfined Permian sandstone aquifer, which is now covered by tidal sediment (Gehrels, 1994; Scott et al., 1995a, 1995b). Tidal sediment consists of a ~50 cm-thick layer of eolian sand, with an average grain size of ~300 μm, mainly composed of quartz (95%) mixed with silt (< 5%; Chaillou et al., 2014). The underlying Permian sandstone aquifer consists of fine red-orange sands (~100 μm) composed of silicate and aluminosilicate with Fe oxides coated silicate grains (Chaillou et al., 2014). Its exact localization in the beach and its offshore extent is unknown. At the top of the sandstone aquifer, there is a fragmented organic-rich layer, with a total organic carbon (TOC) concentration from 5 to 35% weight percent (wt). This old buried soil is mainly composed of terrestrial plant detritus and was formed ~900 years B.P., as revealed by ^{14}C age dating (Juneau, 2012). The site experiences little wave action except during storm events. Tides are semi-diurnal with a spring tide range ≤1 m.

A few recent studies have focused on the biogeochemistry of the STE (Chaillou et al., 2014; Couturier et al., 2017, 2016) and the calculation of groundwater flows (Chaillou

et al., 2017, 2016) at the Martinique Beach site. The shallow superficial unconfined beach aquifer releases both fresh groundwater and recirculated seawater to the coastal embayment. Within the beach, fresh groundwater flows towards the seaward discharge region at a mean velocity of 0.30 m/d (Chaillou et al., 2016) and discharges below a narrow upper saline plume (USP) located near the top of intertidal sediments. This fresh groundwater contributes to at least 70% of the total water flow discharging to the coastal waters (Chaillou et al., 2017). In Chaillou et al. (2014), the authors show that mixing of both organic and inorganic carbon is non-conservative, suggesting a production of DOC and DIC along the groundwater flow path. Based on hydrological approaches and mean DOC and DIC concentrations in the surficial intertidal sediment, Chaillou et al. (2016) calculated a fresh-groundwater carbon load of 147 kg/d of DIC and 27 kg/d of DOC at the discharge zone. Based on optical indices of CDOM, Couturier et al. (2016) recently showed that the degradation of the old buried soil is a probable source of the OC pool in beach groundwater. This degradation along the transit modified the optical fingerprint of groundwater OC by releasing high molecular weight (HMW), aromatic, and lignin-type compounds of terrestrial origin.
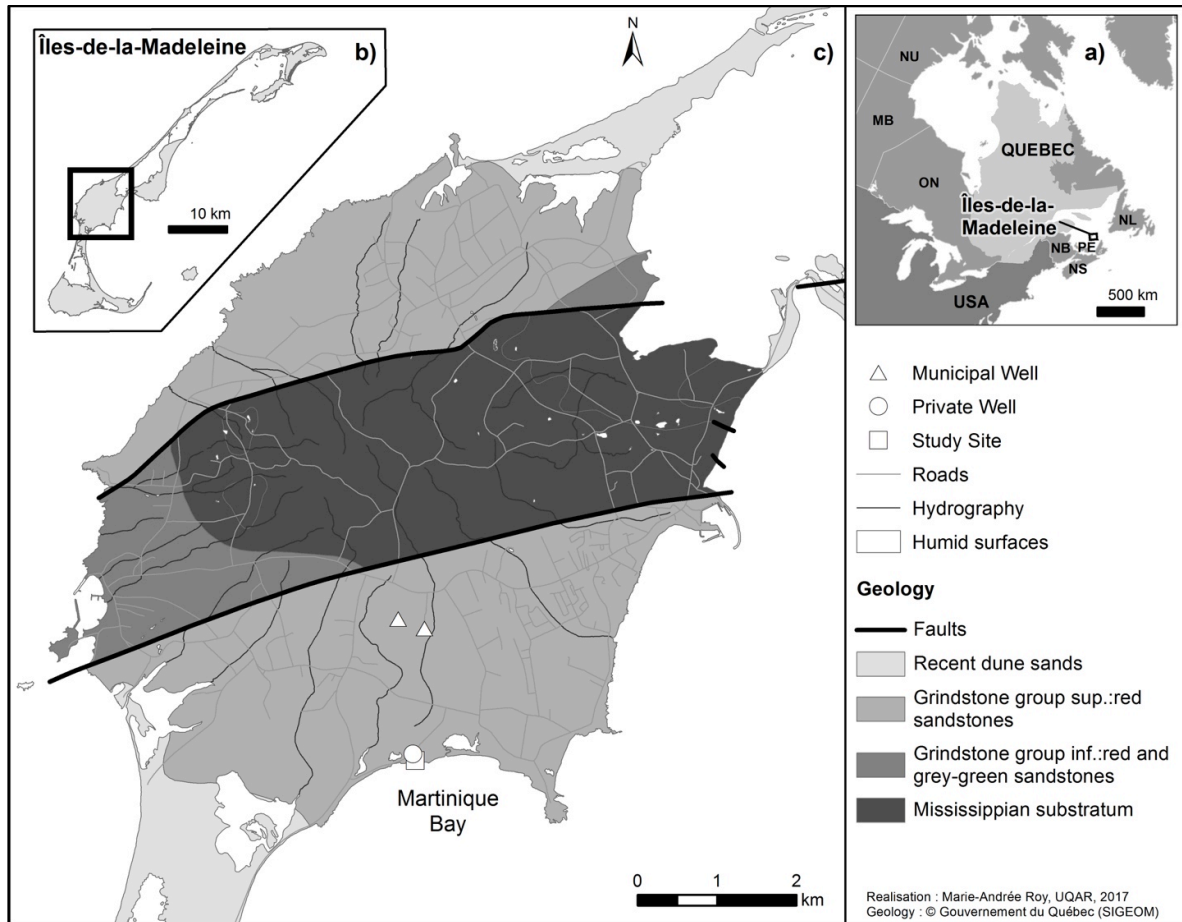
Figure 5 : (a) Province of Quebec, (b) the Îles-de-la-Madeleine and (c) the archipelago's main island (Cap-aux-Meules). The study area of the Martinique Beach and the wells where fresh inland groundwater was collected are shown in panel C. The simplified geology was adapted from Brisebois (1981)

1.4.2 Beach groundwater sampling

Samples were collected during the neap tide period in May and June of both 2013 and 2015. Water samples were collected using 9 multi-level samplers inserted along a ~20 m transect perpendicular to the shoreline (Fig. 6A). The positions of the multi-level samplers covered the intertidal zone and the underlying STE, where fresh groundwater comes in contact with recirculated seawater. In 2013, multi-level samplers M2, M4, M5, M6, M7 and M8 were used to collect beach groundwater. In 2015, groundwater samples

were collected twice following a storm that left seaweed on the beach, using multi-level samplers M1, M3, M6 and M9. The samples were collected one (Fig. 6; 2015-A) and three days (Fig. 6; 2015-B) after the massive deposition of seaweed fragments, which were mainly composed of *Zostera marina*.

Each multi-level sampler was made with PVC, as described by Martin et al. (2003), and allowed collecting beach groundwater at 8 different depths (0, 10, 30, 50, 80, 110, 150, 190 and 230 cm) below the beach surface. To allow sediments around the samplers to reach equilibrium, multi-level samplers were installed for a minimum of two days prior to beach groundwater collection. During collection, groundwater was continuously pumped to the surface using a peristaltic pump and Tygon tubing. Salinity, temperature, and dissolved oxygen were measured in an in-line flow cell with a calibrated YSI-600QS multiparametric probe. After stabilization of these parameters, beach groundwater samples were collected with a clean polypropylene syringe and filtered on combusted 0.7-µm glass fiber filters. Samples were acidified to pH<2 with pure HCl in EPA borosilicate vials with PTFE lined caps for subsequent DOC and δ^{13}C-DOC analyses. For total dissolved Fe, beach groundwater samples were filtered on 0.2-µm Whatman Polycap 75S filters and acidified with pure nitric acid to a pH<2 in polypropylene Falcon® tubes. Samples were stored at 4°C.

Concentrations of DOC, Fe and the δ^{13}C-DOC signatures were systematically measured for fresh inland groundwater and seawater end-members. Samples from the Permian sandstone aquifer were pumped from a municipal well located at 1.5 km from the shore (PU6; Fig. 5), and one private well (PC; Fig. 5) located at only ~50 m inshore from the multi-level sampler transect. Marine end-members were collected 0 to 0.6 km offshore in Martinique Bay using a small boat from which seawater was collected using a submersible pump connected to an on-line flow cell. The physico-chemical parameters, and water samples for subsequent DOC, Fe and δ^{13}C-DOC analyses were collected and stored as described above.
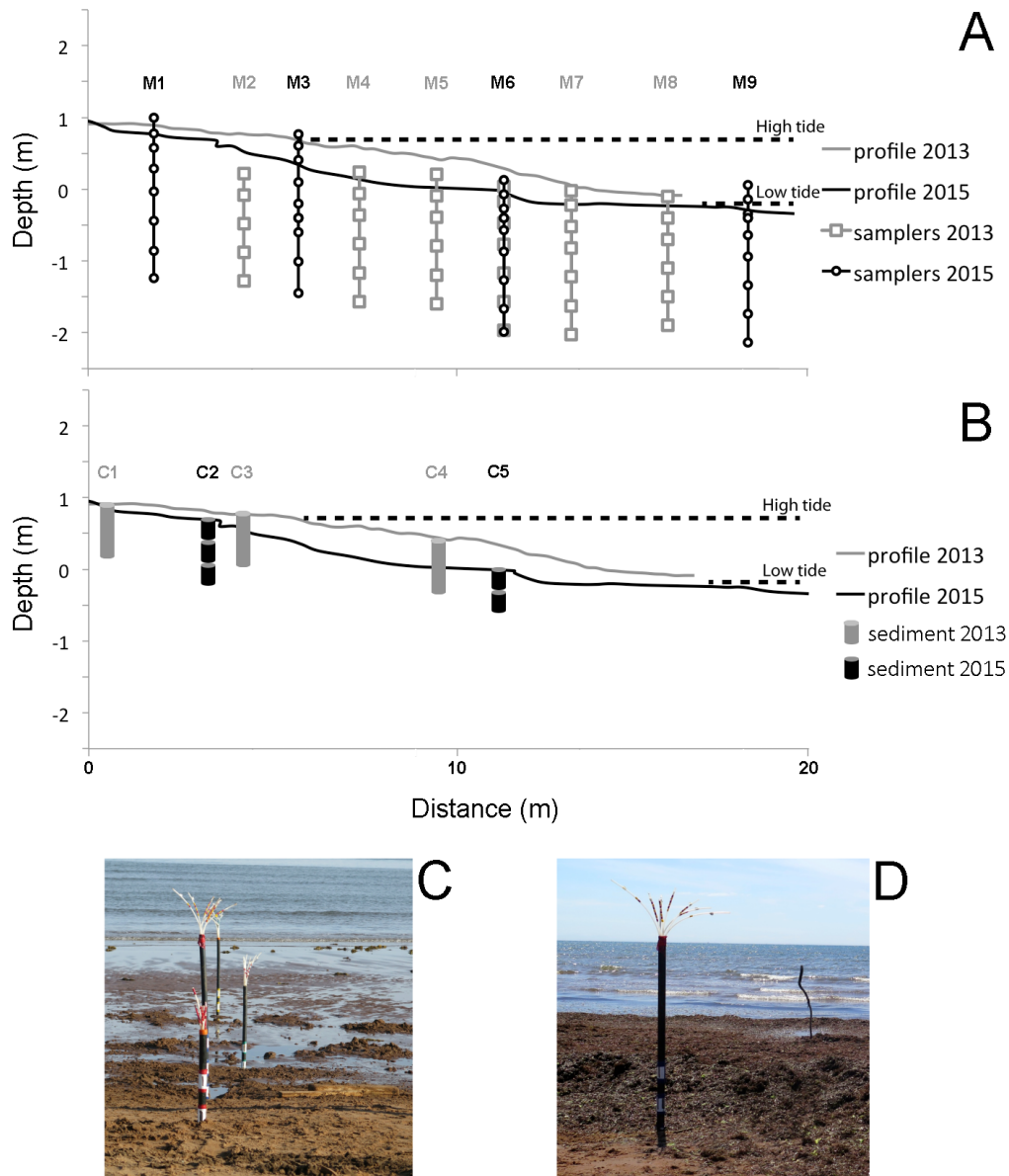
Figure 6 : Cross-shore transect on the studied beach in 2013 (grey) and 2015 (black). A) Location of the different multi-level samplers (M1 to M9). The sampling points are also reported (grey squares for 2013 and black circles for 2015). B) Location of the different sampling point for the sediment. The beach morphology was obtained from differential global positioning system (DGPS) measurements. The indicated depths are relative to mean sea level (i.e., 0m sea level). C) Photography of the studied beach in 2013 and D) in 2015 with the seaweeds deposits

1.4.3 Beach sediment sampling

Three sediment cores were collected in 2013 using standard vibracoring techniques with a clean plastic 1 m liner inserted into an aluminum pipe. The cores were recovered at the top of the beach (C1, Fig. 6B), and at the high and low tide marks (C3 and C4; Fig. 6B). The cores were frozen at -20°C until subsampling. Cores were then opened and the three different sedimentary units (i.e. Holocene sand, organic-rich horizon, and Permian Sandstone) were subsampled to measure their particulate organic carbon (POC) concentration and isotopic signature (δ^{13}C-POC), the reactive Fe-hydroxide content, as well as the concentration and stable isotope signature of POC closely associated to Fe-hydroxides. In 2015, the three different sedimentary units (i.e., Holocene sands, Permian Sandstone and the organic-rich horizon) were collected in the intertidal zone with a manual auger, at the high and low tide marks (C2 and C5 in Fig. 6B). The samples were frozen at -20°C until subsequent analysis. Because they can act as a potential source of DOC into the beach system, seaweeds that accumulated at the surface of the intertidal zone in 2015 were also collected to measure the POC concentration and stable isotope signature (δ^{13}C-POC). Three replicates samples were collected and frozen at -20°C prior to subsequent analysis.

1.4.4 Chemical Analyses

Dissolved Compounds

Total dissolved Fe concentrations were analyzed in acidified and filtered samples using a Microwave Plasma Atomic Emission Spectrophotometer (4200 MP-AES from Agilent Technologies). The detection limit of the method is 2.4 µg/L for Fe concentration at a wavelength of 391 nm. Analytical uncertainties were <5%.

For the samples collected in 2013, DOC was analyzed by high temperature combustion (HTC) using a Total Organic Carbon (TOC) analyzer (TOC-V$_{cpn}$; Shimadzu) based on the method proposed by (Wurl and Tsai, 2009) (see Couturier et al., 2016 for details). The detection limit is 0.05 mg/L and the analytical uncertainties were <2% for

concentrations higher than 1 mg/L. Samples for DOC concentrations in 2015 and δ^{13}C-DOC in 2013 and 2015 were analyzed using a modified Aurora OI 1030 high-temperature catalytic oxidation unit coupled to a chemical trap (GD-100, Graden Instruments) and a GV Isotope Ratio Mass Spectrometer (Isoprime) as described in details in Lalonde et al. (2014a) and Barber et al., (2017b). The standards used for isotopic signatures and DOC concentrations were in-house calibrated β-alanine (40.4 % organic carbon (OC), -26.1 ± 0.1 ‰) and sucrose (42.1 %OC, -11.8 ± 0.1 ‰) dissolved in 18.2 mΩ/cm milli-Q water (Barber et al., 2017b). The precision of the method for fresh and salty waters is ±0.5 ‰ for DOC concentrations of 0.5 mg/L, decreasing regularly from ±0.5 ‰ to ±0.2 ‰ between 0.5 and 1.0 mg/L, and ±0.2 ‰ above 1.0 mg/L (Lalonde et al., 2014a).

Particulate fraction

The citrate-dithionite-bicarbonate Fe reduction method of Mehra and Jackson (1960), modified by Lalonde et al. (2012), was applied to the dried and homogenized sediments. This method allows to quantify the fraction of total POC that is specifically associated to reactive Fe-hydroxides, as well as its δ^{13}C signature. Briefly, reactive Fe-hydroxides are reductively dissolved with dithionite at circumneutral pH (bicarbonate buffer), using citrate as a complexing agent to keep dissolved Fe in solution. The fraction of OC associated with reactive Fe-hydroxides was measured by difference before and after the reduction reaction. The OC concentration and carbon stable isotope signature were analysed with an elemental analyzer (Eurovector EuroEA3000) coupled to a GV Instrument Isoprime isotope ratio mass spectrometer following the removal of inorganic carbon by vapour-phase acidification (Hedges and Stern, 1984). The reactive Fe-hydroxide content in the extract following the reduction step was analyzed by inductively coupled plasma mass spectrometry (Agilent 7500ce). The sedimentary units in each core were analyzed in triplicate in 2013 and 2015. The analytical precision was better than ±0.2 % for organic carbon concentrations, and ±0.2 ‰ for the stable carbon isotope signatures.

1.5 RESULTS

1.5.1 Characteristics of the potential dissolved organic carbon sources

The characteristics of the different potential sources of DOC are presented in Table 2. The fresh inland groundwater samples exhibited DOC concentrations and δ^{13}C-DOC signatures ranging from 0.4 ± 0.1 to 2.3 ± 0.4 mM and -26.0 ± 1.1 ‰ to -20.6 ± 6.2 ‰ respectively. The highest DOC concentrations were measured in the private well PC, located close to the shore. Its δ^{13}C-DOC signature was very depleted. The seawater exhibited low DOC concentrations around 0.15 mM with a mean δ^{13}C signature of -22.2 ± 4.3‰, typical of marine signatures (Barber et al., 2017b; Peterson and Fry, 1987).

Tableau 1 : Mean δ^{13}C-DOC signatures (‰) and concentrations of DOC (mM) of the different potential DOC source (fresh inland groundwater and seawater)

Sample	Source	δ^{13}C-DOC (‰)	DOC (mM)
P4	inland groundwater	-14.4 ± 0.7	0.15 ± 0.02
PU6	inland groundwater	-20.6 ± 6.2	0.40 ± 0.18
PC	inland groundwater	-26.0 ± 1.1	2.39 ± 0.45
SW	marine water	-22.1 ± 4.3	0.15 ± 0.02

1.5.2 Biogeochemical features of the STE

Recent studies have focused on the variations of the physio-chemical parameters (S, T, pH, DO) and DOC concentrations along the groundwater flow path, from inland wells to Martinique Beach and the adjacent bay (Chaillou et al., 2016, 2014, Couturier et al., 2017, 2016). Here, we briefly present the spatial distribution of salinity, Fe and DOC concentrations in May and June 2013 and 2015.

The spatial distribution of salinity along the transect was relatively similar in 2013 and 2015 with an upper recirculation seawater cell just below the beach surface, where salinity was higher than 20 (Fig. 7A-C). In 2013, this zone was vertically constrained with a maximum extension to a depth of 0.5 m. In 2015 (Fig. 7B-C), however, seawater infiltrated deeper, reaching a depth of 1 m below the beach surface. Brackish water, with a salinity ranging from 2 to 20, formed a thin mixing zone along the perimeter of the upper recirculation cell. Below, the deeper part of the STE was dominated by seaward-flowing fresh groundwater with low salinity (<2). The vertical and horizontal distribution of salinity along the transect agreed well with the concept of the subterranean estuary proposed by Moore (1999).

Dissolved Fe exhibited strong vertical gradients with lower concentrations at the surface to concentrations higher than 1000 μM in brackish groundwater. In 2013, Fe concentrations in beach groundwater were very high with a mean value around 600 μM. Dissolved Fe increased just below the upper recirculation seawater cell and reached values higher than 500 μM in the mixing zone (Fig. 7D). In the deep groundwater, the concentrations remained high (i.e., ranging from 500 to 1500 μM) and reached values as high as 2300 μM in M4. In 2015, the patterns of Fe concentrations were different (Fig. 7E-F). Since the upper recirculation cell was deeper, the dissolved Fe-rich zone was located just below the surface at the low tide mark (from M6 to M9; Fig. 7E-F). The concentrations were also lower with mean values around 400 μM and maxima less than 1800 μM.

In beach groundwater, DOC concentrations ranged from 0.14 to 15.28 mM, well above the concentrations measured in the water end-members (Table 1). The distribution patterns were all characterized by low concentrations (< 2 mM) in the intertidal zone, from M5 to M7. The zone enriched in DOC was located at the high tide marks near M3 and M4. However, the mean concentrations were significantly different in the three sampling periods. In 2013, DOC concentrations ranged between 0.14 and 15.28 mM with a mean value of 2.10 ± 2.63 mM. The highest concentrations (>10 mM) were measured near the surface, at about 80 cm depth below the surface in M4 (Fig. 7D). In 2015-A, the DOC

concentrations ranged from 1.18 ± 0.04 mM to 12.41 ± 0.22 mM with a slightly higher mean value of 3.30 ± 2.17 mM. The highest concentration was reached at the interface between seawater and sediment between M3 and M6 (Fig. 7H). Two days after, the mean DOC concentration decreased to 2.72 ± 3.18 mM (from 0.63 ± 0.05mM to 13.62 ± 0.12 mM). The DOC concentration was higher than 12 mM at the top of the intertidal zone, at the top of M3 (Fig. 7I).

The δ^{13}C signatures of DOC were greatly different between 2013 and 2015. In 2013, the δ^{13}C-DOC signatures were between -31.2 ± 0.1 ‰ and -22.7 ± 0.1 ‰, with a mean value at -26.4 ± 1.6 ‰. Values were generally close to -25 ‰ but they were more depleted in ^{13}C at the high tide mark when they dropped to about -30 ‰. These values corresponded to a terrestrial δ^{13}C signature. In 2015-A, just one day after the massive seaweed deposit, values were less depleted in ^{13}C compared to 2013 with signatures between -23.7 ± 0.1 ‰ and -12.4 ± 0.1 ‰ (mean of -16.1 ± 3.0 ‰). The isotopic enrichment was very clear in the intertidal zone, between M6 and M9 where signatures were comprised between -17.0 ± 0.2 ‰ and -12.4 ± 0.1 ‰. Three days later (2015-B), the δ^{13}C-DOC signatures were still enriched in ^{13}C compared to 2013 (between -25.3 ± 0.2 ‰ and -12.2 ± 0.02 ‰; mean = -19.0 ± 3.3 ‰), but not as much as 2015-A. The δ^{13}C-DOC signatures were enriched in ^{13}C in the first 50-80 cm depth of the intertidal zone (between -12.2 ± 0.1 ‰ and -16.9 ± 0.2 ‰) compared to the samples located above the high tide mark where δ^{13}C was around -20 ‰.
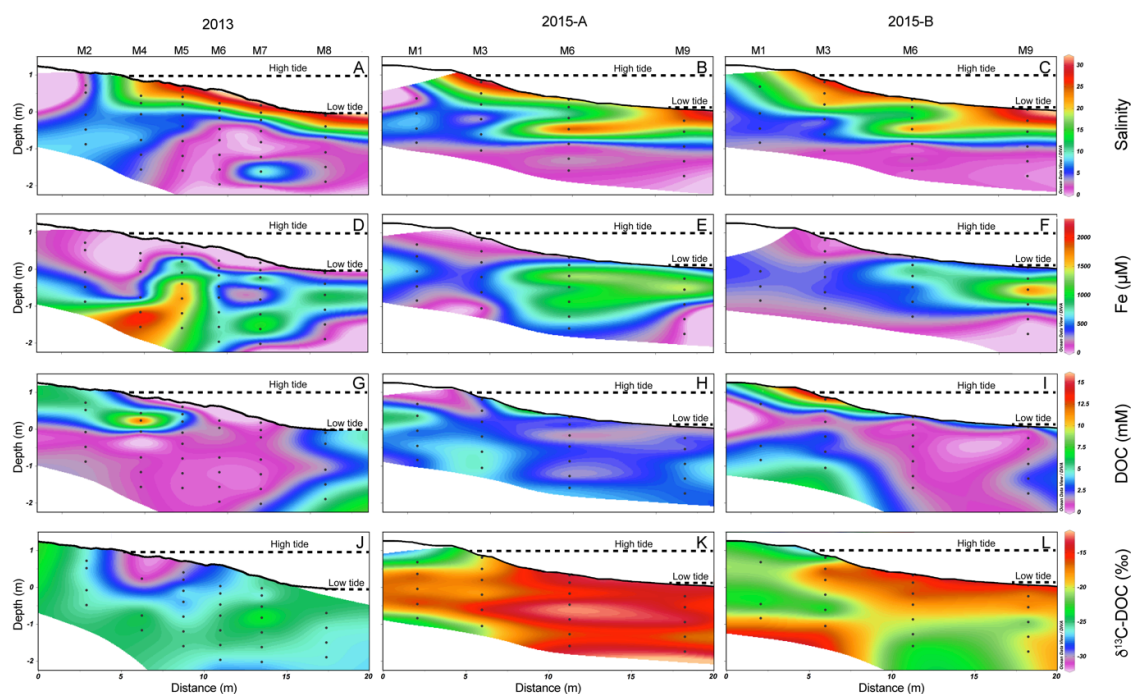
Figure 7 : Cross-section of transect of M1 to M9 showing the topography and distribution of the salinity (A, B, C); the total dissolved Fe concentrations (D, E, F) ; the DOC concentrations (G, H, I) and δ¹³C-DOC (J, K, L) for the three sampling campaigns. Contour lines were determined by spatial interpolation (kriging method). Black dots represent each sampling points. Depths are relative to mean sea level (0 m sea level)

1.5.3 Source, Distribution and Signature of the POC along the transect

The four others investigated source of OC correspond to solid phase terrestrial and marine organic matter (Fig. 8). Two organic-rich source materials were present in the system, namely, the old soil buried below the Holocene sand, and the fresh seaweed deposit at the top of the Holocene sand in the intertidal zone. In the old buried soil, the particulate organic carbon (POC) content was high in the top of the beach with POC content > 19.6 % (Fig. 8). This content tended to decrease towards the shoreline where the old buried soil was eroded away or degraded. This layer was detected only in core C2 in 2015, although it was more diluted with minerals than in 2013 at this site (OC content of about 5%). In all cases, this POC exhibited a δ¹³C signature typical of terrestrial soil (i.e., -26.70 ± 0.50 ‰;

n=9) (Peterson and Fry, 1987). The marine seaweeds collected on the beach were enriched in POC (30.30 ± 0.80 %) and were characterized by a less depleted δ^{13}C-POC signature (i.e., -12.00 ± 0.20 ‰, n=3) typical of *Zostera marina* (Chmura and Aharon, 1995). The Holocene sand and Permian sandstone were poor in OC with concentrations below 0.5 % of dry sediment. In both cases, the δ^{13}C-POC signatures were depleted and ranged between -25.20 ± 1.60 ‰ (n=17) and -26.50 ± 0.10 ‰ (n=15) in the sands and sandstone, respectively.
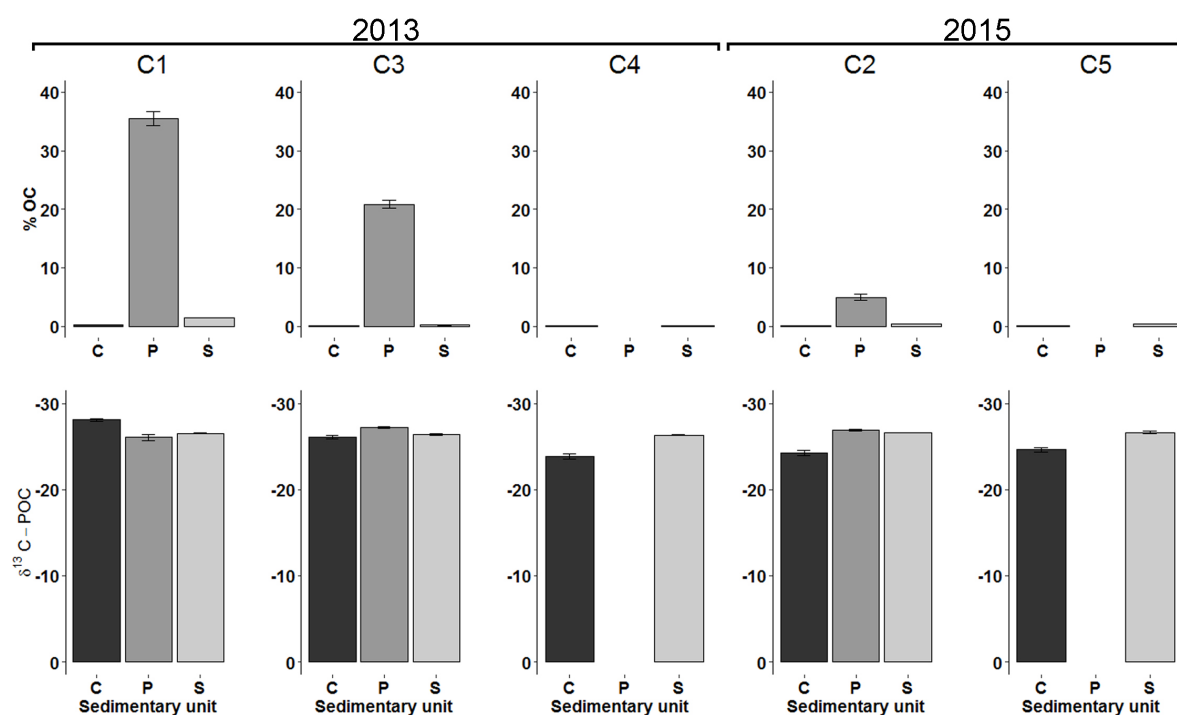
Figure 8 : Percent OC and δ^{13}C-POC of each sediment cores in 2013 (C1, C3 and C4) and 2015 (C2 and C5). Results are given for each sedimentary unit (C = Holocene Sand; P = organic-rich layer horizon; S = Permian sandstone). The location of the different sedimentary cores is reported in Fig. 6B. The sedimentary unit P is absent at the low tide marks, which explains why there is no result for C4 and C5 for this unit

1.5.4 Distribution and Signature of the Organic Carbon trapped by Fe-oxides along the STE

The relative amounts of OC associated to reactive Fe-hydroxides in the different sedimentary units are reported in Fig. 9. The percentage of total OC associated with reactive Fe-hydroxides was low in the 2013 samples with values below 13.9 % in the three units. In the seaward core (C4) where the total OC concentrations were very low (<1 wt%), the proportion of OC associated to reactive Fe-oxides was below the detection limit of the method. Higher percentages of total OC associated to Fe were measured in sediment samples collected in 2015, particularly for core C2, where Fe-stabilized OC accounted for about 24% in the surficial sand unit and increased with depth to reach a maximum value of 56% in the Permian Sandstone (Fig. 9). The δ^{13}C-POC signature of the OC associated to reactive Fe was very depleted and ranged between -24.30 and -33.60 ‰.
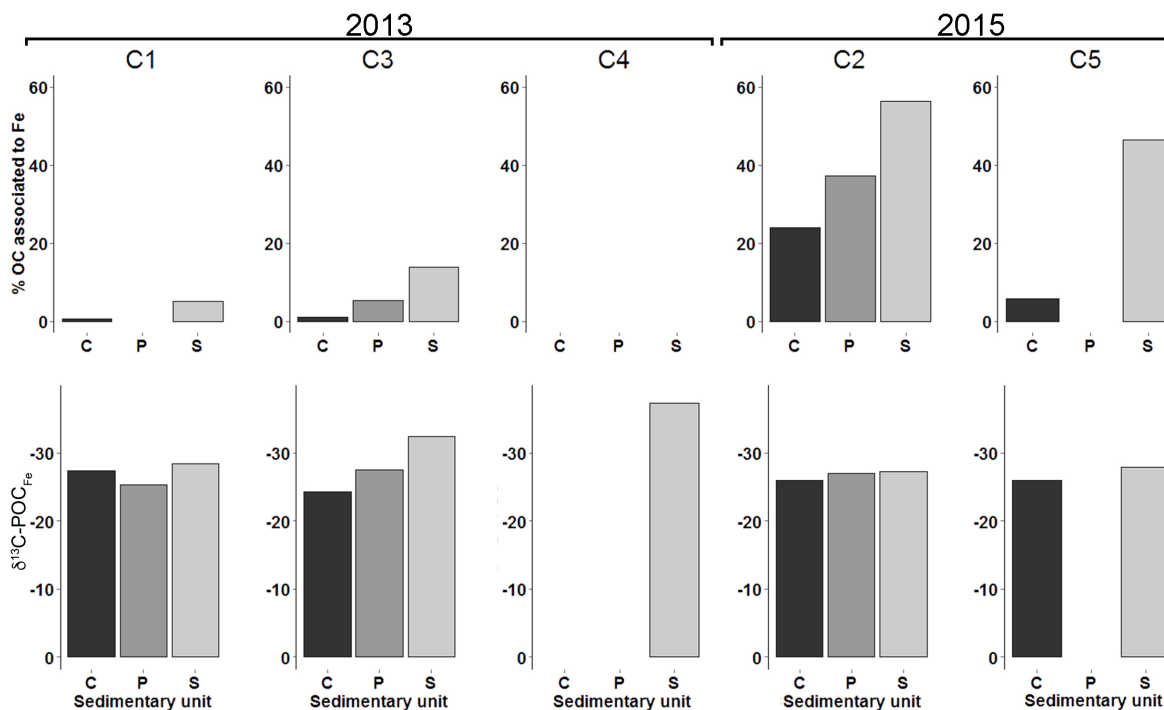
Figure 9 : Percentage of total OC associated with Fe and δ^{13}C-POC of the OC associated with Fe for each sediment cores in 2013 (C1, C3 and C4) and 2015 (C2 and C5). Results are given for each sedimentary unit (C = Holocene Sand; P = organic-rich layer horizon; S

= Permian sandstone). The location of the different sedimentary cores is reported in Fig. 2B. The sedimentary unit P is absent at the low tide mark, which explains why there is no result for C4 and C5 for this unit

1.6 DISCUSSION

1.6.1 Biogeochemical process along the STE

The STE of the Martinique Beach is a highly dynamic system characterized by transient biogeochemical conditions where dissolved oxygen saturation, DOC and Fe concentrations vary greatly within centimeter-scales. As in surficial estuaries, different processes, such as mineralization, flocculation, adsorption, and coprecipitation, can affect the fate of DOC and Fe in beach groundwater. The absence of light and the continuous water-sediment interaction provide an ideal environment for the transformation and sorption of OC onto mineral particles in the absence of photochemical oxidation processes (Kaiser et al., 2004). In addition, the mineralization of OC leads to a decrease in DOC concentrations and the production of DIC and reduced metabolites such as dissolved ferrous iron (Bauer et al., 2013; Dorsett et al., 2011; Nevin and Lovley, 2002; Roy et al., 2013). As in surficial estuaries, the salinity gradient also induces the flocculation of OC and the formation of Fe colloids (Boyle et al., 1977; Charette and Sholkovitz, 2002; Haese, 2006).

In the sandy beach STE, DOC showed clearly a non-conservative pattern, with significant internal inputs as groundwater transits along the intertidal zone (Fig. 7G-I), similar to already observed at the same site (Chaillou et al., 2016; Couturier et al., 2016) and in other STEs, including Turkey Point Beach (Gulf of Mexico, Florida; Santos et al., 2009), Hampyeong Bay (Korea; Kim et al., 2012), and North Inlet (South Carolina; Goñi and Gardner, 2004). The low dissolved oxygen saturation (~20%) and high DOC concentrations (> 2 mM) suggested a suitable environment for anaerobic microbial respiration. The high DIC concentrations previously reported by Chaillou et al. (2014, 2016), combined with high dissolved Fe concentrations (and other reduced compounds

such as NH_4^+ and Mn^{2+}; Couturier et al., 2017), as well as the characteristic H_2S odour detected during sample collection, all support the idea that suboxic to anoxic solid-phase OC mineralization processes occurred along the flow path, supporting the loss of DOC towards the discharge zone.

The spatial distributions of dissolved Fe also showed a non-conservative pattern and a significant difference between the high Fe concentrations from the deep part of the STE, where fresh groundwater flowed in 2013 (Fig. 7D), and the low tide mark of USP in 2015, where seawater recirculated (Fig. 7F). The accumulation and degradation of the fresh seaweed deposit likely increased the OC mineralization rates and, therefore, enhanced the consumption of oxidants and the production of reduced chemicals near the beach surface. This finding agrees well with the high NH_4^+ concentrations observed by Couturier et al. (2017) in the upper saline plume (USP). The redox oscillation within the mixing zone along the USP creates favorable conditions for Fe-OC flocculation and oxidative precipitation mechanisms as the oxidation of ferrous Fe from anoxic groundwater is efficient near the groundwater-seawater interface, where dissolved oxygen levels and salinity increase due to tidal inputs (Charette and Sholkovitz, 2002; Edzwald et al., 1974; Sholkovitz, 1976). The low mean concentrations of dissolved Fe in beach groundwater in 2015 suggest a general loss of dissolved Fe to the solid phase compared to 2013. The oxidation and precipitation of reactive Fe-hydroxides were probably more efficient at this sampling period. Because the Fe-hydroxides content of the solid phase is very high in both the Holocene sand and underlying Permian sandstone aquifer, the direct measurement of newly formed amorphous Fe-hydroxides was not possible using this extraction method. In addition to reactive Fe-hydroxide precipitation, Riedel et al. (2013) reported that the oxic-anoxic transition enhances the mechanism of Fe-OC flocculation, particularly with terrestrial OC, controlling the export of both Fe and lignin-type compounds to the overlying water column.

1.6.2. Source of the DOC in the study beach based on δ^{13}C-DOC signatures

Based on the stable isotopes of water along the STE, Chaillou et al. (2017) confirmed the contribution of only two water end-members s (i.e. fresh inland groundwater and seawater) and the absence of additional skeptic tank seepages, which could act as a source of OC into beach groundwater. They also highlighted the high contribution of fresh inland groundwater and the limited infiltration of seawater in shallow beach groundwater in the spring when the water table is high due to the snowmelt. However, in groundwater, solutes and water could have a different origin.

In contrast to the spatial distribution of DOC, the δ^{13}C-DOC signatures exhibited different values and patterns in 2013 and 2015. Despite the DOC concentrations were in the same range (Fig. 7G-I; Fig. 10), the average isotopic signatures varied greatly, from -31.2 ± 0.1 ‰ in 2013 to -12.2 ± 0.1 ‰ in 2015-A when seaweeds were deposited on the surface of the beach. In both cases, the groundwater end-members did not seem to be the primary source of DOC in beach groundwater because their respective signatures (i.e. -14.4 ± 0.1 ‰, -20.6 ± 6.2 ‰ and -22.1 ± 4.3 ‰ for fresh inland groundwater of P4 and PU6 and seawater, respectively; Table 1) were very different from the beach groundwater DOC signatures. Even if there was a limited infiltration of seawater below the USP, we cannot exclude that some DOC derived from marine primary production was present in the system. It was, however, clearly not the main source of DOC. This suggests that the beach groundwater DOC pool was unrelated to the water end-members. With a maximum groundwater flow rate of ~0.30 m/d (Chaillou et al., 2016), the groundwater transit time through the STE (~20 m) is about 66 days, which is long enough to allow DOC production from the degradation of POC from both marine and terrestrial origin, along with other processes that can influence the measured δ^{13}C-DOC signatures such as the degradation of DOC, and the biochemical fractionation of the dissolved organic compounds based on their size and affinity for the mineral phase. As an example, the DOC production rates from

seaweeds degradation is highest in the first 1-2 days and decreases afterward (Wada et al. 2007 and reference therein).
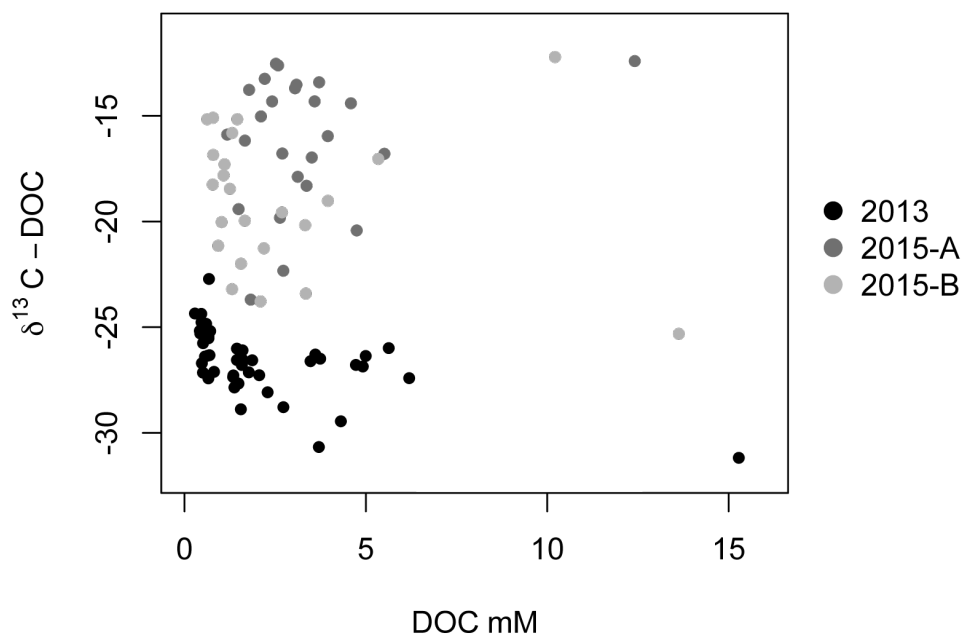
Figure 10 : Relationship between δ^{13}C-DOC (‰) and DOC concentration (mM). The black dots represent the values measured in 2013, while the dark gray dots represent the 2015-A values and the light gray dots represent the 2015-B values

In the 2013 samples, the beach groundwater δ^{13}C-DOC signatures ranged from -31.2 ± 0.1 ‰ to -22.7 ± 0.1 ‰ (Fig. 7J-L, Fig. 10) and were typical of terrestrial plants that use the Rubisco enzyme in C fixation during photosynthesis (C_3 plants). These signatures were strongly depleted compared to the values measured in fresh inland groundwater samples, with the exception of the nearshore well (PC) where δ^{13}C-DOC signature was -26.0 ± 1.1 ‰ (Table 1). The variations in δ^{13}C-DOC signatures along the flow path from the aquifer to the beach groundwater reflect the spatial distribution of land cover and soil, which are the main sources of DOC into groundwater (Shen et al., 2015; and references therein). The unsaturated zone acts as a chromatographic column where surface and plant-derived DOC are removed by microbial degradation and sorption onto minerals prior to

reaching the saturated zone (Shen et al., 2015). The proximity of the PC well to the studied transect (Fig. 5C) and the thickness and the lithology of the unsaturated zone probably prevent a strong removal of surficial and plant-derived DOC. There, significantly higher SUVA$_{254}$ values (i.e. DOC-normalized absorbance at 254 nm; Weishaar et al., 2003) were measured compare to those measured in municipal wells, corroborating the relatively high concentrations of plant-derived CDOM in beach groundwater (Couturier et al., 2016). The δ^{13}C-DOC signatures were close to the δ^{13}C value of POC from the old buried soil and sediments, which exhibited a signature typical of terrestrial C3 plants (Aravena et al., 2004; Aravena and Wassenaar, 1993; Palmer et al., 2011). This result suggests that the degradation of this terrestrial POC supported the production of DOC, in agreement with the findings of Couturier et al. (2016). This process probably supported both the production of DIC with depleted isotopic signature (e.g. about -30‰; Chaillou et al., 2016), and the release of DOC, probably as aromatic lignin-type compounds, in agreement with the findings of Filip and Smed-Hildmann (1992), who have shown that fossil plant materials could release humic acids to groundwater.

The DOC concentrations and δ^{13}C-DOC signatures measured in the 2015 beach groundwater samples were, however, significantly different from those measured in 2013. During the first sampling campaign in 2015 (2015-A), only one day following the massive deposition of seaweeds on the surface of the beach, less depleted δ^{13}C-DOC signatures, ranging between -23.7 ± 0.1 and -12.4 ± 0.1 ‰ (Fig. 7K), were measured compared to 2013 (Fig. 7J). As in 2013, the degradation of a specific POC source material might control the isotopic signatures of DOC in the beach groundwater samples. The massive seaweed deposit represented a source of organic material with an OC content of 30.3 ± 0.8 % (wt) and a stable isotope signature of -12.0 ± 0.2 ‰, similar to some of the δ^{13}C-DOC signatures measured in 2015-A. The seaweed deposits, which accumulate sporadically along the shore during storm events, may fuel the *in situ* release of DOC with a C4 plant signature. This release of DOC determines the stable isotopic signature of DOC near the surface of the beach for as long as the seaweed deposit is present at the surface. Only three days after the

deposit event however, the isotopic imprint of seaweeds was diluted and δ^{13}C-DOC signatures reached more depleted values (Fig. 7L and Fig. 10). The DOC originating from seaweed degradation likely is rapidly flushed through the discharge zone by both the tidal pump and hydraulic head gradient. Based on the specific groundwater discharge measured in this site (~0.03 m^3/s; Chaillou et al., 2016), we calculated that around 8000 m^3 of beach groundwater were exported from the intertidal zone in only three days. The seaweed-derived DOC was probably transported by submarine groundwater discharge to coastal water and the isotopic signature was probably diluted by more depleted δ^{13}C signatures derived from the buried soil and aquifer matrix.

The δ^{13}C-DOC signal in beach groundwater seems to rapidly respond to OC inputs. We show a terrestrial imprint from the aquifer matrix resulting from the POC degradation from the old buried soil and sediment. However, the system can be sporadically affected by massive inputs of marine OC, which hides the terrestrial imprint. This transient marine imprint seems to be rapidly evacuated from the STE. The stable isotope signature of the DOC pool likely is an efficient tracer of these rapid changes in source material in the sandy beach STE.

1.6.3 Fe-OC interactions along the STE

Mineralogy, and more specifically mineral surface chemistry and area, largely controls the stabilization of OM in soils (Kaiser and Guggenberger, 2003) and sediment (Hedges and Keil, 1995). In a broad range of cohesive marine sediments, for example, Lalonde et al. (2012) have shown that on average 21.5 ± 8.6 % of total OC was closely associated to, or trapped, by reactive Fe-hydroxides through adsorption onto and/or co-precipitation with reactive Fe-hydroxides (Barber et al., 2017a). In the non-cohesive sediments of the STE, the average grain size decreases with depth, from ~300 μm in surficial Holocene sand to ~100 μm in Permian sandstone. Surprisingly, this decreasing trend is not paralleled by an increase in reactive Fe-hydroxides concentrations, which vary between about 1 and 6% of the total sediment dry weight, with slightly higher

concentrations in 2015A and 2015B compared to 2013 (Table S1). The amount of OC associated with Fe (percent of total OC) shown in Fig. 9 are thus not controlled by the amount of available reactive Fe-hydroxides, as also suggested by the very low OC:Fe molar ratios (<2.07, Table S1) calculated for both years. While the total OC concentrations in the organic-poor layers (Holocene sand and Permian sandstone) were low in both years, a higher fraction of this OC was stabilized through its association with reactive Fe-hydroxides in 2015 (5.8 to 56.3 % of total OC) compared to 2013 (non-detectable to 13.9% of total OC), with a maximum in the high tide mark core C2 (Fig. 9). The difference was not directly due to the generally higher, seaweed-derived, DOC concentrations measured in 2015 close to the beach surface (Fig. 7G-I) as the $\delta^{13}C$ signature of Fe-associated OC was typical of soils (about -27 ‰) rather than seaweeds (about -12 ‰). The absence of a seaweed signal in the Fe-associated POC fraction could be due to the fact that this large input of fresh seaweed-derived DOC enhanced microbial activity, which in turn resulted in mildly reducing conditions, thus limiting the trapping of this fresh material onto the solid phase. The resulting displacement of the oxic-anoxic transition zone then led to an enhancement in Fe-OC trapping when reducing groundwater enriched in dissolved ferrous iron was oxidized and dissolved Fe re-precipitated as reactive Fe-hydroxides in contact with oxygenated seawater. This newly precipitated reactive Fe-hydroxides probably acted as a "transient" barrier to the DOC pool that has the highest affinity with amorphous reactive Fe-oxides (Gregory and Duan, 2001; Linkhorst et al., 2017). The concomitant dissolution of Fe and DOC under anaerobic conditions and the subsequent precipitation of Fe-OC at the anoxic-oxic transition support the idea of a highly dynamic nature of such Fe curtain in response to fresh organic matter inputs.

The increase with depth in the relative proportion of total OC associated to reactive Fe-hydroxides measured in both years (Fig. 9) could be due in part to the downward increase in particle surface area, although the mineral grains in the three sedimentary units all belonged to the sandstone category (i.e., large particle size, low mineral surface reactivity). Other factors such as the local redox conditions, the bacterial degradation of non-Fe-stabilized OC, the molecular composition of the Fe-stabilized OC, and others

remaining to be identified, could have played a role but the challenge associated with the sampling of pore water corresponding exactly to the analyzed solid phase samples in non-cohesive sediments such as a sandy beach, the fact that the cores were not all sampled during the same year, and the highly dynamic nature of STE make the interpretation of the data extremely difficult. More work is needed to fully understand the mechanism(s) and types of chemical bonds that lead to the trapping of terrestrial OC through adsorption onto and/or co-precipitation within reactive Fe-oxides in this system.

The interactions between Fe and DOC are modulated by the local redox conditions and by the molecular composition and concentrations of OC (Riedel et al., 2013; Sholkovitz, 1976). The measured δ^{13}C-POC signatures shown in Fig. 9 indicate that the Fe-associated POC pool is of terrestrial origin regardless the sedimentary unit. Reactive Fe-oxides have a greater affinity for HMW compounds enriched in aromatic, carboxylic and hydroxyl moieties, such as altered lignin and polysaccharide compounds of terrestrial origin, compared to the more aliphatic-rich compounds characteristic of marine OC (Linkhorst et al., 2017; Riedel et al., 2012; Shields et al., 2016). Ferric iron in STE groundwater preferentially interacts with and traps terrestrial OC independently of the origin of the DOC in beach groundwater. The molecular fractionation of DOC along the STE and preferential trapping of terrestrial compounds and favor the *in situ* degradation and/or export of non-Fe-stabilized marine-derived molecules to coastal waters, explaining in part, along with the preferential photodegradation of aromatic-rich compounds (Lalonde et al., 2014b), the globally low concentrations of humic-like DOM observed in coastal embayments (Kim and Kim, 2017). The exact mechanism controlling these Fe-OC interactions (i.e., adsorption or coprecipitation of OC on mineral surface; Barber et al., 2017a) remains to be determined and further laboratory experiments are required to explore the role of the Fe curtain as a permanent or transient terrestrial carbon sink at the groundwater – seawater interface. Whether on a transient or long-term basis, this trapped iron-associated OC can also form a seeding template that eventually leads to the accumulation of even more OC as the beach system evolves, as suggested by Shields et al. (2016). In agreement with the idea of Linkhorst et al. (2017) however, we propose that STE

acts as transient sink for terrestrial OC at the land-sea interface and contributes to the regulation of the exports of marine vs. terrestrial carbon to coastal waters. This inorganic regulator may contribute to the "missing" terrestrial OC in the ocean (Bianchi, 2011; Hedges et al., 1997).
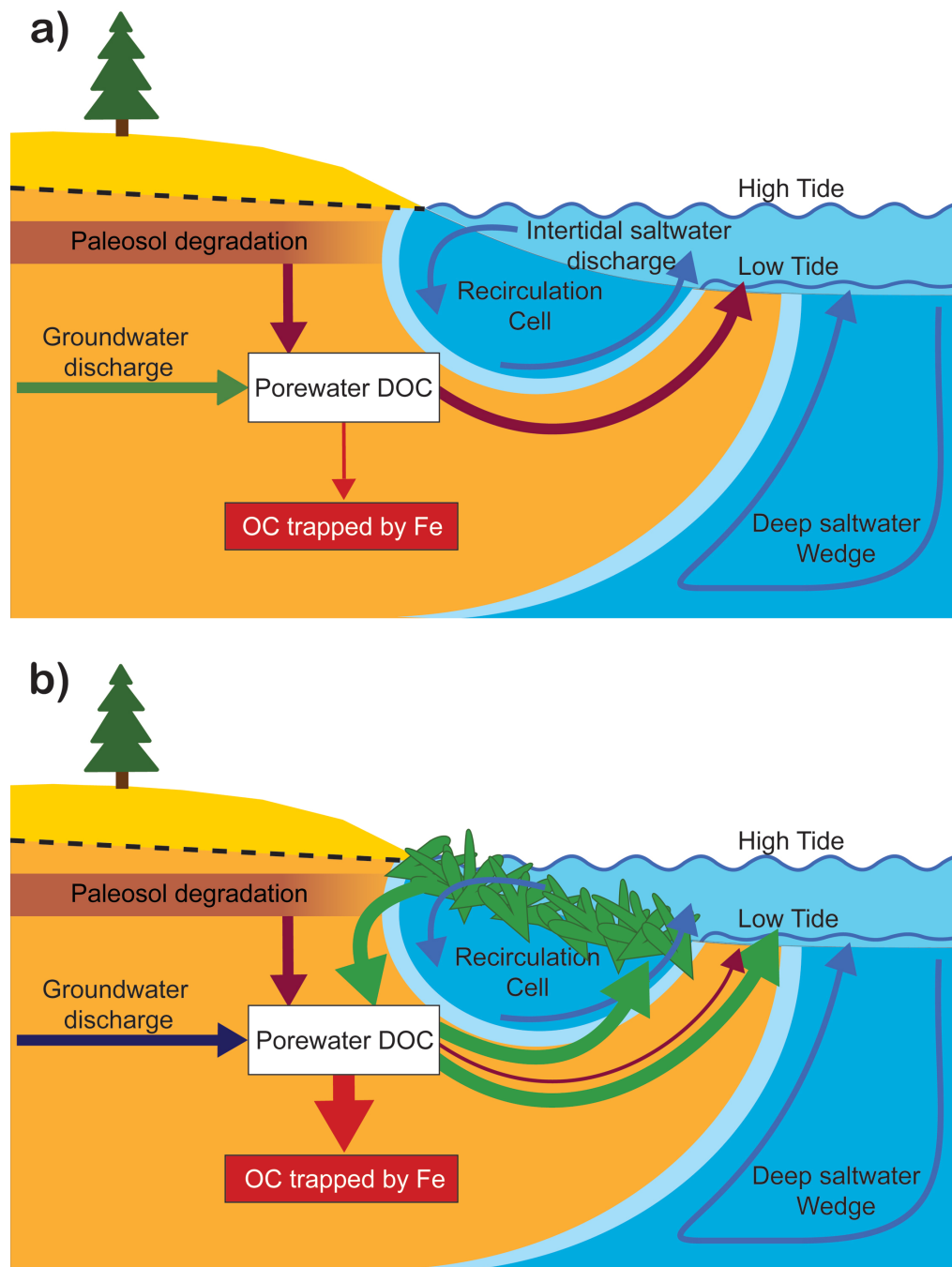
Figure 11 : Conceptual schematics of the Martinique Beach STE a) in 2013 where DOC was mainly originated from terrestrial POC degradation and b) in 2015 where fresh marine OM was accumulated at the sediment-water interface. See the text for details

1.7 CONCLUSION

The analysis of δ^{13}C signatures of DOC allowed discriminating between its sources in the studied STE. The OC sources appeared partly decoupled from the water masses of STE. The first one is terrestrial and originates in large parts from an old buried soil present in the aquifer matrix, which releases ^{13}C-depleted DOC as it is degraded. This DOC constitutes the baseline signal in the beach aquifer. The other major source of DOC detected in this system is the rapidly degrading seaweed accumulating on the beach during sporadic storm events. This intensity of this transient signal can be so high that it can mask the baseline δ^{13}C-DOC signal, as was the case in this study in 2015. These results further confirm that a high frequency sampling approach should be adopted to adequately decipher the cycling of OC in systems as dynamic as this one since individual sampling efforts reflect a snapshot view of the OC pools and fluxes.

Our study highlights that Fe-OC trapping occurs in the non-cohesive sediment of a sandy beach STE. Newly precipitated reactive Fe-hydroxides probably plays a pivotal role as a transient barrier to the DOC pool, and specifically on terrestrial-derived organic carbon. As in soil and in cohesive marine sediment, the molecular fractionation of DOC along the STE and preferential trapping of terrestrial compounds favors the *in situ* degradation and/or export of non-Fe-stabilized marine-derived molecules to coastal waters. These mechanisms contribute to the regulation of the exports of marine vs. terrestrial carbon to coastal waters. The exact role of the Fe curtain as a permanent or transient terrestrial carbon sink at the groundwater – seawater interface remains and should be explore in future studies. Whether on a transient or long-term basis, this trapped iron-associated OC can also form a seeding template that eventually leads to the accumulation of even more OC as the beach system evolves. Within the context of climate change and the inevitable sea level rise, the imprint of buried terrestrial horizons on carbon fluxes need to be understood in order to assess the consequences of landward migration of the coastline on the biogeochemistry of coastal ocean.

1.8 ACKNOWLEDGMENTS

CONCLUSION GÉNÉRALE

Ce mémoire a permis pour la première fois d'identifier les sources de COD dans un estuaire souterrain à l'aide du δ^{13}C-COD. Avec cet outil, il a été possible de montrer que le COD provenait généralement de la dégradation du COP, autant terrigène que marin, contrairement à ce qui était présenté dans la littérature où le COD est considéré comme issu de la phase particulaire d'origine marine uniquement (Anschutz et al., 2009; Charbonnier et al., 2013; Kim et al., 2012). La dégradation du paléosol dans la matrice de l'aquifère serait la source principale de COD en 2013 (Couturier et al. 2016) en raison de la similitude entre la signature du δ^{13}C-COD dans la plage et celle du δ^{13}C-COP du paléosol. Cependant, la signature de cette source pourrait être rapidement camouflée par des apports sporadiques de Zostère marine, lors d'événements comme des tempêtes. Ces apports d'algue sont rapidement dégradés, dilués et probablement évacués jusqu'à la zone de décharge. Les sources de COD ont donc changé rapidement au gré des différents apports de COP et le δ^{13}C-COD a permis de voir ce changement rapide. Ces résultats montrent qu'un échantillonnage fréquent doit être fait dans des systèmes dynamiques afin de bien comprendre l'origine du carbone.

Ensuite, en plus de la floculation entre le Fe dissous et le COD lors du changement de salinité, jusqu'à 60 % du CO peut être piégé par les oxydes de Fe réactifs dans les sédiments non cohésifs de la plage. Le Fe réactif nouvellement précipité joue un rôle de barrière pour le DOC, plus spécifiquement le DOC terrigène. En effet, lors du premier échantillonnage en 2013, le COD présent était majoritairement terrigène et $\leq$13,9 % de CO terrigène était piégé par les oxydes de Fe réactifs. De plus, le piégeage était plus important en profondeur en raison des grains plus fins (e.i. : grains avec une plus grande surface de contact pour accueillir les complexes de Fe et de CO). Lors du deuxième échantillonnage,

en 2015, l'apport de MO fraiche à la surface de la zone intertidale aurait eu pour effet d'augmenter la minéralisation de la MO. Cette minéralisation rapide aurait engendré une remontée vers la surface de la production de différents produits de la diagenèse précoce comme le Fe dissous. Le déplacement du front oxique-anoxique aurait augmenté le piégeage du CO par le Fe jusqu'à ~60 % lors de la réduction des eaux souterraines enrichies en Fe dissous a été oxydé. Ce nouveau Fe précipité au contact de l'eau de mer oxygénée en hydroxydes de Fe réactif aurait alors piégé du CO. Dans un système dynamique comme un ES d'une plage, les interactions entre le Fe et le COD sont affectées de façon importante par l'oscillation rédox, les sources *in situ* de CO ainsi que les apports sporadiques de CO (voir Fig. 11 dans chapitre 1). Ce piégeage favorise la dégradation *in situ* et l'exportation de molécules marines vers les eaux côtières.

Cette étude a aussi permis de montrer qu'il y a des interactions entre le Fe et le COD dans les ES. À notre connaissance, il s'agit de la première étude à quantifier, par l'analyse de la phase dissoute et de la phase particulaire, le processus de piégeage du CO par le Fe dans un ES. Cette étude est originale, car elle montre que le piégeage du CO peut même se produire dans les sédiments non cohésifs. Elle améliore également notre compréhension des SGD, des plages et des bilans de carbone.

LIMITES DU PROJET

Quelques questions restent encore en suspend et des études plus spécifiques devraient permettre de résoudre ces différentes limites. Tout d'abord, il y a 1) la variabilité spatio-temporelle des dépôts sporadiques d'algues. Étant donné qu'il n'y a que deux années d'échantillonnage (2013 et 2015), il n'est pas possible de dire à quelle fréquence arrivent les dépôts sporadiques d'algues. Un échantillonnage plus long, soit plusieurs fois pendant l'année et à différentes saisons, permettrait de voir si ce phénomène se produit régulièrement ou pas. Ensuite, 2) on ne connaît pas le temps de retour à l'état stationnaire du site d'étude après une accumulation d'algues. Afin de savoir combien de temps il faut à l'ES pour passer d'une signature marine à une signature terrigène, il faudrait aller sur le

terrain et faire plusieurs prélèvements sur plusieurs jours, au moins 1 ou 2 semaines, après un événement d'accumulation d'algues. Il serait donc possible de voir la transition de la signature marine à la signature terrigène. Une autre limite de cette étude est 3) qu' il n'est pas encore possible de confirmer si le mécanisme principal de piégeage du CO par les oxydes de Fe réactifs dans les sédiments est l'adsorption ou bien la coprécipitation malgré le fait que la quantité de CO piégé varie et suggère de l'adsorption du CO sur la matrice minérale. Il faudrait échantillonner des carottes de sédiments connexes à chacun des multipréleveurs d'eau afin d'associer directement les valeurs de la phase dissoute avec celles de la phase particulaire. Finalement, 4) la caractérisation des flux de carbone n'a pas été possible, donc on ne sait pas si le CO sort réellement de la plage d'étude et, s'il sort, qu'elle est la source de ce dernier. Une solution serait de mettre en place des chambres advectives afin de mesurer directement les flux d'eau et de CO qui sortent de la plage. De plus, avec ces chambres advectives, le COD qui sort de la plage pourrait être caractérisé pour en connaître l'origine et pour montrer si les ES peuvent être des sources de CO terrigène à l'océan côtier. Il serait alors intéressant de voir si l'hydrogéologie dans la plage d'étude affecte le piégeage du CO par les oxydes de Fe réactifs comme elle peut affecter le comportement des espèces dissoutes

PERSPECTIVES

À plus long terme, en raison de la hausse relative du niveau marin sur la côte Est de l'Amérique du Nord (Douglas, 1990; Gehrels et al., 2004, 2002), la plage de la Martinique et son paléosol représentent un modèle de système transgressif. Cette hausse relative du niveau marin pourrait avoir comme effet une augmentation de nombre de systèmes avec des paléosols en plus de modifier les écoulements des SGD et les apports de différents composés chimiques à l'océan côtier. Ces changements affectant les bilans de carbone en milieu côtier modifieraient les modèles sur l'export de CO terrigène à l'océan dans cette partie du monde. De nouveaux modèles pourraient permettre de voir si une augmentation de paléosol ainsi qu'une modification des écoulements affecteraient la biogéochimie des eaux côtières de la côte Est de l'Amérique du Nord. De plus, s'il est démontré que les

plages sont des sources de carbone terrigène, donc plus réfractaire, à l'océan côtier, la théorie du *Priming Effect* pourrait être plus étudiée en vue de la confirmer. Les SGD des plages méritent donc d'être plus considérés dans les apports de carbone vu leur importance dans la biogéochimie des milieux côtiers.

ANNEXE I : NITROGEN TRANSFORMATIONS ALONG A SHALLOW SUBTERRANEAN ESTUARY

Couturier, M., Tommi-Morin, G., Sirois, M., Rao, A., Nozais, C., Chaillou, G., 2017. *Nitrogen transformations along a shallow subterranean estuary*. Biogeosciences. 14. 3321–3336. doi:10.5194/bg-2016-535

Biogeosciences

Nitrogen transformations along a shallow subterranean estuary

Mathilde Couturier[1,2], **Gwendoline Tommi-Morin**[1,2], **Maude Sirois**[1,3], **Alexandra Rao**[3], **Christian Nozais**[2], **and Gwénaëlle Chaillou**[1,2]

[1]Canada Research Chair on the Geochemistry of Coastal Hydrogeosystems, BOREAS, group on Nordic System,
Département de Biologie, Chimie, Géographie, Université du Québec à Rimouski, Rimouski, G5L3A1, Canada
[2]Département de Biologie, Chimie, Géographie, Université du Québec à Rimouski, Rimouski, G5L3A1, Canada
[3]Institut des sciences de la mer de Rimouski, Université du Québec à Rimouski, Rimouski, Quebec, G5L 3A1, Canada

Correspondence to: Mathilde Couturier (mathilde.couturier@uqar.ca)

Abstract. The transformations of chemical constituents in subterranean estuaries (STEs) control the delivery of nutrient loads from coastal aquifers to the ocean. It is important to determine the processes and sources that alter nutrient concentrations at a local scale in order to estimate accurate regional and global nutrient fluxes via submarine groundwater discharge (SGD), particularly in boreal environments, where data are still very scarce. Here, the biogeochemical transformations of nitrogen (N) species were examined within the STE of a boreal microtidal sandy beach located in the Magdalen Islands (Quebec, Canada). This study revealed the vertical and horizontal distribution of nitrate (NO_3^-), nitrite (NO_2^-), ammonia (NH_4^+), dissolved organic nitrogen (DON) and total dissolved nitrogen (TDN) measured in beach groundwater during four spring seasons (June 2011, 2012, 2013 and 2015) when aquifer recharge was maximal after snowmelt. Inland groundwater supplied high concentrations of NO_x and DON to the STE, whereas inputs from seawater infiltration were very limited. Non-conservative behaviour was observed along the groundwater flow path, leading to low NO_x and high NH_4^+ concentrations in the discharge zone. The long transit time of groundwater within the beach ($\sim$ 166 days), coupled with oxygen-depleted conditions and high carbon concentrations, created a favourable environment for N transformations such as heterotrophic and autotrophic denitrification and ammonium production. Biogeochemical pathways led to a shift in nitrogen species along the flow path from NO_x-rich to NO_x-poor groundwater. An estimate of SGD fluxes of N was determined to account for biogeochemical transformations within the STE based on a N-species inventory and Darcy's flow. Fresh inland groundwater delivered 37 mol NO_x yr^{-1} per metre of shoreline and 63 mol DON m^{-1} yr^{-1} to the STE, and NH_4^+ input was negligible. Near the discharge zone, the potential export of N species was estimated around 140, 1.5 and 33 mol yr^{-1} per metre of shoreline for NH_4^+, NO_x and DON respectively. In contrast to the fresh inland groundwater, the N load of beach groundwater near the discharge zone was dominated by NH_4^+ and DON. Our study shows the importance of tidal sands in the biogeochemical transformation of the terrestrial N pool. This local export of bioavailable N probably supports benthic production and higher trophic levels leading to its rapid transformation in surface sediments and coastal waters.

1 Introduction

Land–ocean interfaces are critical transition zones that may affect the ecology and quality of coastal ecosystems (Schlacher and Connolly, 2009). Chemical constituents in submarine groundwater discharge (SGD) are now widely recognized to have a significant impact on coastal ecosystems (Knee and Jordan, 2013; McCoy and Corbett, 2009; Null et al., 2012; Slomp and Van Cappellen, 2004). SGD is conventionally defined as "any flow of water out across the seafloor without regards to its composition and its origin" (Burnett et al., 2006). Thus, before entering coastal waters, fresh groundwater travels through a shallow subterranean estuary (STE) (Moore, 1999), a region where mixing between fresh and marine groundwater promotes biogeochemical processes that can lead to rapid changes in nutrient concentrations and induce non-conservative input or re-

moval (Gonneea and Charette, 2014). The STE supports extensive chemical reactions near the discharge interface and is often assumed to be a non-steady-state system (Kroeger and Charette, 2008). Continental factors (e.g. local hydrogeology, recharge, precipitation) as well as marine factors (e.g. tidal and wave pumping, hydrography, and density) induce temporal and spatial variability in biogeochemical conditions (see Santos et al., 2012, and references therein). The mixing zone is subject to oscillating conditions, with rapid changes in oxygen saturation, redox potential and organic matter input controlled by tidal stage and amplitude, sea level and seasonal water table fluctuations (Abarca et al., 2013; Gonneea et al., 2013; Heiss and Michael, 2014; Robinson et al., 2014). These physical processes are likely to impact the distribution and biogeochemical reactivity of many dissolved constituents (Beck et al., 2007; Kroeger and Charette, 2008). In this context, the STE either can be a source of nutrients or act as a barrier and limit nutrient discharge to coastal environments. Assessing the role of the STE in nutrient transformations is crucial to better quantifying global chemical fluxes via SGD (Moore, 2010).

Rivers have long been considered the main conveyors of N to the ocean (Seitzinger et al., 2005, and references therein). Beusen et al. (2013) recently provided evidence that SGD also plays a major role in regional and global marine N cycles. N loads from SGD to nearshore ecosystems have been estimated to be $4 \, \mathrm{Tg \, N \, yr^{-1}}$ (Voss et al., 2013), and the role of SGD in coastal eutrophication has also been demonstrated (Valiela et al., 1990). These N loads may be an important factor in the development of harmful algal blooms in coastal waters (Anderson et al., 2008; Glibert et al., 2014). Fresh groundwater is often rich in nutrients and other materials from anthropogenic inputs due to coastal development (agriculture, urbanization) (Howarth and Marino, 2006; Null et al., 2012; Rocha et al., 2015), and models predict a 20 % increase in N loads from SGD within the next few decades due to coastal development (Beusen et al., 2013).

Estimates of nutrient loads from the SGD to the coastal ocean have often been based on nutrient concentrations in fresh groundwater, with the assumption that nutrient transport through the STE is conservative (Burnett et al., 2006). However, numerous studies have demonstrated that concentrations of dissolved N change throughout the STE because of biological and chemical reactions (Beck et al., 2007; Loveless and Oldham, 2010; Moore, 2010; Santos et al., 2009). Variations in oxygen and organic matter input along the hydraulic gradient lead to a combination of heterotrophic processes that can enhance or attenuate the export of N to the coastal ocean (Santoro, 2010). For example, in the Gulf of Mexico (Turkey Point, Florida), the STE acts as a source of ammonium because remineralization of marine organic matter throughout the STE provides nutrients to the SGD exported to the embayment (Santos et al., 2008). In Waquoit Bay (Cape Cod, Massachusetts), Kroeger and Charette (2008) demonstrated that ammonium accumu-

lates in the STE because remineralization of organic matter transported by marine and fresh groundwater outpaces nitrification. In contrast, based on the N attenuation observed in a shallow STE due to denitrification (Cockburn Sound, Australia), Loveless and Oldham (2010) calculated nitrate loads to coastal waters that were 1–2 times lower than previous estimates based on nutrient concentrations from fresh groundwater. As these studies show, ignoring non-conservative mixing can lead to an over- or underestimation of nutrient loads to coastal waters (Beck et al., 2007).

STEs are transient systems where steady state and thus the classical diagenetic sequence of redox reactions are rarely achieved (Sundby, 2006). In transient systems, diagenetic reactions reflect redox oscillations and environmental conditions far from steady state. Redox oscillations, with alternating oxic and anoxic conditions in sediments, allow coupled nitrification–denitrification to take place in the same location within the sediment (Aller, 1994). Alternative pathways of nitrate reduction, such as dissimilatory nitrate reduction to ammonium (DNRA) and Anammox, have also been reported in the STE (Erler et al., 2014; Kroeger and Charette, 2008; Rocha et al., 2009; Sáenz et al., 2012). Many of these processes transform dissolved inorganic nitrogen (DIN) and dissolved organic nitrogen (DON) along the groundwater flow path. DON is assumed to be from natural rather than anthropogenic sources and is often neglected (Hansell and Carlson, 2014). Nevertheless, DON concentrations can be high in SGD and should be considered (Kroeger et al., 2007; Santos et al., 2014).

Martinique Beach, located in the Magdalen Islands (Quebec, Canada) at the southern limit of the boreal climatic zone, is exposed to little or no external contamination. Site-specific studies in boreal and cold environments are still scarce, and climate and hydrology change rapidly in cold climates (Hinzman et al., 2005). Thus nutrient fluxes by SGD to the coastal ocean in boreal regions and their contribution at local and global scales remain to be elucidated. The objective of this 4-year study was to investigate the spatial and temporal variation of N species (inorganic and organic N) through a shallow boreal STE, from inland groundwater to coastal ocean. SGD fluxes of the different N species that are discharged to coastal waters by shallow groundwater at this specific-site were also estimated.

2 Materials and methods

2.1 Study area

Martinique Beach is located on the main island of the Magdalen Islands archipelago in the Gulf of St. Lawrence (Quebec, Canada; Fig. 1). The Martinique Beach system originates from a recent transgression sequence. Rapid rates of sea-level rise along the Atlantic coast of Canada over the middle to late Holocene buried the unconfined Permian sandstone aquifer, which is now covered by tidal sediment
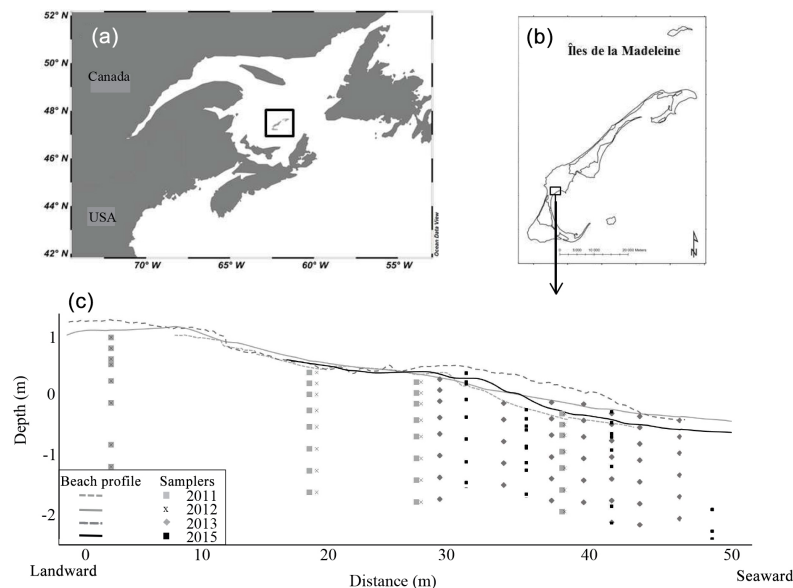
Figure 1. Position of the study site in the Magdalen Islands (Quebec, Canada) **(a, b)**. Beach profile of Martinique Beach in 2011, 2012, 2013 and 2015; beach profiles were determined using a DGPS; locations of sampling sites (2011–2013, 2015) along the sandy beach transect; depths are relative to mean sea level (i.e. 0 m is mean sea level) **(c)**.

(Gehrels, 1994; Scott et al., 1995a, b). The site experiences semi-diurnal tides with a mean range of 0.8 m and a maximum range of 1.7 m during spring tide. The archipelago has no rivers; thus the aquifer recharge is only from rain and snow, with the highest recharge during spring snowmelt. The mean yearly recharge is about 230 mm (Madelin'Eau, 2004). Because groundwater constitutes the only source of drinking water in the archipelago, the hydrogeology is well known, and the aquifer constantly monitored (Chaillou et al., 2012; Madelin'Eau, 2007, 2009, 2011). Since anthropogenic pressures like urbanization and agriculture are limited in the archipelago, the main sources of N contamination are from residential and recreational areas. Therefore, Martinique Beach is an ideal system in which to study N transformations in a boreal microtidal subterranean estuary.

The Martinique Beach STE acts as a shallow unconfined aquifer at the nearshore limit of the Permian aquifer; it releases both fresh and recirculated saline groundwater to the coastal embayment (Chaillou et al., 2016). It is a low-energy beach under a microtidal regime (Jackson et al., 2002; Masselink and Short, 1993). The upper centimetres (20 cm) of the beach consist of marine sands with a median particle size of 0.30 mm (silt content < 5 %), mainly composed of quartz (95 %). The hydraulic conductivity of this sedimentary unit

is about $11.40 \pm 4.40 \, \mathrm{m \, d^{-1}}$ (Chaillou et al., 2016). Lower hydraulic conductivity was measured in the underlying sandstone aquifer ($K \sim 1.80 \, \mathrm{m \, d^{-1}}$; Madelin'Eau, 2007), which is composed of fine silicate and aluminosilicate sands with Fe-coated silicate grains (Chaillou et al., 2014). These two layers are organic-poor (total organic carbon ([TOC]) < 0.20 % weight percent (wt) and total nitrogen [TN] < 0.10 wt %; Chaillou et al., 2014). In the landward part of the beach, however, an old-age soil horizon dated to ~ 900 BP (^{14}C dating; Juneau, 2012) occurs a few centimetres below the beach surface. This horizon is carbon-rich ([TOC] > 20 wt %) but has a low nitrogen content ([TN] < 0.50 wt %; Chaillou et al., 2014).

In the Magdalen Islands, the snowmelt leads to a high water table from April to June in the Permian sandstone aquifer (Madelin'Eau, 2004) and in the adjacent beach aquifer (Chaillou et al., 2016). Under these hydrologic conditions, the saline circulation cell and its associated mixing zone are spatially limited, and the inland hydraulic gradient is the main control of total SGD (Heiss and Michael, 2014; Robinson et al., 2007a). Based on the stable isotopes of water along the STE, Chaillou et al. (2017) confirmed the contribution of only two water endmembers (i.e. fresh meteoric groundwater and seawater) and the absence of additional sep-

tic tank seepages. They also highlighted the high contribution of fresh groundwater and the limited infiltration of seawater in shallow beach groundwater. The regional seaward fresh groundwater flow (Q_{inland}) of about 0.021 m^3 s^{-1} was estimated based on mean and multi-annual regional water table levels from municipal wells (Chaillou et al., 2016). Q_{inland} is then the theoretical inland groundwater export from the Permian sandstone aquifer to Martinique Beach. At Martinique Beach, fresh groundwater flow was also evaluated based on a mean hydraulic gradient through the 50 m length of the beach. This specific flow (Q_{beach}) was 0.029 m^3 s^{-1}, suggesting that fresh inland groundwater flux contributes to at least 70 % of the water flow discharging to the coastal waters.

2.2 Groundwater sampling

Sampling was carried out in June 2011, 2012, 2013 and 2015 along a 50 m cross-shore transect. In 2011 and 2012, groundwater samples were collected in the landward part of the STE. In 2013 and 2015, we focused on the intertidal and discharge zone, where fresh meteoric groundwater comes in contact with recirculated seawater. Groundwater extraction was done using multi-level samplers in 2.5 m long PVC pipes (Fig. 1), similar to those described by Martin et al. (2003). Groundwater was collected at 10, 30, 50, 80, 100, 150, 190 and 230 cm below the beach surface. Samplers were re-inserted at the same locations each year using differential GPS (DGPS) coordinates. To allow sediments around the samplers to reach equilibrium, sampling started 2 days after their insertion. Groundwater was sampled using a peristaltic pump, and physico-chemical parameters (pH, temperature, oxygen, salinity) were measured directly using an online flow cell with a calibrated multi-parameter probe (600QS, YSI Inc.). Oxygen measurements are not available for 2015, due to sensor malfunction. After stabilization of physico-chemical parameters, all groundwater samples were filtered through a 0.2 µm polypropylene capsule filter. Samples for nutrient analyses (NH$_4^+$, NO$_3^-$ and NO$_2^-$) were stored in acid-washed polyethylene tubes that were rapidly frozen for later analysis; samples for total dissolved iron were stored at 4 °C in 50 mL acid-washed polyethylene tubes and acidified with 50 µL of 10 % HNO$_3$; and total dissolved nitrogen (TDN) samples were stored in baked 7 mL vials and acidified with 25 µL of high-purity 10 % HCl. TDN measurements were only performed in 2012. Groundwater endmember samples were collected in the manner described above from four private and municipal wells (two or three replicates per well) located 50 to 2000 m landward of the most inland sampler in the sandstone aquifer. Seawater endmember samples (N = 6) were collected about 50 cm above the seabed using a submersible pump at about 900 m offshore in Martinique Bay.

2.3 Chemical analyses

NH$_4^+$ samples were measured by flow injection gas exchange–conductivity analysis based on the method described by Hall and Aller (1992). The precision was ±5 % with a detection limit of 0.1 µmol L^{-1}. NO$_3^-$ and NO$_2^-$, referred to as NO$_x$, were analysed by the colorimetric method developed by Schnetger and Lehners (2014) and measured with a powerwave XS2 microplate spectrophotometer. The precision was 2 %, and the limit of detection was 0.4 µmol L^{-1}. DIN was calculated as the sum of NH$_4^+$, NO$_3^-$ and NO$_2^-$. TDN was analysed in 2012 by high-temperature combustion (HTC) using a total organic carbon analyser (TOC-vpn, Shimadzu) with a TNM-1 module, and a precision of 2 %. DON was calculated as the difference between TDN and DIN (i.e. DON = TDN − [NH$_4^+$ + NO$_x$]). DON calculations were only possible in 2012 based on TDN measurements. The DON measurement is still problematic since it combines the analytical errors and uncertainties of the three analyses. Nevertheless, there is currently no single accepted method for the measurement of DON (Hansell and Carlson, 2014). Here we estimated the precision to be around 10 %. Dissolved iron was analysed using a 5100PC flame atomic absorption spectrophotometer (5100ZL Zeeman Furnace). Analytical uncertainties were < 5 %.

3 Results

3.1 Distribution of salinity and oxygen saturation

Previous studies have already discussed the distribution of physico-chemical parameters along the groundwater flow path at Martinique Beach based on 2012 and 2013 data (Chaillou et al., 2014, 2016; Couturier et al., 2016). Here, we will briefly present an overview of the salinity and redox conditions in the STE (Fig. 2).

In 2011 and 2012, the landward part of the STE was mostly characterized by suboxic freshwater (dissolved oxygen ([DO]) < 20 %, salinity < 10). The discharge zone with the saline circulation cell was salty and oxygenated ([DO] > 60 %, salinity > 20). A sharp salinity gradient occurred below the saline circulation cell, with salinity falling to 0 within the upper 50 cm of the sediment. In 2013 and 2015, the focus on the intertidal zone confirmed the occurrence of a small saline circulation cell with sharp gradients of salinity and DO along its perimeter. Fresh and suboxic water were recurrent at 60 cm below the surface in the discharge zone of the beach. A mixing zone composed of brackish water (salinity comprised between 7 and 15) occurred along the perimeter of the saline circulation cell resulting from a mixture of fresh and saline groundwater. This mixing zone appeared to be depleted in DO ([DO] < 20 %). The rest of the system was composed of fresh groundwater. In 2013, some measurements showing high DO concentrations in the deepest samples may indicate atmospheric contamination during sampling.
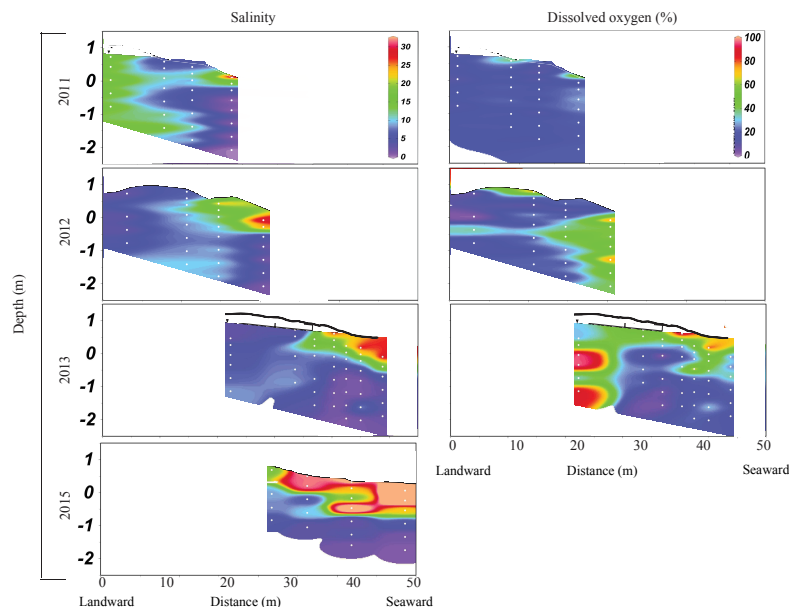
Figure 2. Cross-sections of the transect (see Fig. 1c) showing the beach profile and mean distribution of salinity and dissolved oxygen in 2011, 2012, 2013 and 2015 (no dissolved oxygen data are available for 2015). Depths are relative to mean sea level (i.e. 0 m is mean sea level). Contour lines were derived by spatial interpolation (kriging method) of data points; the interpolation model reproduced the empirical data set with a 97 % confidence level. White dots represent the depths at which samples were collected using multi-level samplers. The dashed line represents the water table level.

Table 1. Mean concentrations ($\mu mol\,L^{-1}$) of nitrogen species in the groundwater and seawater endmembers as well as ranges in beach groundwater measured during the study. NO_x and NH_4^+ were measured in 2011, 2012, 2013 and 2015; TDN and DON were measured in 2012.

	Inland wells	Seawater	Beach groundwater
2011–2015	N = 10	N = 6	N = 245
NO_x	65.5 ± 26.7	0.5 ± 0.5	$0–26.1$
NH_4^+	0.1 ± 0.3	0.8 ± 0.5	$0.1–1056.2$
2012	N = 2	N = 3	N = 54
DON	110.9 ± 3.4	7.3 ± 0.8	$0–1481.8$
TDN	203 ± 4.5	9.1 ± 1.1	$7.4–1704.4$

3.2 Nutrient distribution from inland groundwater to beach groundwater

The concentrations of NO_x ($\Sigma NO_3^- + NO_2^-$) measured in four inland wells ranged from 14 to 94 $\mu mol\,L^{-1}$ with a mean concentration of 65.5 ± 26.7 $\mu mol\,L^{-1}$ (Table 1). In the nearshore well, located 50 m from the shoreline, the concentration reached 20 $\mu mol\,L^{-1}$. NH_4^+ concentrations were low, with concentrations varying between 0 and 1 $\mu mol\,L^{-1}$. The fresh inland groundwater endmember was rich in TDN as measured in wells in 2012, with DON making up 53 % of the TDN (i.e. DON $= 110.9 \pm 3.4$ $\mu mol\,L^{-1}$). Compared to fresh inland groundwater, the seawater samples were largely depleted in NO_x with a mean concentration of 0.5 ± 0.5 $\mu mol\,L^{-1}$ (N = 6, Table 1). NH_4^+ concentrations were also low with 0.8 ± 0.5 $\mu mol\,L^{-1}$. As in fresh inland groundwater, TDN in seawater was largely dominated by DON that represented ~ 80 % of the N budget with a mean concentration of 7.3 ± 0.8 $\mu mol\,L^{-1}$. Overall, TDN concentrations in the seawater endmember were 20 times lower than in the groundwater endmember.

Within the STE, NO_x concentrations were low (0–26 $\mu mol\,L^{-1}$ with a mean concentration of 1.9 $\mu mol\,L^{-1}$). These concentrations were 5 times lower than those measured within the fresh groundwater endmember (Table 1, Fig. 3a). However, some samples collected in the deep and fresh part of the STE reached concentrations greater than
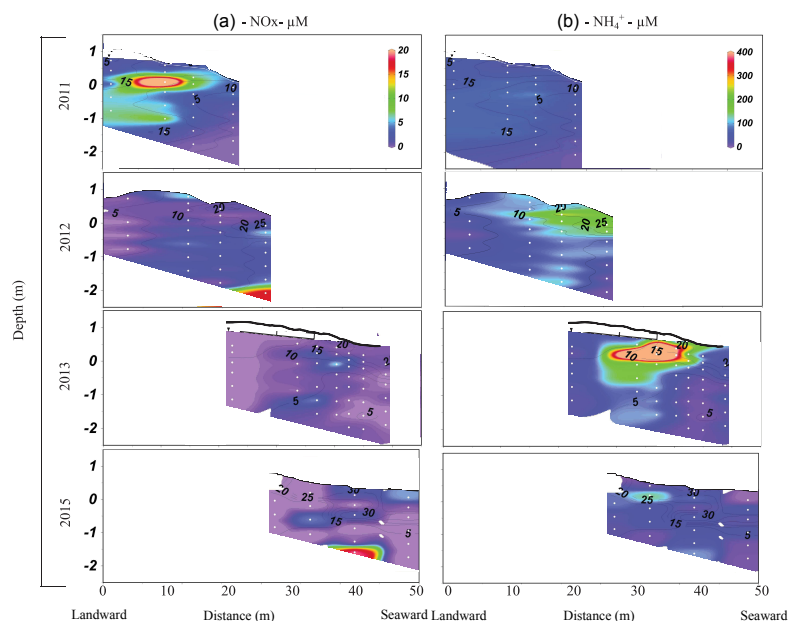
Figure 3. Cross-sections of the transect (see Fig. 1c) showing the beach profile and distributions of **(a)** nitrate + nitrite (NO_x) and **(b)** ammonium in $\mu mol\,L^{-1}$ in 2011, 2012, 2013 and 2015. Black contour lines refer to salinity. Depths are relative to mean sea level (i.e. 0 m is mean sea level). All contour lines were derived by spatial interpolation (kriging method) of data points. White dots represent the depths at which samples were collected using multi-level samplers.

$20\,\mu mol\,L^{-1}$ (Fig. 3a). Such hot spots of NO_x concentrations were also recorded in 2011 (up to $15.2\,\mu mol\,L^{-1}$), 2012 (up to $26.1\,\mu mol\,L^{-1}$) and 2015 (up to $19.5\,\mu mol\,L^{-1}$). In contrast to NO_x, NH_4^+ concentrations were high in the STE, with concentrations ranging from $\sim 20\,\mu mol\,L^{-1}$ to $>500\,\mu mol\,L^{-1}$ (Fig. 3b), and up to $1056\,\mu mol\,L^{-1}$ (2013, Fig. 3b). Ammonium (NH_4^+) concentrations measured in the STE were 1 to 1000 times higher than endmember values (Table 1, Fig. 3b). In 2013, an area of high concentrations was observed in the mixing zone, in front of the saline circulation cell, where NH_4^+ concentrations reached values greater than $400\,\mu mol\,L^{-1}$ (Fig. 3b). NH_4^+ concentrations were still high in the saline circulation cell (e.g. 84–$92\,\mu mol\,L^{-1}$), and these were also high compared to the overlying seawater endmember (Table 1). NH_4^+ concentrations decreased sharply with depth in the mixing zone. For example, in June 2013 maximum NH_4^+ concentrations were around $400\,\mu mol\,L^{-1}$ at 30 cm below the beach surface of the intertidal zone and decreased to $50\,\mu mol\,L^{-1}$ at 230 cm (Fig. 3b). NH_4^+ was the main TDN species in the STE (on average NH_4^+ concentrations accounted for 60 % of TDN in all samples). Thus, in 2012, the TDN distribution was quite similar to the NH_4^+

distribution (Fig. 4), with high values in the mixing zone. TDN decreased sharply below the saline circulation cell and the mixing zone; values ranged from 50 to $100\,\mu mol\,L^{-1}$ and dropped below detection below the saline circulation cell. DON represented 31 % of the TDN in beach groundwater, and the highest concentrations were observed in the mixing zone ($>200\,\mu mol\,L^{-1}$, Fig. 4). DON levels decreased below the saline circulation cell, with concentrations close to 0.

N species showed different distributions relative to groundwater salinity and DO saturation along the STE (Fig. 5). N species were characterized by non-conservative behaviour relative to the theoretical two-endmember mixing between seawater and fresh inland groundwater. NO_x declined from $60\,\mu mol\,L^{-1}$ in fresh inland groundwater to concentrations below detection in brackish and saline groundwater (Fig. 5a). The highest concentrations of NO_x were encountered when DO saturation was below 60 %. While dissolved NO_x showed removal in the flow path, NH_4^+ exhibited excess concentrations relative to conservative mixing between the two endmembers (Fig. 5b). NH_4^+ concentrations clearly showed strong production along the salinity gradient of the STE. The highest concentrations of NH_4^+ oc-

M. Couturier et al.: Nitrogen transformations along a shallow subterranean estuary 3327
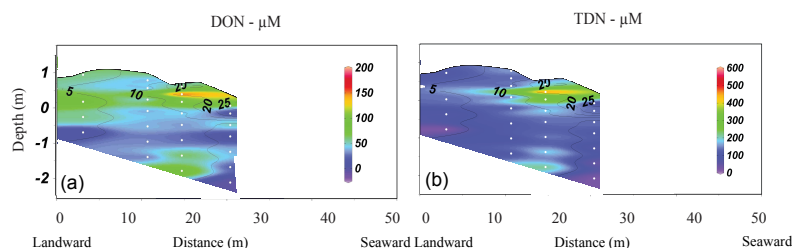
Figure 4. Cross-sections of the transect (see Fig. 1c) showing the topography and distributions of DON and TDN in µmol L^{-1} in 2012. Black contour lines refer to salinity. Depths are relative to mean sea level (i.e. 0 m is mean sea level). All contour lines were derived by spatial interpolation (kriging method) of data points. White dots represent the depths at which samples were collected using multi-level samplers.
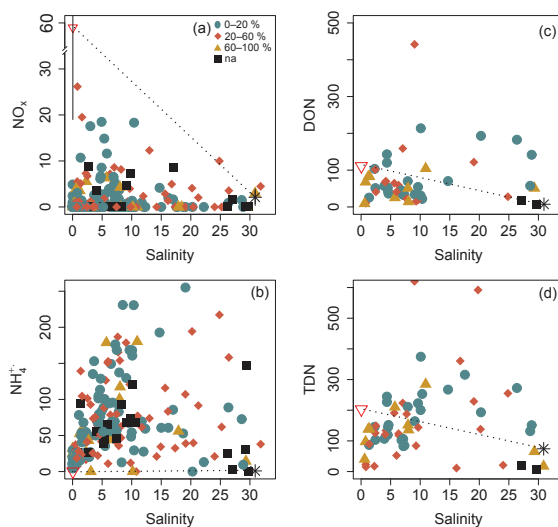
Figure 5. Distribution of NO$_x$ and NH$_4^+$ groundwater concentration in µmol L^{-1} collected in 2011, 2012, 2013 and 2015 **(a, b)** and DON and TDN in 2012 **(c, d)** within the STE relative to salinity grouped for different DO saturation from 0 to 20, 20 to 60 and 60 to 100 %. Extra points are not included to allow for better visibility. Black dots were used when no data on DO saturation were available. Red triangles are mean groundwater endmember values, and black squares are mean seawater endmember values. Standard deviations are black lines associated with endmembers. Dashed lines represent the theoretical mixing line between groundwater and seawater endmembers.

curred mainly under suboxic conditions ([DO] < 20 %) and decreased significantly with increased DO (p value < 0.05). Both NH$_4^+$ and NO$_x$ were observed in 81 of 245 samples (∼ 33 % of the data set). These samples were mainly located just below the saline circulation cell and the associated mixing zone, where oxygen-depleted conditions prevailed ([DO] < 20 %). In contrast to the behaviour of NO$_x$ and NH$_4^+$, TDN and DON exhibited a distinct trend along

the salinity gradient: (i) they fell below the theoretical mixing line in fresh and brackish waters (salinity 0–10), and this removal occurred in suboxic–anoxic conditions, and (ii) their concentrations increased above the theoretical mixing line in saline waters (salinity > 10). There was no significant relationship with DO.

Total dissolved iron concentrations were high in the STE and ranged from 1 to 2700 µmol L^{-1} with a mean concen-
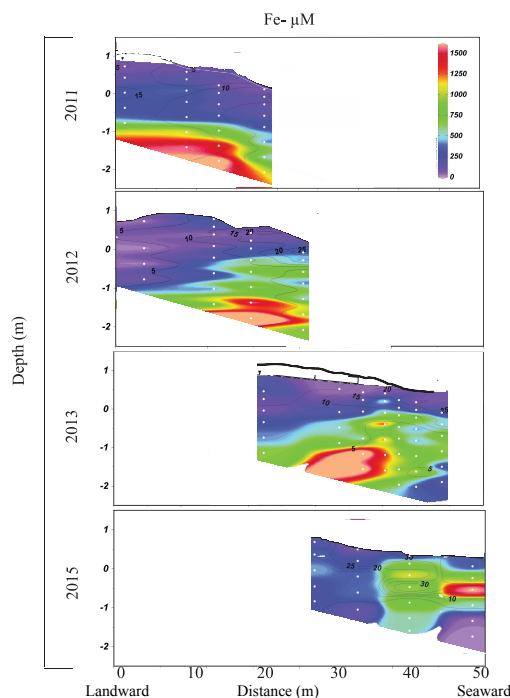
Figure 6. Cross-sections of the transect (see Fig. 1c) showing the topography and distributions of dissolved iron in μmol L^{-1} in 2011, 2012, 2013 and 2015. White contour lines refer to salinity. Depths are relative to mean sea level (i.e. 0 m is mean sea level). All contour lines were derived by spatial interpolation (kriging method) of data points. White dots represent the depths at which samples were collected using multi-level samplers.

tration of 520 μmol L^{-1} (Fig. 6). Concentrations increased sharply with depth and below the saline circulation cell. Concentrations of dissolved iron in the upper metre of the STE and in the saline circulation cell were lower, but still high (from 1 to 100 μmol L^{-1}) compared to the overlaying water.

4 Discussion

4.1 Biogeochemical controls of DIN concentrations along the groundwater flow path

The non-conservative behaviour of DIN along the groundwater flow path influences the nutrient concentration in discharging groundwater, while at the same time making it difficult to estimate the flux of groundwater-derived DIN to the coastal ocean (Johannes, 1980; Moore, 2010; Valiela et al., 1990). The calculation of chemical fluxes using samples from inland wells may result in significant errors in estimated chemical fluxes. Processes occurring in the STE must

be elucidated to improve our understanding of the role of the STE in altering groundwater-derived N. The DIN pool changed from NO_x-rich groundwater in the aquifer to NH_4^+-rich groundwater in the STE. In our study, NO_x represented 99 % of the DIN pool in the fresh inland groundwater end-member but only 37 % in the seawater endmember. In the next section, the potential biogeochemical mechanisms controlling the N pool along the flow path are explored.

4.1.1 Nitrate loss along the STE

NO_x concentrations were low within the STE in contrast to the high concentrations measured in fresh inland groundwater. There was strong attenuation in NO_x, with mean concentrations of 60 μmol L^{-1} in inland wells ($\sim$ 500 to 1500 m from the shoreline), dropping to $\sim$ 20 μmol L^{-1} in the nearshore well (50 m from the shoreline) and to 2 μmol L^{-1} in the STE, near the discharge zone. Such attenuation of NO_x is common in groundwater (Rivett et al.,

2008), and denitrification is generally recognized as the most significant mass removal process along the flow path (Korom, 1992). Denitrification is central to the nitrogen cycle in the subsurface groundwater environment. It involves the reduction of NO_x to N_2 gas via a chain of microbial reduction reactions.

As oxygen-depleted conditions and high dissolved organic carbon (DOC) concentrations are encountered along the STE (Couturier et al., 2016), denitrification may be one of the processes driving rapid groundwater-borne NO_x loss. The stoichiometry of nitrate reduction and the oxidation of organic matter by denitrification, given by Jørgensen et al. (2014), are as follows:

$$5CH_2O + 4NO_3^- + 4H^+ = 2N_2 + 5CO_2 + 7H_2O. \qquad (R1)$$
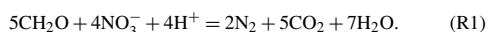
According to this stoichiometry, the mean concentration of DOC observed in the STE (i.e. $1940\,\mu mol\,C\,L^{-1}$; Couturier et al., 2016) could be used to reduce $1550\,\mu mol\,L^{-1}$ of nitrate to dinitrogen by denitrification. With concentrations of NO_x around $20\,\mu mol\,L^{-1}$ in the nearshore well, this means that all groundwater-borne NO_3^- may conceivably be reduced by DOC. However, even if the concentration of DOC in groundwater is high, Couturier et al. (2016) showed that dissolved organic matter (DOM) had a strong terrestrial signature along the STE at Martinique Beach. This OC was characterized by a high-molecular-weight and was enriched in lignin-derived compounds. In an alluvial aquifer, Baker and Vervier (2004) confirmed that the rate of denitrification was best predicted by the concentration of low-molecular-weight organic acids compared to high-molecular-weight compounds. In an unconfined sandy aquifer, Postma et al. (1991) reported that nitrate reduction was minimal when OC was present as lignin and lignite fragments (i.e. as high-molecular-weight compounds). Thus, the terrestrial DOC present in the Martinique Beach STE may not promote high rates of heterotrophic denitrification at the study site.

Nitrate reduction can be supported, however, by electron donors other than organic matter such as Fe^{2+} (Aller, 1994; Postma, 1990). There is evidence that groundwater containing Fe^{2+} contains little or no nitrate (Korom, 1992). The presence of reduced iron is assumed to facilitate the occurrence of denitrification according to Reactions 2 and 3:

$$5Fe^{2+} + NO_3^- + 12H_2O = Fe(OH)_3 + \frac{1}{2}N_2 + 9H^+, \qquad (R2)$$

$$10Fe^{2+} + 2NO_3^- + 14H_2O = 10FeOOH + N_2 + 18H^+ \qquad (R3)$$

High DOC concentrations (Couturier et al., 2016) support the reductive dissolution of Fe oxyhydroxides and lead to total dissolved iron concentrations as high as 1000–$1600\,\mu mol\,L^{-1}$, with concentrations reaching $2700\,\mu mol\,L^{-1}$ in deep groundwater below the saline circulation cell (Fig. 6). Thus Fe^{2+} can act as an electron donor and may have induced a loss of nitrates along the flow path. This autotrophic denitrification is most efficient in aquifers with low nitrate input

(Postma et al., 1991) and in margin sediments (Anschutz et al., 2002; Chaillou et al., 2007; Hulth et al., 1999; Hyacinthe et al., 2001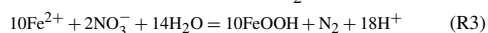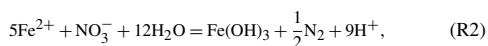). The stoichiometry of Reactions 2 and 3 shows that $1\,mol\,Fe^{2+}$ can reduce $0.2\,mol\,NO_3^-$. Based on the range of Fe^{2+} concentrations measured along the transect, this process is capable of completely reducing groundwater-borne NO_x.

With a maximum groundwater flow rate of $0.029\,m^3\,s^{-1}$ in beach groundwater (Chaillou et al., 2016), the groundwater transit time through the STE ($\sim 50\,m$) is about 166 days, which is long enough to support denitrification reactions and subsequent N transformations. Hot spots of NO_x concentrations (e.g. $7.5\,\mu mol\,L^{-1}$ at 50 cm depth with $[DO] < 10\,\%$ in 2013, $15.2\,\mu mol\,L^{-1}$ at 80 cm depth with $[DO] < 30\,\%$ in 2012 and 2015; Fig. 3a) were likely the result of local and sporadic production rather than traces of groundwater-borne NO_x. The downward infiltration of oxygenated seawater by tides could be large enough to oxidize NH_4^+ and produce NO_3^- along the saline circulation cell. These concentrations of NO_3^- remained low ($< 6\,\mu mol\,L^{-1}$) in the STE probably because of the multiple electron donors that can be used to reduce NO_3^- to N_2 under anoxic conditions (i.e. DOC, Fe^{2+}, NH_4^+, H_2S and FeS).

4.1.2 Ammonium production along the STE

Mineralization of organic matter is likely the most important source of NH_4^+ in the Martinique Beach STE. DON measurements in 2012 were high (0–$1481\,\mu mol\,L^{-1}$), with a mean value of $80\,\mu mol\,L^{-1}$. DON is a complex mixture of primarily uncharacterized compounds, of which 10 to 70 % are estimated to be bioavailable (Seitzinger et al., 2002). DON bioavailability is often reported to be dependent on the nature of compounds (Sipler and Bronk, 2014). In the beach groundwater, DON represented 39 % of the TDN, so its mineralization by heterotrophic microorganisms could be responsible for part of the NH_4^+ production in the STE (Kroeger et al., 2006). Ammonium production is mainly located upstream of the saline circulation cell (Fig. 3b) and is linked to the presence of high DON concentrations as observed in June 2012 (Fig. 4). Because ammonification is highly dependent on the bioavailability of DON, it is difficult to estimate what fraction of NH_4^+ could be derived from DON mineralization. Based on the estimate that 10 to 70 % of DON is bioavailable as proposed by Seitzinger et al. (2002), mineralization of DON could lead to the production of 8 to $56\,\mu mol\,L^{-1}$ of NH_4^+, which represents between 2 and 10 % of the NH_4^+ concentration observed in beach groundwater.

In coastal sediments, where sulfate is not limiting, sulfate reduction produces NH_4^+ according to the following reaction:

$$53SO_4^{2-} + (CH_2O)_{106}(NH_3)_{16}(H_3PO_4) = 39CO_2$$
$$+ 67HCO_3^- + 16NH_4^+ + 53HS^- + 39H_2O + HPO_4^{2-} \qquad (R4)$$
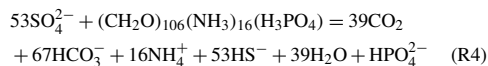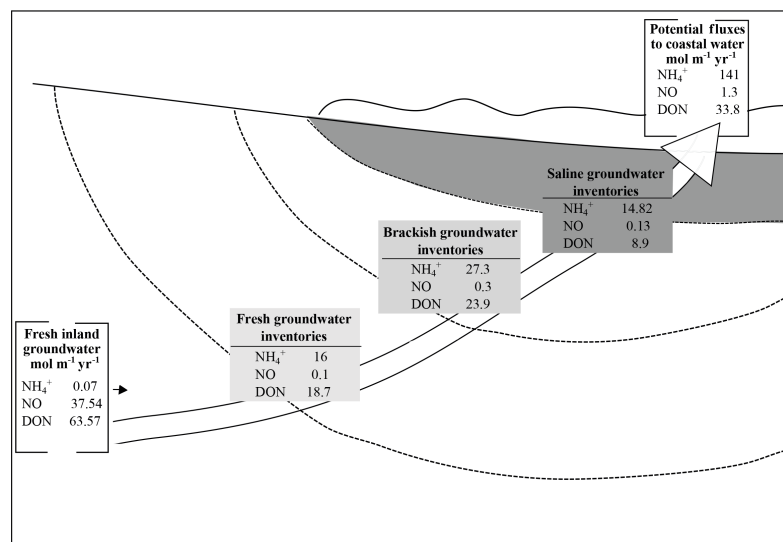
Figure 7. Schematic representation of (1) N inventories in fresh, brackish and saline beach groundwater (boxes from light grey to dark grey; dashed lines represent the schematic salinity separation) and of (2) fresh inland groundwater fluxes and potential exported fluxes to coastal water (white boxes). White arrow schematizes the groundwater flow path from the inland groundwater to the seepage face. The increase in TDN along the groundwater flow path is attributed to release of N from particulate organic matter of terrestrial origin.

NH_4^+ was observed in samples with salinity > 4, with the highest concentrations ($\sim 1.25\,\mathrm{mmol\,L^{-1}}$) at salinity around 15. At salinity 15, we estimate a SO_4^{2-} concentration of $12\,\mathrm{mmol\,L^{-1}}$ in beach surface groundwater, which is sufficient to produce $3.6\,\mathrm{mmol\,L^{-1}}$ NH_4^+ by sulfate reduction. This reaction could therefore explain the remainder of NH_4^+ production in beach groundwater.

The breakdown of macro-algal deposits derived from wave and tidal action in sediments can also increase N input to beach groundwater (Kelaher and Levinton, 2003; Rossi et al., 2011) and can potentially add NH_4^+. At Martinique Beach, algal deposits were not specifically measured but were often observed after storm events. In addition, external contamination from wastewater or sceptic tank seepages cannot be completely excluded. Nevertheless, the absence of traces of NH_4^+ contamination in the landward part of the beach and the stable isotopes of water reported by Chaillou et al. (2017) do not support an anthropogenic NH_4^+ input.

4.2 Nutrient transport along the flow path

The non-conservative behaviour of nutrients within the STE makes it difficult to estimate the export of nutrients to the coastal ocean. As pointed out in the review by Moore (2010), robust measurements of nutrient fluxes are needed on a site-specific scale to obtain accurate regional and global estimates. In non-conservative systems, however, the determination of appropriate nutrient endmember concentrations for flux calculations is not straightforward. Beck et al. (2007) previously highlighted the need to closely scrutinize the biogeochemical processes in the STE to refine nutrient export fluxes to coastal areas. Here, inorganic and organic N inventories were estimated along the groundwater flow path based on salinity. Then the potential nitrogen fluxes out of the STE were estimated and compared to the fresh inland groundwater-borne nutrient fluxes. Fluxes and inventories of the different N species along the groundwater flow path are summarized in Fig. 7.

4.2.1 Nitrogen inventories

Nutrient inventories were calculated by integrating nutrient concentrations at sampling locations according to salinity and multiplying by the sediment porosity (i.e. 0.25; Chaillou et al., 2012). Salinity was used to delimit zones to calculate N inventories along the flow path in deep fresh groundwater with low salinity ($S < 5$; N $= 57$); in the brackish beach groundwater ($5 < S < 15$; N $= 19$) that runs parallel to the surficial saline circulation cell; and, finally, in saline groundwa-

Table 2. Nutrient inventories estimated along the STE. Inventories were calculated in fresh, brackish and saline beach groundwater; the 2013 data set was used. For dissolved organic nitrogen, concentrations measured in 2012 were used.

Beach groundwater	N	Inventories [$\mu mol\,m^{-2}$]				
		NH_4^+	NO_3^-	DIN	DON[a]	TDN[a]
Freshwater ($S < 5$)	57	16	0.1	16.1	18.7	34.8
Brackish water ($5 < S < 15$)	19	27.3	0.3	27.6	23.9	51.5
Saline water ($S > 15$)	15	14.8	0.1	15	8.9	24

[a] Calculated on 2012 sampling.

ter ($S > 15$; N = 15). Inorganic and organic nitrogen inventories are presented in Table 2.

In the inland groundwater wells, fresh groundwater was rich in DON (Table 1). DIN represented only 33 % of the TDN, with NO_x making up 95 % of the inorganic pool (Table 1). In the fresh beach groundwater ($S < 5$), nutrient inventories showed that DON was still the main N species with an inventory of 18.7 $\mu mol\,m^{-2}$ (Table 2), which represented more than 50 % of the TDN pool. In DIN, a shift from NO_x to NH_4^+ occurred from the inland groundwater to deep fresh beach groundwater: NO_x became a negligible fraction (NO_x inventory $< 0.5\,\mu mol\,m^{-2}$), whereas NH_4^+ was the main inorganic fraction, representing 46, 53 and 61% of the TDN in fresh, brackish and saline beach groundwater respectively.

NH_4^+ was clearly produced along the groundwater flow path through the STE. In brackish groundwater, a strong production of TDN was observed: DIN, NH_4^+ and DON increased by 169, 168 and 127 % respectively (Fig. 7). Based on the previous work of Couturier et al. (2016), the source of nitrogen released in the STE is thought to be mineralization of terrestrial rather than marine organic matter. This strong in situ TDN production in the brackish beach groundwater altered the groundwater-borne N pool. Indeed, TDN concentrations in the saline circulation cell are much higher than the input from inland groundwater, even if this TDN is subsequently attenuated in surface sediment in the saline circulation cell due to biogeochemical processes and dilution (Table 2). Our findings showed that, even if groundwater-borne TDN in the form of NO_3^- and DON was mostly attenuated along the groundwater flow path, a "new" N pool was produced within the STE as it was already observed for DOM (Couturier et al., 2016).

4.2.2   Nitrogen fluxes

The fresh groundwater-borne N fluxes to the STE have been calculated as the product of the mean DON, NO_x and NH_4^+ concentrations of the fresh inland groundwater endmember and the flow of fresh groundwater on shore (Chaillou et al., 2016). The fresh inland groundwater-derived N input estimated in this way was < 0.07 and 37 $mol\,m^{-1}\,yr^{-1}$ for NH_4^+ and NO_x respectively. Estimated DIN and DON fluxes are 37 $mol\,m^{-1}\,yr^{-1}$ and 63 $mol\,m^{-1}\,y^{-1}$ respectively (Ta-

Table 3. N fluxes delivered to STE and exported to coastal ocean in $mol\,m^{-1}\,yr^1$. Fresh inland groundwater-borne fluxes were computed as the product of average concentrations of N in groundwater endmembers and the volume of fresh groundwater discharge (Q_{inland}). The exported N fluxes were the product of N inventory at the high-tide mark and the flow measured in the beach (Q_{beach}). Inorganic N fluxes were estimated based on 2013 sampling, and DON fluxes were based on 2012 sampling.

Fluxes $mol\,m^{-1}\,yr^{-1}$	NH_4^+	NO_x	DIN	DON[a]
Fresh inland groundwater	0.07	37	37	63
Exported N	141	1.3	142.3	33.8

[a] Calculated based on 2012 sampling with hydrologic flow determined in 2013.

ble 3). The estimated groundwater-borne TDN flux was approximately 102 $mol\,m^{-1}\,yr^{-1}$, corresponding to an annual N input of $\sim 1700\,kg$ along the 1200 m Martinique Beach shoreline. This flux is dominated by DON and NO_x. Inland groundwater clearly acts as a source of nitrogen to the beach groundwater, as has been observed in other STEs, such as in Dor Bay (Mediterranean coast; Weinstein et al., 2011), Cockburn Sound (western Australia; Loveless and Oldham, 2010) and Waquoit Bay (Cape Cod, MA; Talbot et al., 2003; Gonneea and Charette, 2014). However, the groundwater-borne N load at Martinique Beach was very low in comparison to the above-mentioned sites, where fresh groundwater NO_x concentrations as high as 300 $\mu mol\,L^{-1}$ were reported.

Estimates of nutrient export from the STE to the coastal ocean are more difficult to obtain. Direct measurements (from surface sediment incubations) are probably the most accurate ways to measure export. However, the spatial patchiness of seeps at the discharge zone and the effect of tides on the hydraulic gradient in the beach aquifer lead to significant variability in direct measurements of SGD (Blanco et al., 2008; Welti et al., 2015). Furthermore, indirect estimates – based on the product of solute concentrations in fresh inland groundwater and SGD flux estimates based on isotopic tracers or hydraulic gradients – are more often used to obtain a spatially integrated estimate of chemical discharge (Beck et al., 2011; Burnett et al., 2006), though they often ignore transformations occurring in surface sediments at the seep-

age face (Rao and Charette, 2012). Integrating the role of in situ N transformations is also critical to accurately estimating the impact that coastal boreal systems have on regional and global nutrient budgets. Here, the potential nutrient export from the STE at Martinique Beach to the seepage face has been calculated based on Darcy's flow through the 50 m length of the STE reported by Chaillou et al. (2016). To estimate the potential nitrogen export to the seepage face, we assumed that the TDN produced in the Martinique Beach STE is flushed out of the system by the continental hydraulic gradient.

This potential N export corresponds to 141, 1.3 and 33.8 mol m^{-1} yr^{-1} for NH$_4^+$, NO$_x$ and DON respectively (Table 3), corresponding to an annual N input of $\sim$3100 kg along the 1200 m Martinique Beach shoreline, which is twice the groundwater-borne fluxes. DIN exported to the seepage face ($\sim$142 mol m^{-1} yr^{-1}) was in the range of previous measurements at other sites, such as the Mediterranean coast (France; 530 mol m^{-1} yr^{-1}; Weinstein et al., 2011), the Gulf of Mexico (FL, USA; 414 mol m^{-1} yr^{-1}; Santos et al., 2009) and the Atlantic coast (Aquitania coast, France; 150 mol m^{-1} yr^{-1}; Anschutz et al., 2016). However, in most of these studies, the DIN pool was mainly dominated by NO$_x$, while at Martinique Beach NH$_4^+$ represented more than 90 % of the potential DIN supply to the seepage face. It is noteworthy that fewer studies report NH$_4^+$ as the main N species exported to the coastal ocean compared to NO$_x$. Kroeger et al. (2007) showed high proportions of NH$_4^+$ and DON in SGD fluxes to Tampa Bay (FL, USA), which may be explained in part by historical eutrophication, local hypoxia and anoxia in this area (Janicki et al., 2001). Measurements of DON flux to the coastal ocean are scarce. Kim et al. (2013) reported conservative mixing of DON, with export fluxes of 1.31 × 10^5 mol d^{-1} in Hwasun Bay (Jeju Island, Korea) and in the Gulf of Mexico; Santos et al. (2009) estimated that land-derived DON makes up $\sim$52 % of the total N exported to the coastal ocean.

It is difficult to estimate N fluxes by SGD to Martinique Bay, as coupled nitrification–denitrification in the upper 5–10 cm of sediments at the seepage face may remove much of the TDN flux exported from the STE (Gao et al., 2009; Gihring et al., 2010; Rao et al., 2008). Since NH$_4^+$ and DON are N species highly bioavailable to microorganisms, this N export can further be directly transformed by the microphytobenthos and higher trophic levels (Miller and Ullman, 2004). While fresh inland groundwater provides little input of N to Martinique Beach, biogeochemical processes in the beach groundwater lead to the transformation of organic N to inorganic N. These biogeochemical processes affect the N species potentially discharged to the coastal ocean. This N supply from the beach groundwater could therefore change the local benthic biogeochemical cycles and associated communities (Sawyer, 2015; Welti et al., 2015).

5 Conclusion

This study highlights the role of the STE in processing groundwater-derived N in a shallow boreal STE, far from anthropogenic pressures. N was mobilized within the STE since in situ production of NH$_4^+$ and DON were observed in beach groundwater. Fresh inland groundwaters delivered to the STE are rich in NO$_x$ and DON and depleted in NH$_4^+$. DON represented the main N species along the flow path. However, a shift from NO$_x$ to NH$_4^+$ occurred due to the removal of NO$_x$ and the addition of NH$_4^+$ within the STE. Nitrate loss along the flow path could be attributed to alternative reduction pathways such as Fe oxidation and to the mineralization of OC, since DOC concentrations were high in the STE. A part of NH$_4^+$ production could be attributed to mineralization of DON. The increase of TDN (i.e. the sum of DON and NH$_4^+$) in beach groundwater is likely the result of release of N from particulate organic matter of terrestrial origin. As a consequence, TDN in beach groundwater was higher than the inland fresh groundwater, revealing the reactivity of the system. While the input of NO$_x$ represents 32 % (37 mmol m^{-1} yr^{-1}) of the fresh groundwater input of TDN to the STE, NO$_x$ fluxes potentially exported from the STE to the seepage face only represent 1 % of the total exported TDN. Thus, near the discharge zone, NH$_4^+$ and DON dominated the TDN load exported to surface sediments and Martinique Bay. This local export of bioavailable N is probably removed in surface sediments, or it supports benthic production and higher trophic levels. This study highlights the impact of biogeochemical transformations on N species in a boreal STE. Our study showed that biogeochemical transformations, along a continuum between fresh inland groundwater and the ocean, modify the distribution of N species, providing new N species from terrestrial origin to the coastal ocean. These biogeochemically active and dynamic systems reflect the challenge of accurately estimating groundwater nutrient fluxes to the coastal ocean.

References

Abarca, E., Karam, H., Hemond, H. F., and Harvey, C. F.: Transient groundwater dynamics in a coastal aquifer: the effects of tides, the lunar cycle and the beach profile, Water Resour. Res., 49, 2473–2488, https://doi.org/10.1002/wrcr.20075, 2013.

Aller, R. C.: Bioturbation and remineralization of sedimentary organic matter: effects of redox oscillation, Chem. Geol., 114, 331–345, https://doi.org/10.1016/0009-2541(94)90062-0, 1994.

Anderson, D. M., Burkholder, J. M., Cochlan, W. P., Gobler, C. J., Heil, C. A., Kudela, R. M., Parsons, M. L., Rensel, J. E. J., Townsend, D. W., Trainer, V. L., and Vargo, G. A.: Harmful algal blooms and eutrophication: examining linkages from selected coastal regions of the United States, Harmful Algae, 8, 39–53, https://doi.org/10.1016/j.hal.2008.08.017, 2008.

Anschutz, P., Jorissen, F. J., Chaillou, G., Abu-Zied, R., and Fontanier, C.: Recent turbidite deposition in the eastern Atlantic: early diagenesis and biotic recovery, J. Mar. Res., 60, 835–854, https://doi.org/10.1357/002224002321505156, 2002.

Anschutz, P., Charbonnier, C., Deborde, J., Deirmendjian, L., Poirier, D., Mouret, A., Buquet, D., and Lecroart, P.: Terrestrial groundwater and nutrient discharge along the 240-km-long Aquitanian coast, Mar. Chem., 185, 38–47, https://doi.org/10.1016/j.marchem.2016.04.002, 2016.

Baker, M. A. and Vervier, P.: Hydrological variability, organic matter supply and denitrification in the Garonne River ecosystem, Freshwater Biol., 49, 181–190, https://doi.org/10.1046/j.1365-2426.2003.01175.x, 2004.

Beck, A. J., Tsukamoto, Y., Tovar-Sanchez, A., Huerta-Diaz, M., Bokuniewicz, H. J., and Sanudo-Wilhelmy, S. A.: Importance of geochemical transformations in determining submarine groundwater discharge-derived trace metal and nutrient fluxes, Appl. Geochem., 22, 477–490, https://doi.org/10.1016/j.apgeochem.2006.10.005, 2007.

Beck, M., Riedel, T., Graue, J., Köster, J., Kowalski, N., Wu, C. S., Wegener, G., Lipsewers, Y., Freund, H., Böttcher, M. E., Brumsack, H.-J., Cypionka, H., Rullkötter, J., and Engelen, B.: Imprint of past and present environmental conditions on microbiology and biogeochemistry of coastal Quaternary sediments, Biogeosciences, 8, 55–68, https://doi.org/10.5194/bg-8-55-2011, 2011.

Beusen, A. H. W., Slomp, C. P., and Bouwman, A. F.: Global land–ocean linkage: direct inputs of nitrogen to coastal waters via submarine groundwater discharge, Environ. Res. Lett., 8, 34035, doi:1748-9326/8/3/034035, 2013.

Blanco, A. C., Nadaoka, K., and Yamamoto, T.: Planktonic and benthic microalgal community composition as indicators of terrestrial influence on a fringing reef in Ishigaki Island, Southwest Japan, Mar. Environ. Res., 66, 520–535, https://doi.org/10.1016/j.marenvres.2008.08.005, 2008.

Burnett, W., Aggarwal, P., Aureli, A., Bokuniewicz, H., Cable, J., Charette, M. A., Kontar, E., Krupa, S., Kulkarni, K., Loveless, A., Moore, W., Oberdorfer, J., Oliveira, J., Ozyurt, N., Povinec, P., Privitera, A., Rajar, R., Ramessur, R., Scholten, J., Stieglitz, T., Taniguchi, M., and Turner, J.: Quantifying submarine groundwater discharge in the coastal zone via multiple methods, Sci. Total Environ., 367, 498–543, https://doi.org/10.1016/j.scitotenv.2006.05.009, 2006.

Chaillou, G., Anschutz, P., Dubrulle, C. and Lecroart, P.: Transient states in diagenesis following the deposition of a gravity layer: dynamics of O$_2$, Mn, Fe and N-species in experimental units, Aquat. Geochem., 13, 157–172, https://doi.org/10.1007/s10498-007-9013-0, 2007.

Chaillou, G., Touchette, M., Rémillard, A., Buffin-Bélanger, T., St-Louis, R., Hétu, B., and Tita, G.: Synthèse de l'état des connaissances sur les eaux souterraines aux Îles-de-la-Madeleine – Impacts de l'exploration et de l'exploitation des ressources naturelles sur celles-ci, Université du Québec à Rimouski, 2012.

Chaillou, G., Couturier, M., Tommi-Morin, G., and Rao, A. M.: Total alkalinity and dissolved inorganic carbon production in groundwaters discharging through a sandy beach, Procedia Earth Planet. Sci., 10, 88–99, https://doi.org/10.1016/j.proeps.2014.08.017, 2014.

Chaillou, G., Lemay-Borduas, F., and Couturier, M.: Transport and transformations of groundwater-borne carbon discharging through a sandy beach to coastal ocean, Can. Water Resour. J., 38, 809–828, https://doi.org/10.1080/07011784.2015.1111775, 2016.

Chaillou, G., Lemay-Borduas, F., Larocque, M., Couturier, M., Biehler, A., and Tommi-Morin, G.: Flow and discharge of groundwater from a snowmelt-affected sandy beach, J. Hydrol., in revision, 2017.

Couturier, M., Nozais, C., and Chaillou, G.: Microtidal subterranean estuaries as a source of fresh terrestrial dissolved organic matter to coastal ocean, Mar. Chem., 186, 46–57, https://doi.org/10.1016/j.marchem.2016.08.001, 2016.

Erler, D. V, Santos, I. R., Zhang, Y., Tait, D. R., Befus, K. M., Hidden, A., Li, L., and Eyre, B. D.: Nitrogen transformations within a tropical subterranean estuary, Mar. Chem., 164, 38–47, https://doi.org/10.1016/j.marchem.2014.05.008, 2014.

Gao, H., Schreiber, F., Collins, G., Jensen, M. M., Kostka, J. E., Lavik, G., de Beer, D., Zhou, H., and Kuypers, M. M.: Aerobic denitrification in permeable Wadden Sea sediments, ISME J., 4, 417–426, https://doi.org/10.1038/ismej.2009.127, 2009.

Gehrels, W. R.: Determining relative sea-level change from salt-marsh foraminifera and plant zones on the coast of Maine, USA, J. Coastal Res., 10, 990–1009, 1994.

Gihring, T. M., Canion, A., Riggs, A., Huettel, M., and Kostka, J. E.: Denitrification in shallow, sublittoral Gulf of Mexico permeable sediments, Limnol. Oceanogr., 55, 43–54, https://doi.org/10.4319/lo.2010.55.1.0043, 2010.

Glibert, P. M., Icarus Allen, J., Artioli, Y., Beusen, A., Bouwman, L., Harle, J., Holmes, R., and Holt, J.: Vulnerability of coastal ecosystems to changes in harmful algal bloom distribution in response to climate change: projections based on model analysis, Glob. Change Biol., 20, 3845–3858, https://doi.org/10.1111/gcb.12662, 2014.

Gonneea, M. E. and Charette, M. A.: Hydrologic controls on nutrient cycling in an unconfined coastal aquifer, Environ. Sci. Technol., 48, 14178–14185, https://doi.org/10.1021/es503313t, 2014.

Gonneea, M. E., Mulligan, A. E., and Charette, M. A.: Climate-driven sea level anomalies modulate coastal groundwater dynamics and discharge, Geophys. Res. Lett., 40, 2701–2706, https://doi.org/10.1002/grl.50192, 2013.

Hall, P. J. and Aller, R. C.: Rapid, small-Volume, flow injection analysis for CO_2 and NH_4+ in marine and freshwaters, Limnol. Oceanogr., 37, 1113–1119, 1992.

Hansell, D. A. and Carlson, C. A.: Biogeochemistry of marine dissolved organic matter, Academic Press, Elsevier, San Diego, Ca, USA, 2014.

Heiss, J. W. and Michael, H. A.: Saltwater-freshwater mixing dynamics in a sandy beach aquifer over tidal, srping-neap and seasonal cycles, Water Resour. Res., 50, 6747–6766, https://doi.org/10.1002/2014WR015574, 2014.

Hinzman, L. D., Bettez, N. D., Bolton, W. R., Chapin, F. S., Dyurgerov, M. B., Fastie, C. L., Griffith, B., Hollister, R. D., Hope, A., Huntington, H. P., Jensen, A. M., Jia, G. J., Jorgenson, T., Kane, D. L., Klein, D. R., Kofinas, G., Lynch, A. H., Lloyd, A. H., Mcguire, A. D., Nelson, F. E., Oechel, W. C., Osterkamp, T. E., Racine, C. H., Romanovsky, V. E., Stone, R. S., Stow, D. A., Sturm, M., Tweedie, C. E., Vourlitis, G. L., Walker, M. D., Walker, D. A., Webber, P. J., Welker, J. M., Winker, K. S., and Yoshikawa, K.: Evidence and implications of recent climate change in northern Alaska and other Arctic regions, Clim. Change, 72, 251–298, https://doi.org/10.1007/s10584-005-5352-2, 2005.

Howarth, R. W. and Marino, R.: Nitrogen as the limiting nutrient for eutrophication in coastal marine ecosystems: evolving views over three decades, Limnol. Oceanogr., 51, 364–376, https://doi.org/10.4319/lo.2006.51.1_part_2.0364, 2006.

Hulth, S., Aller, R. C., and Gilbert, F.: Coupled anoxic nitrification/manganese reduction in marine sediments, Geochim. Cosmochim. Ac., 63, 49–66, https://doi.org/10.1016/S0016-7037(98)00285-3, 1999.

Hyacinthe, C., Anschutz, P., Carbonel, P., Jouanneau, J. M., and Jorissen, F. J.: Early diagenetic processes in the muddy sediments of the bay of biscay, Mar. Geol., 177, 111–128, https://doi.org/10.1016/S0025-3227(01)00127-X, 2001.

Jackson, N., Nordstrom, K., Smith, D., and Virginia, W.: Geomorphic – biotic interactions on beach foreshores in estuaries, J. Coastal Res., 424, 414–424, doi:0749-0208, 2002.

Janicki, A., Pribble, R., Janicki, S., and Winowitch, M.: An analysis of long-term trends in Tampa Bay water quality, Tampa Bay Estuary Program, St Petersburg, FL, USA, 2001.

Johannes, R. E.: The ecological significance of the submarine discharge of groundwater, Mar. Ecol.-Prog. Ser., 3, 365–373, 1980.

Jørgensen, L., Lechtenfeld, O. J., Benner, R., Middelboe, M., and Stedmon, C. A.: Production and transformation of dissolved neutral sugars and amino acids by bacteria in seawater, Biogeosciences, 11, 5349–5363, https://doi.org/10.5194/bg-11-5349-2014, 2014.

Juneau, M.-N.: Hausse récente du niveau marin relatif aux Îles de la Madeleine, Master's thesis, Université du Québec à Rimouski, Rimouski, Canada, 2012.

Kelaher, B. and Levinton, J.: Variation in detrital enrichment causes spatio-temporal variation in soft-sediment assemblages, Mar. Ecol.-Prog. Ser., 261, 85–97, https://doi.org/10.3354/meps261085, 2003.

Kim, T., Kwon, E., Kim, I., Lee, S., and Kim, G.: Dissolved organic matter in the subterranean estuary of a volcanic island, Jeju: importance of dissolved organic nitrogen fluxes to the ocean, J. Sea Res., 78, 18–24, https://doi.org/10.1016/j.seares.2012.12.009, 2013.

Knee, K. L. and Jordan, T. E.: Spatial distribution of dissolved radon in the Choptank river and its tributaries: implications for groundwater discharge and nitrate inputs, Estuar. Coast., 36, 1237–1252, 2013.

Korom, S. F.: Natural denitrification in the saturated zone: a review, Water Resour. Res., 28, 1657–1668, https://doi.org/10.1029/92WR00252, 1992.

Kroeger, K. D. and Charette, M.: Nitrogen biogeochemistry of submarine groundwater discharge, Limnol. Oceanogr., 53, 1025–1039, 2008.

Kroeger, K. D., Cole, M. L., and Valiela, I.: Groundwater-transported dissolved organic nitrogen exports from coastal watersheds, Limnol. Oceanogr., 51, 2248–2261, https://doi.org/10.4319/lo.2006.51.5.2248, 2006.

Kroeger, K. D., Swarzenski, P. W., Greenwood, W. J., and Reich, C.: Submarine groundwater discharge to Tampa Bay: nutrient fluxes and biogeochemistry of the coastal aquifer, Mar. Chem., 104, 85–97, https://doi.org/10.1016/j.marchem.2006.10.012, 2007.

Loveless, A. M. and Oldham, C. E.: Natural attenuation of nitrogen in groundwater discharging through a sandy beach, Biogeochemistry, 98, 75–87, https://doi.org/10.1007/s10533-009-9377-x, 2010.

Madelin'Eau: Gestion des eaux souterraines aux Îles-de-la-Madeleine Un défi de développement durable Rapport final, 2004.

Madelin'Eau: Secteur sud-est de l'île de grande entrée – Rapport hydrologique, 2007.

Madelin'Eau: Secteur de grande-entrée – flanc nord alimentation en eau potable, 2009.

Madelin'Eau: Projet de réalisation d'un forage gazier vertical et conventionel d'une profondeur de 2500 m, municipalité des îles de la Madeleine – Rapport d'étape 1, expertise hydrogéologique, 2011.

Martin, J. B., Hartl, K. M., Corbett, D. R., Swarzenski, P. W., and Cable, J. E.: A multi-level pore-water sampler for permeable sediments, J. Sediment. Res., 73, 128–132, https://doi.org/10.1306/070802730128, 2003.

Masselink, G. and Short, A.: The effect on tide range on beach morphodynamics and morphology: a conceptual beach model, J. Coastal Res., 9, 785–800, 1993.

McCoy, C. and Corbett, D. R.: Review of submarine groundwater discharge (SGD) in coastal zones of the Southeast and Gulf Coast regions of the United States with management implications, J. Environ. Manage., 90, 644–51, https://doi.org/10.1016/j.jenvman.2008.03.002, 2009.

Miller, D. C. and Ullman, W. J.: Ecological consequences of ground water discharge to Delaware Bay, United States, Groundwater, 42,(959–970, https://doi.org/10.1111/j.1745-6584.2004.tb02635.x, 2004.

Moore, W. S.: The subterranean estuary: a reaction zone of ground water and sea water, Mar. Chem., 65, 111–125, https://doi.org/10.1016/S0304-4203(99)00014-6, 1999.

M. Couturier et al.: Nitrogen transformations along a shallow subterranean estuary 3335

Moore, W. S.: The effect of submarine groundwater discharge on the ocean., Ann. Rev. Mar. Sci., 2, 59–88, https://doi.org/10.1146/annurev-marine-120308-081019, 2010.

Null, K. A., Dimova, N. T., Knee, K. L., Esser, B. K., Swarzenski, P. W., Singleton, M. J., Stacey, M., and Paytan, A.: Submarine groundwater discharge-derived nutrient loads to San Francisco bay: implications to future ecosystem changes, Estuar. Coast., 35, 1299–1315, https://doi.org/10.1007/s12237-012-9526-7, 2012.

Postma, D.: Kinetics of nitrate reduction by detrital Fe (II)-silicates, Geochim. Cosmochim. Ac., 54, 903–908, 1990.

Postma, D., Boesen, C., Kristiansen, H., and Larsen, F.: Nitrate reduction in an unconfined sandy aquifer: water chemistry, reduction processes and geochemical modeling, Water Resour. Res., 27, 2027–2045, https://doi.org/10.1029/91WR00989, 1991.

Rao, A. M. F. and Charette, M. A.: Benthic nitrogen fixation in an eutrophic estuary affected by groundwater discharge, J. Coastal Res., 280, 477–485, https://doi.org/10.2112/JCOASTRES-D-11-00057.1, 2012.

Rao, A. M. F., McCarthy, M. J., Gardner, W. S., and Jahnke, R. A.: Respiration and denitrification in permeable continental shelf deposits on the South Atlantic Bight: N2: Ar and isotope pairing measurements in sediment column experiments, Cont. Shelf Res., 28, 602–613, 2008.

Rivett, M. O., Buss, S. R., Morgan, P., Smith, J. W. N., and Bemment, C. D.: Nitrate attenuation in groundwater: A review of biogeochemical controlling processes, Water Res., 42, 4215–4232, https://doi.org/10.1016/j.watres.2008.07.020, 2008.

Robinson, C., Li, L., and Barry, D. A.: Effect of tidal forcing on a subterranean estuary, Adv. Water Resour., 30, 851–865, https://doi.org/10.1016/j.advwatres.2006.07.006, 2007a.

Robinson, C., Xin, P., Li, L., and Barry, D. A.: Groundwater flow and salt transport in a subterranean estuary driven by intensified wave conditions, Water Resour. Res., 50, 165–181, https://doi.org/10.1002/2013WR013813, 2014.

Rocha, C., Ibanhez, J., and Leote, C.: Benthic nitrate biogeochemistry affected by tidal modulation of Submarine Groundwater Discharge (SGD) through a sandy beach face, Ria Formosa, Southwestern Iberia, Mar. Chem., 115, 43–58, https://doi.org/10.1016/j.marchem.2009.06.003, 2009.

Rocha, C., Wilson, J., Scholten, J., and Schubert, M.: Retention and fate of groundwater-borne nitrogen in a coastal bay (Kinvara Bay, Western Ireland) during summer, Biogeochemistry, 125, 275–299, https://doi.org/10.1007/s10533-015-0116-1, 2015.

Rossi, F., Incera, M., Callier, M., and Olabarria, C.: Effects of detrital non-native and native macroalgae on the nitrogen and carbon cycling in intertidal sediments, Mar. Biol., 158, 2705–2715, https://doi.org/10.1007/s00227-011-1768-6, 2011.

Sáenz, J. P., Hopmans, E. C., Rogers, D., Henderson, P. B., Charette, M. A., Schouten, S., Casciotti, K. L., Sinninghe Damsté, J. S., and Eglinton, T. I.: Distribution of anaerobic ammonia-oxidizing bacteria in a subterranean estuary, Mar. Chem., 136, 7–13, https://doi.org/10.1016/j.marchem.2012.04.004, 2012.

Santoro, A. E.: Microbial nitrogen cycling at the saltwater-freshwater interface, Hydrogeol. J., 18, 187–202, https://doi.org/10.1007/s10040-009-0526-z, 2010.

Santos, I., Burnett, W. C., Dittmar, T., Suryaputra, I. G. N., and Chanton, J.: Tidal pumping drives nutrient and dissolved organic matter dynamics in a Gulf of Mexico subter-

ranean estuary, Geochim. Cosmochim. Ac., 73, 1325–1339, https://doi.org/10.1016/j.gca.2008.11.029, 2009.

Santos, I., Eyre, B. D., and Huettel, M.: The driving forces of porewater and groundwater flow in permeable coastal sediments: A review, Estuar. Coast. Shelf S., 98, 1–15, https://doi.org/10.1016/j.ecss.2011.10.024, 2012.

Santos, I. R., Burnett, W. C., Chanton, J., Mwashote, B., Suryaputra, I. G. N. A., and Dittmar, T.: Nutrient biogeochemistry in a Gulf of Mexico subterranean estuary and groundwater-derived fluxes to the coastal ocean, Limnol. Oceanogr., 53, 705–718, https://doi.org/10.4319/lo.2008.53.2.0705, 2008.

Santos, I. R., Bryan, K. R., Pilditch, C. A., and Tait, D. R.: Influence of porewater exchange on nutrient dynamics in two New Zealand estuarine intertidal flats, Mar. Chem., 167, 57–70, https://doi.org/10.1016/j.marchem.2014.04.006, 2014.

Sawyer, A. H.: Enhanced removal of groundwater-borne nitrate in heterogeneous aquatic sediments, Geophys. Res. Lett., 42, 403–410, https://doi.org/10.1002/2014GL062234, 2015.

Schlacher, T. A. and Connolly, R. M.: Land–ocean coupling of carbon and nitrogen fluxes on sandy beaches, Ecosystems, 12, 311–321, https://doi.org/10.1007/s10021-008-9224-2, 2009.

Schnetger, B. and Lehners, C.: Determination of nitrate plus nitrite in small volume marine water samples using vanadium(III)chloride as a reduction agent, Mar. Chem., 160, 91–98, https://doi.org/10.1016/j.marchem.2014.01.010, 2014.

Scott, D. B., Brown, K., Collins, E. S., and Medioli, F. S.: A new sea-level curve from Nova Scotia: evidence for a rapid acceleration of sea-level rise in the late mid-Holocene, Can. J. Earth Sci., 32, 2071–2080, https://doi.org/10.1139/e95-160, 1995a.

Scott, D. B., Gayes, P. T., and Collins, E. S.: Mid-holocene precedent for a future rise in sea-level along the Atlantic coast of North America, J. Coastal Res., 11, 615–622, 1995b.

Seitzinger, S. P., Sanders, R. W., and Styles, R.: Bioavailability of DON from natural and anthropogenic sources to estuarine plankton, Limnol. Oceanogr., 47, 353–366, https://doi.org/10.4319/lo.2002.47.2.0353, 2002.

Seitzinger, S. P., Harrison, J. A., Dumont, E., Beusen, A. H. W., and Bouwman, A. F.: Sources and delivery of carbon, nitrogen and phosphorus to the coastal zone: an overview of global Nutrient Export from Watersheds (NEWS) models and their application, Global Biogeochem. Cy., 19, GB4S01, https://doi.org/10.1029/2005GB002606, 2005.

Sipler, R. E. and Bronk, D. A.: Dynamics of dissolved organic nitrogen, in: Biogeochemistry of marine dissolved organic matter, edited by: Hansell, D. A. and Carlson, C. A., 127–184, Academic Press, San Diego, Ca, USA, 2014.

Slomp, C. P. and Van Cappellen, P.: Nutrient inputs to the coastal ocean through submarine groundwater discharge: controls and potential impact, J. Hydrol., 295, 64–86, 2004.

Sundby, B.: Transient state diagenesis in continental margin muds, Mar. Chem., 102, 2–12, https://doi.org/10.1016/j.marchem.2005.09.016, 2006.

Talbot, J. M., Kroeger, K. D., Rago, A., Allen, M. C., and Charette, M. A.: Nitrogen flux and speciation through the subterranean estuary of Waquoit Bay, Massachusetts, Biol. Bull., 205, 244–245, https://doi.org/10.2307/1543276, 2003.

Valiela, I., Costa, J., Foreman, K., Teal, J. M., Howes, B., and Aubrey, D.: Transport of groundwater-borne nutrients from wa-

tersheds and their effects on coastal waters, Biogeochemistry, 10, 177–197, 1990.

Voss, M., Bange, H. W., Dippner, J. W., Middelburg, J. J., Montoya, J. P., and Ward, B.: The marine nitrogen cycle: recent discoveries, uncertainties and the potential relevance of climate change, Philos. T. R. Soc., 368, https://doi.org/10.1098/rstb.2013.0121, 2013.

Weinstein, Y., Yechieli, Y., Shalem, Y., Burnett, W., Swarzenski, P. W., and Herut, B.: What is the role of fresh groundwater and recirculated seawater in conveying nutrients to the coastal ocean?, Environ. Sci. Technol., 45, 5195–5200, https://doi.org/10.1021/es104394r, 2011.

Welti, N., Gale, D., Hayes, M., Kumar, A., Gasparon, M., Gibbes, B. and Lockington, D.: Intertidal diatom communities reflect patchiness in groundwater discharge, Estuar. Coast. Shelf S., https://doi.org/10.1016/j.ecss.2015.06.006, 2015.

ANNEXE II : STABLE ISOTOPE ANALYSIS OF DISSOLVED ORGANIC CARBON IN CANADA'S EASTERN COASTAL WATERS

Barber, A., Sirois, M., Chaillou, G., Gélinas, Y., 2017. *Stable isotope analysis of dissolved organic carbon in Canada's eastern coastal waters*. Limnology and Oceanography. 00. 00–00. doi : 10.1002/lno.10666

Stable isotope analysis of dissolved organic carbon in Canada's eastern coastal waters

Andrew Barber,[1] Maude Sirois,[2] Gwénaëlle Chaillou,[2] Yves Gélinas [1]*
[1]GEOTOP and the Department of Chemistry and Biochemistry, Concordia University, Montréal, Quebec, Canada
[2]Geochemistry of Coastal Hydrogeosystems, Université du Québec à Rimouski, Rimouski, Quebec, Canada

Abstract

The application of carbon stable isotope analysis of dissolved organic carbon (δ^{13}C-DOC) from natural seawater has been limited owing to the inherent difficulty of such analysis, with order of magnitude differences in interfering ions and analyte concentrations. High temperature catalytic oxidation allows for the attenuation of these interferences by precipitation of inorganic ions on quartz chips upstream from the oxidation catalyst. Using a chemical trap, the OI 1030C combustion DOC analyzer unit can be coupled to an IRMS, allowing for the analysis of low DOC content saline waters with relatively high throughput. The analytical limitations and large water volumes traditionally required for these types of analyses have prevented any large-scale δ^{13}C-DOC studies. Here, we present δ^{13}C-DOC signatures for surface and bottom waters obtained along Canada's East Coast. Included in the study are samples from the Esquiman channel (between Newfoundland and Labrador), Lake Melville, the Saglek and Nachvak Fjords, the Hudson Strait and finally covering the salinity gradient across the St. Lawrence Estuary and Gulf. Measured δ^{13}C-DOC signatures ranged from predominantly marine values of $-19.9 \pm 0.3‰$ (vs. VPDB) off the coast of Newfoundland to predominantly terrestrial signatures of $-26.9 \pm 0.1‰$ in Lake Melville. We observed a large spread in δ^{13}C-DOC signatures for samples with a salinity of ≈ 35 between $-19.9‰$ and $-23.3‰$ demonstrating the difficulty associated to selecting a marine end-member to be used in stable isotope mixing models to determine the fate of organic matter along the freshwater-marine continuum.

Dissolved organic carbon (DOC), ubiquitous in all marine and lacustrine environments, is one of the largest pools of organic carbon on the planet, comparable in magnitude to the atmospheric CO_2 pool. Virtually all natural waters contain some form of DOC, ranging from highly reactive freshly produced DOC to low reactivity recalcitrant DOC escaping remineralization for upwards of 6000 yr (Druffel and Williams 1992). This broad range of DOC composition and reactivity can be encountered in spatially limited areas such as the transition zones between terrestrial and marine environments, which are a key component of the hydrological and biogeochemical continuum linking surface waters and the ocean (Ward et al. 2017). Organic matter is extensively reworked along this continuum through biotic processes such as bacterial degradation, as well as by abiotic processes such as photo-oxidation, co-precipitation alongside inorganic minerals, and salting out. These fresh to saline transition zones are particularly interesting in terms of carbon sequestration as they have been shown to act as both sources and sinks for organic carbon and atmospheric CO_2 (Cai 2011; Laruelle et al. 2015).

The advent of high precision and accuracy DOC determination instruments has allowed for more complete oceanic and riverine carbon budgets, yet DOC concentration measurements alone are insufficient for tracking the fate of organic matter. A series of DOC concentration interlaboratory comparison studies (ring-tests) was launched to better explain the discrepancy in reported DOC concentrations for similar samples (Sharp 1997; Sharp et al. 2002). The unavailability of organic carbon free water, insufficient blank corrections, and method artifacts (such as the inadvertent generation of oxidation inhibitors) were the primary sources of error in DOC concentration determination. Equally important to the routine analysis of DOC has been the increase in availability and widespread use of consensus

reference materials, such as those offered by the Hansel lab at the University of Miami, which has been provided to over 240 laboratories worldwide (http://yyy.rsmas.miami.edu/groups/biogeochem/CRM.html).

The now routine nature of DOC analysis has allowed for DOC determination to be coupled with isotope ratio mass spectrometers (IRMS) to determine not only DOC concentrations in natural waters but also the δ^{13}C signature of the DOC. While DOC-IRMS coupling is straightforward for the analysis of freshwater, low DOC concentration (usually < 100 μmol L^{-1}) marine samples present a complex analytical challenge. The high dissolved salt content (> 3% wt) leads to incomplete organic matter oxidation in wet chemical oxidation instruments, as the oxidation of DOC by persulfate is inhibited by inorganic ions found in seawater, such as Cl$^-$ (Aiken 1992; Peyton 1993) and limited sample throughput due to salt build-up within the inner workings of the instrument. Only recently have instrument developments made this measurement possible with sufficient precision and accuracy to acquire meaningful data (Bouillon et al. 2006; Osburn and St-Jean 2007; Federherr et al. 2014; Lalonde et al. 2014*a*).

Natural abundance carbon stable isotope (δ^{13}C) signatures can be exploited to track the sources and transformations of the various carbon pools along this continuum. Differences in δ^{13}C signatures arise either from differences in carbon fixation mechanisms or initial carbon source used during carbon fixation (Farquhar et al. 1989; Guy et al. 1993). These differences allow for the use of δ^{13}C signatures as source indicators, with marine organic matter being more enriched in ^{13}C (e.g., Williams and Druffel 1987; Bauer and Druffel 1998; Wang and Druffel 2001), leading to less negative δ^{13}C signatures, compared to higher order terrestrial plant organic matter (Hedges et al. 1997; Lalonde et al. 2014*b*). In marine environments, newly photosynthesized organic matter is created through the fixation of dissolved inorganic carbon, which has an initial δ^{13}C signature of approximately 0‰, while in terrestrial environments the source material for carbon fixation is atmospheric CO_2, with a signature ranging from $-8‰$ to $-9‰$ (Earth System Research Laboratory Global Monitoring Division of NOAA; https://www.esrl.noaa.gov/gmd/dv/iadv/). These variations in source material and fractionation factors for different photosynthetic C fixation pathways lead to marine planktonic organic matter having δ^{13}C-DOC signatures of $-19‰$ to $-24‰$ compared to typical woody terrestrial organic matter δ^{13}C-DOC signatures of $-28‰$ (Peterson and Fry 1987).

These natural changes in δ^{13}C-DOC can be exploited in conjunction with isotope mass balance calculations to decipher the fate of terrestrial and/or marine organic matter (Bauer et al. 2002; Osburn and St-Jean 2007; Bouillon et al. 2012; Lalonde et al. 2014*b*). They are most useful for looking at the freshwater to saline continuum, where δ^{13}C-DOC signatures are different enough to discriminate between terrestrial and marine organic matter. The St. Lawrence Estuary and the Hudson Bay/Strait north of Quebec are important systems in terms of both total water and organic carbon discharge. Of particular note is the St. Lawrence Valley river system between the Great Lakes to the Atlantic Ocean (Québec, Canada), the second largest freshwater discharge in North America (Xie et al. 2012), where the estimated seaward DOC flux reaches 1.55×10^9 kg C yr^{-1} (Telang et al. 1991). Coupled with the hypoxic and acidic bottom waters found in this region (Mucci et al. 2011), the high riverine DOC to particulate organic carbon (POC) ratio of 10 : 1 (Hélie 2004) makes it an important study site for understanding terrestrial DOC export and molecular level transformations during its transit.

The importance of the Hudson Bay and surrounding regions, in the context of carbon cycling, arises from its large drainage basin (1/3 the size of Canada) and high water discharge rates, with a total of 5.5×10^9 kg of DOC flowing into the Hudson Bay from the surrounding large river systems and hydrological dams on a yearly basis (Déry et al. 2005). The bulk of the discharged organic matter originates from southernmost rivers (4.6×10^9 kg of the 5.5×10^9 kg of total organic C per year) draining the surrounding boreal forest (Mundy et al. 2010); as well as from Quebec's large river systems and hydro-reservoirs to the north. This is in contrast to the eastern coast of Quebec and Labrador which is sparsely vegetated with several fjords, located north of the tree-line, discharging out to the Labrador Sea (Bentley and Kahlmeyer 2012).

Importantly, several processes are known to alter the bulk isotopic signature of organic matter through the preferential removal of specific organic functionalities (Wang and Druffel 2001). Changes in DOC stable isotope signatures along the freshwater-marine continuum and throughout the water column are either due to differences in organic matter sources or through the re-working of this organic matter during degradation. While bacterial degradation does not lead to significant ^{13}C fractionation between the initial material and the altered organic remnants, (Shaffer et al. 1999; Bauer 2002), photo-oxidation of riverine organic matter leads to an increase in δ^{13}C-DOC signatures, owing to the preferential removal of conjugate carbon-carbon double bonds, which are more sensitive to UV degradation than saturated C-C bonds and other carbon containing functionalities (Lalonde et al. 2014*b*). Unfortunately, the changes in the signature of the terrestrial end-member upon photo-degradation, combined to the broad range of reported values for the marine end-member, make the use of isotopic mass balance calculations to quantify the proportion of terrestrial and marine DOC in a sample extremely uncertain.

Here, using carbon stable isotopes and DOC concentrations, we discuss DOC dynamics in Canada's eastern coastal waters, including the St. Lawrence Estuary, East Coast of Newfoundland, and Labrador and the Hudson Strait.

Coupled with previous terrestrial vs. marine proxy studies (Tremblay and Gagné 2009; Xie et al. 2012; Zhang and Xie 2015), we explore different processes, such as photo-oxidation, leading to variations in carbon stable isotope signatures for DOC from different locations and water column depths. We also discuss the limitations of isotopic mass balance calculation approaches to apportion DOC sources along the freshwater-ocean continuum, which arise from the uncertainties in δ^{13}C signatures of the end-members used in the model.

Materials and methods

St. Lawrence Valley river system

Draining the North American Great Lakes, the St. Lawrence River is the Canadian river with the highest water discharge, transporting approximately 413 km^3 of water per year to the Gulf of the St. Lawrence (Telang et al. 1991). Based on differences in water column depth and salinity, it can be separated into three major regions, the Upper and Lower Estuaries, and the Gulf (Fig. 1a). The Upper Estuary (USLE) begins near Quebec City and extends toward Tadoussac and the mouth of the Saguenay Fjord (Sta. 1–12; Fig. 1b). It is characterized by relatively shallow water and a steep salinity gradient ranging from under 0.1 near Quebec City to approximately 22.5 near Tadoussac. Seaward of the USLE, the water column is characterized by a strong vertical stratification. Differences in density between surface waters flowing seaward and the colder, denser waters flowing into the estuary from the Atlantic, coupled with changes in surface water density during the warmer summer months, allow for the formation of a cold intermediate layer (CIL), characterized by a local temperature minimum (Gilbert and Pettigrew 1997), as low as −1°C during the May 2016 sampling mission. The Lower St. Lawrence Estuary (LSLE) begins near Tadoussac, where there is a steep change in water column depth, dropping by over 200 m as this is the head of the Laurentian Channel, a trough that extends out to the Atlantic Ocean, through the Cabot Strait. Here, the stratified water masses of the St. Lawrence River valley system mix owing to the upwelling currents originating from the Atlantic (Mucci et al. 2011). The LSLE (Sta. 13–19 in this study) is characterized by higher surface water salinities (22–30) and lower DOC concentrations. Finally, the Gulf of the St. Lawrence incorporates water from the lower estuary as well as high salinity waters flowing in from the northeast and southeast through the Belle-Isle Strait and Cabot Strait, respectively.

Hudson Strait

The Hudson Strait joins Hudson Bay to the Labrador Sea and sits between the northern tip of Quebec and Baffin Island (Fig. 2). Along the northern coast, water flows westward toward the Hudson Bay, while flowing eastward toward the Labrador Sea along the southern coast (Straneo and Saucier 2008). The Hudson Strait joins the largest body of water

that completes a yearly freeze/thaw cycle (the Hudson Bay) to the Labrador Sea, acting as an important source of freshwater (salinity < 28) to the Labrador Current and global thermohaline circulation.

Sample collection

Water samples were collected aboard the R/V *Maria S. Merian* and the R/V *Coriolis II* (September 2015 and May 2016 respectively) using a CTD Rosette fitted with 12.5 L Niskin bottles. Combusted (450°C for 6 h) EPA borosilicate vials (40 mL) with PTFE lined caps were filled with water filtered through combusted 0.7 μm glass fiber filters. All samples were acidified to pH 2 using 12N TRACE select grade HCl and stored at 4°C in the dark prior to their analysis in the laboratory. Surface water (depth of between 2 m and 3 m) was collected at all stations (11 in the USLE, 12 in the Saguenay Fjord, 20 in the LSLE and Gulf, as well as 7 on the Labrador Coast and Hudson Strait; Figs. 1–3, and Supporting Information Tables S1–S3). In addition, one deep-water sample was collected about 10 m above the sediment–water interface at four USLE stations where the water column is stratified (Sta. 6, 9, 10, and 11), as well as at one station in the Saguenay Fjord (Station SAG 30). In the LSLE and Gulf, partial profiles (four depths) were collected at each station (surface, in the middle of the CIL layers at depths between 30 m and 70 m, middle of the deep water mass between 200 m and 250 m, and about 10 m above the sediment–water interface at depths varying between 196 m and 437 m).

Analytical methods

DOC concentrations and δ^{13}C-DOC signatures were determined using a modified Aurora OI 1030 high-temperature catalytic oxidation unit coupled to a chemical trap (GD-100, Graden Instruments, Ontario, Canada) and a GV/V Isotope Ratio Mass Spectrometer (Isoprime Ltd., Manchester, UK). The total organic carbon analyzer was modified in order to decrease the baseline CO_2 content by replacing the original PTFE tubing with PEEK tubing, which is less permeable to CO_2, even at elevated temperatures. A system pressure of 30 psi was used, while the combustion column was maintained at 680°C. For each sample, four replicate injections of 1.5 mL were sent to the combustion column after 2.5-min sparge at 90°C to remove any dissolved inorganic carbon in the water. The analysis of one replicate injection takes approximately 17.5 min. A full description of the GD-100 trap valve configuration can be found in Lalonde et al. (2014*a*). For the fully saline samples approximately 60 injections could be performed before cleaning the combustion column due to salt build-up.

In-house calibrated β-alanine (40.4% OC, $−26.18 \pm 0.10‰$), sucrose (42.1% OC, $−11.77 \pm 0.09‰$) and potassium hydrogen phthalate (47.0% OC, $−28.14 \pm 0.10‰$), dissolved in 18.2 mΩ cm^{-1} milli Q water, were used as isotopic standards while β-alanine was used as a standard for DOC concentration. The post calibration isotope signature was then blank subtracted using an isotope mass balance correction modified from (Brand 2004; Panetta et al. 2008; Lalonde et al. 2014*a*),
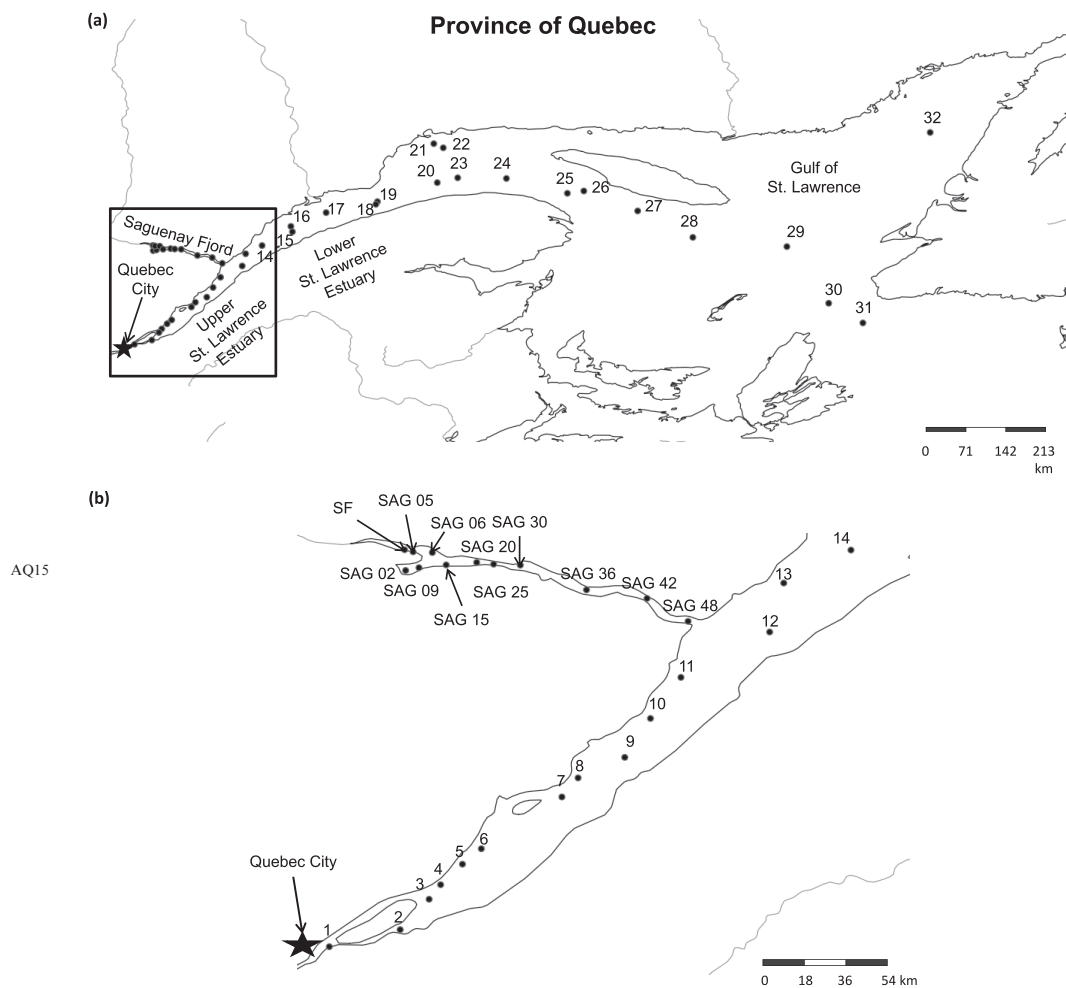
Fig. 1. (**a**) Map of all sampling stations in the Upper and Lower St. Lawrence Estuaries, Gulf of the St. Lawrence and Saguenay Fjords. Station numbers increase from 1 to 33 starting near Quebec City and increasing seaward. The station numbers for the boxed area can be found in the inset map (**b**) the sampling stations from the Upper St. Lawrence Estuary and Saguenay Fjord.

$$\delta^{13}C_{sample} = \frac{\delta^{13}C_m \; \eta_m - \delta^{13}C_b \; \eta_b}{\eta_m - \eta_b} \qquad (1)$$

where η_m and η_b are the measured and blank intensities respectively, assuming that the measured $\delta^{13}C$ signature is determined by only the sample and blank contributions in a linear fashion. The intensity of the blank was determined through repeated blank measurements while the $\delta^{13}C$ signature of the blank was extrapolated using a 4 or 5 point β-alanine calibration curve of varying concentration plotted
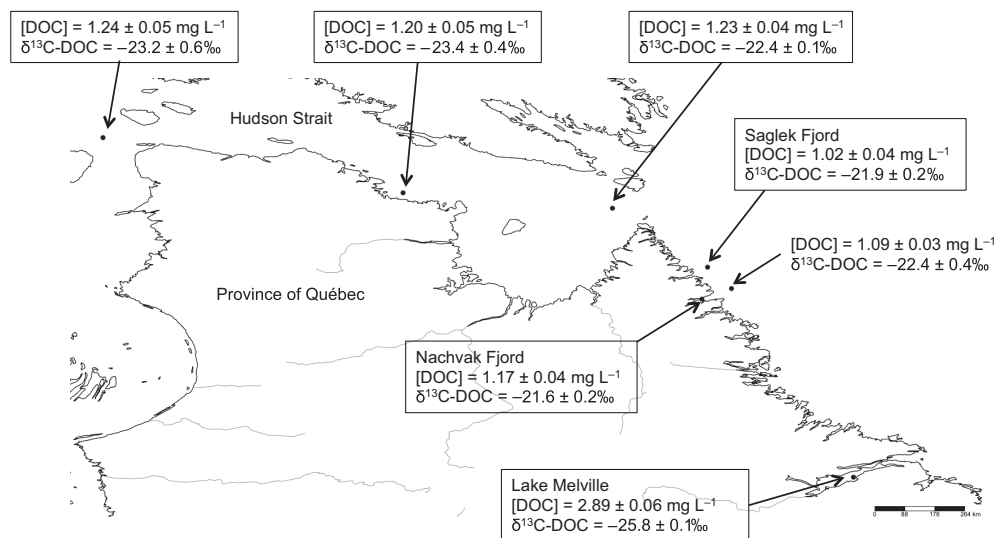
Fig. 2. Map of all northern sampling stations including their respective surface water DOC concentration and δ^{13}C-DOC signatures.

against the inverse intensity (Fry et al. 1992), which also served to ensure instrument linearity over the desired range of concentrations. Solving for the intercept gives the blank corrected δ^{13}C (δ_{bc}) signature, but the actual true blank δ^{13}C signature (δ_b) can be solved for using the following formula (Lalonde et al. 2014*a*),

$$\delta_b = \left(\frac{\text{slope}}{\eta_b}\right) + \delta_{bc} \qquad (2)$$

where the slope is taken from the plot of 1/intensity vs. δ^{13}C.

Results

Saguenay Fjord

The Saguenay Fjord is considered an important contributor of terrestrial organic matter as it discharges into the St. Lawrence Estuary near Tadoussac (Tremblay and Gagné 2009; Xie et al. 2012; Zhang and Xie 2015). The surface δ^{13}C-DOC signatures measured across the Saguenay Fjord were practically invariant with an average δ^{13}C-DOC across all surface stations of $-26.6 \pm 0.4\%$ and DOC concentrations ranging between 4.05 and 5.25 mg L^{-1} OC ($N = 12$) (Supporting Information Table S1). Where the water column is deepest, at station SAG 30 (Smith and Walton 1980; Locat and Levesque 2009), a significant decrease in DOC concentration was observed between the surface and deep waters,

from 5.25 ± 0.01 mg L^{-1} to 1.46 ± 0.02 mg L^{-1} respectively, alongside an enrichment in δ^{13}C-DOC of 2.1%. These deep, high salinity waters have a mixed terrestrial and marine carbon stable isotope signature of $-24.6 \pm 0.2\%$ (Supporting Information Table S1). Surface waters from the Saguenay have a low salt content (salinity between ~ 0 and 4.3) with the exception of station SAG 48, the closest from the St. Lawrence Estuary, where the salinity reaches 12.4.

Northern Quebec and Labrador

DOC in water from the Saglek and Nachvack fjords and surrounding coast was predominantly of marine origin with δ^{13}C-DOC signatures ranging between $-21.6 \pm 0.2\%$ and $-22.4 \pm 0.4\%$ (Fig. 2) and concentrations ranging from 1.02 ± 0.04 mg L^{-1} to 1.17 ± 0.04 mg L^{-1}. This is in contrast to the Hudson Strait, which had slightly higher DOC concentrations (approximately 1.2 mg L^{-1}) while being more depleted in ^{13}C (Fig. 2). The DOC concentrations across the Hudson Strait were fairly similar but the δ^{13}C-DOC signatures became more depleted going west, from $-22.4 \pm 0.1\%$ to $-23.2 \pm 0.6\%$. Finally, surface water samples collected from Lake Melville contained more DOC than the other northern stations, with a concentration of 2.89 ± 0.06 mg L^{-1} and a δ^{13}C-DOC signature of $-25.8 \pm 0.1\%$ (Fig. 2).

Across the St. Lawrence Estuary and Gulf

Samples collected from the USLE had an average δ^{13}C-DOC signature of $-26.7 \pm 0.4\%$ (Fig. 3, up to ~ 210 km
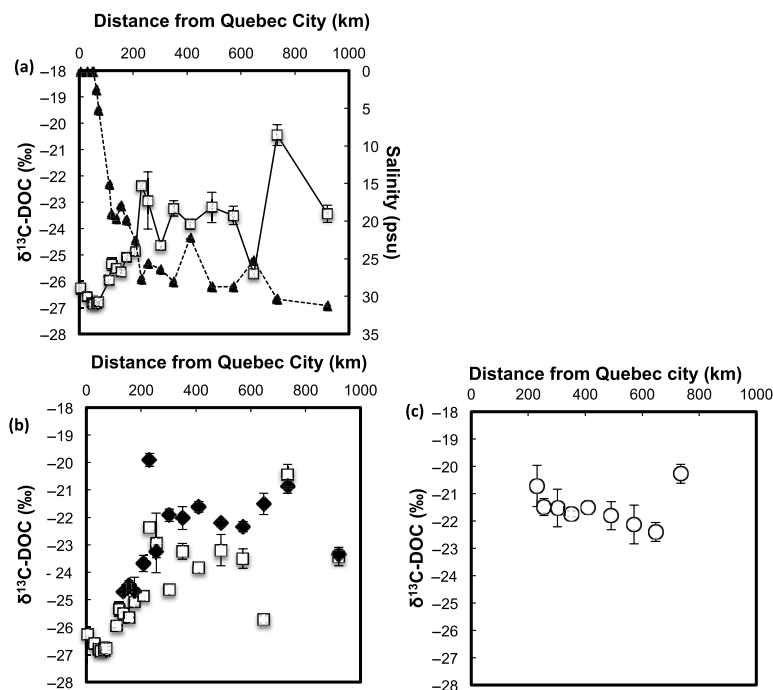
Fig. 3. (**a**) δ^{13}C-DOC signatures (open squares) and salinity (filled triangles) for the surface waters across the St. Lawrence Estuary and Gulf (**b**) δ^{13}C-DOC signatures for the surface (open squares) and cold intermediate (filled diamonds) water layers (CIL) as a function of the distance from Quebec City (**c**) δ^{13}C-DOC signatures for the deep water layers (open circles), all as a function of the distance seaward from Quebec City. Error bars represent the reproducibility from four replicates. Deep waters were collected approximately 3 m above the sediment–water interface.

from Quebec City), the lowest δ^{13}C-DOC signatures observed in this study along with those from the Saguenay Fjord. Within the mixing zone, there is a gradual enrichment in δ^{13}C-DOC signature for the surface samples ranging from $-26.9 \pm 0.1\%$ at Sta. 5 ($\sim$ 65 km from Quebec City) to $-22.4 \pm 0.1\%$ at Sta. 24 ($\sim$ 571 km from Quebec City), with salinities of 2.5 and 27.7, respectively (Fig. 3).

Within the Gulf of the St. Lawrence, DOC concentrations are lower compared to the upper estuary, ranging from 2.03 $\pm$ 0.10 mg L^{-1} for surface waters immediately south of Anticosti Island (Sta. 25) to 0.64 $\pm$ 0.05 mg L^{-1} for deep water at Sta. 27 (Supporting Information Tables S2, S3). These samples are also among by the most extreme δ^{13}C-DOC signatures observed for this region with the near shore sample near Anticosti Island (Sta. 25) having a strong terrestrial signature of $-25.7 \pm 0.1\%$, while the low concentration, salty bottom waters at Sta. 27 is typically marine ($-20.3 \pm 0.7\%$; Supporting Information Table S3).

Across both sampling missions, a trend toward more positive δ^{13}C-DOC signatures was observed for the St. Lawrence Estuary samples from the CIL compared to surface water samples (Supporting Information Table S3; representative profiles are shown as examples on Figs. 3b, 4). This enrichment in ^{13}C of DOC within the CIL was observed at 16 of the 20 stations, with statistically significant differences being observed at eight stations ($\alpha = 0.05$). The largest differences in δ^{13}C-DOC signatures between the surface and CIL water layers were found off the coast of Anticosti Island (Sta. 25), with signatures of $-25.7 \pm 0.1\%$ and $-21.5 \pm 0.4\%$ for the surface and cold intermediate layers, respectively (Fig. 3b, Supporting Information Table S3). Samples from Sta. 29 and 31 (Fig. 4), near the transition between the Gulf of the St. Lawrence and the Atlantic Ocean, showed no change in δ^{13}C-DOC down the water column. This is in contrast to samples from the Esquiman Chanel (Sta. 32) where the δ^{13}C-DOC signatures were more depleted within the CIL but then
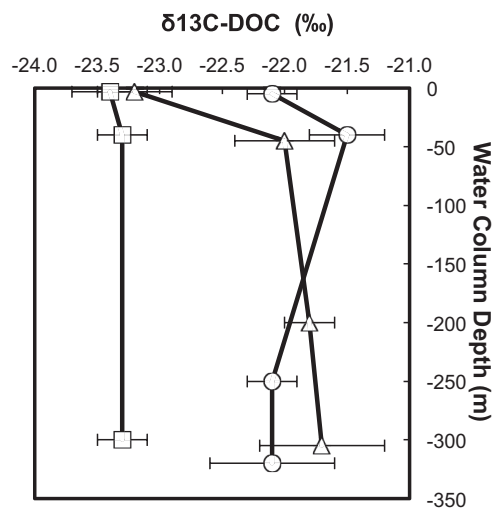
δ13C-DOC (‰)

Fig. 4. Sample water column δ^{13}C-DOC signatures profiles showing invariable δ^{13}C-DOC signatures at Sta. 29 (open squares), or enrichment in δ^{13}C-DOC between the surface and cold intermediate layer at Sta. 17 (open triangles) and Sta. 33 (open circles). All three stations are located in the Gulf of St. Lawrence (Fig. 1). Error bars are 1σ standard deviations from four replicates.

returned to values similar to those at the surface at depth (Fig. 4). A compilation of all the DOC concentrations and δ^{13}C signatures collected in this study is available in Supporting Information Table S1.

Discussion

Terrestrial organic matter inputs from the Saguenay Fjord

The DOC concentrations for the surface waters from the Saguenay Fjord were the highest among the regions analyzed in this study. These high DOC concentration surface waters discharge into the St. Lawrence Estuary near Tadoussac and account for a large fraction of the total discharge of terrestrial organic matter in the estuary (Schafer et al. 1990; Tremblay and Gagné 2009; El-Sabh and Silverberg 2012). The measured δ^{13}C-DOC signatures in these surface waters are predominantly terrestrial in nature, in agreement with the previously reported bulk organic C/N molar ratios of 21–25 (Pocklington and Leonard 1979; Louchouarn et al. 1997; St-Onge and Hillaire-Marcel 2001) and the terrestrial-specific lignin degradation products (Louchouarn and Lucotte 1998). This result reflects the fact that the surrounding vegetation is dominated by boreal forest and, more specifically, woody gymnosperms (Louchouarn et al. 1997).

Although surface DOC concentrations and carbon stable isotope signatures remain relatively constant throughout the Saguenay Fjord, variations in both concentrations and δ^{13}C-DOC were observed between surface waters and those just above the sediment water interface (Supporting Information Table S1). The waters of the Saguenay remain distinct and vertically stratified (Yeats and Bewers 1976), with high DOC, brackish surface waters flowing above the mostly saline deep waters, which flow into the Fjord from the St. Lawrence Estuary (Bourgault et al. 2012). The mixed terrestrial/marine δ^{13}C-DOC signature for the deep waters arises from a combination of the degradation of the more labile components of particulate organic matter as it sinks within the water column, as well as from mixing of relatively fresh terrestrial organic matter discharged from the surrounding boreal forest and the less reactive, partly marine organic matter transported into the Saguenay from the St. Lawrence Estuary.

Despite the vast amount of work exploiting bulk and compound-specific stable carbon isotope analysis done on sediment organic matter from terrestrial-to-marine transition zones, relatively few stable isotope analyses can be found in the literature for non-fractionated, bulk dissolved organic matter using an appropriate analytical methodology. A study on fjords from the Fiordland National Park in New Zealand (Yamashita et al. 2015) reported surface δ^{13}C-DOC signatures between -28.1‰ and -31.8‰, several permil more depleted than those reported here, a difference likely due to differences in the type of vegetation found in Fiordland compared to the Saguenay River watershed. The most depleted terrestrial values reported in this study (-26.9 ± 0.1‰; Supporting Information Table S1, S2) are similar to those measured by Osburn and Stedmon (2011) in the Baltic-North Sea transition zone, reflecting the fact that both regions drain catchments dominated by boreal forest (Stepanauskas et al. 2002; Mundy et al. 2010). These results highlight the importance of constraining and selecting an appropriate signature for the terrestrial δ^{13}C-DOC end-member value based on the surrounding vegetation and organic matter inputs when attempting to perform isotope mass balance calculations.

Dependence of δ^{13}C-DOC signatures on the vegetation in the drainage basin

As opposed to the Saguenay Fjord which receives large quantities of organic matter in the form of woody gymnosperms, the stations from Northern Québec and the North-Eastern Coast of Labrador (Nunatsiavut) are located above the tree line in the Torngat Mountains National Park (Elliott and Short 1979). Notably, the DOC in samples from within the Saglek Fjord as well as at the mouth of the Saglek and Nachvak Fjords were less depleted in ^{13}C relative to the Saguenay, with comparatively lower DOC concentrations. The erosion-resistant bedrock (Wilton 1996) coupled with the decreasing abundance of woody trees in this region (Bentley and Kahlmeyer 2012) likely explains the absence of

terrestrial signatures in these fjord systems despite the presence of riverine water inputs. A similar marine-like signature $(-22.3 \pm 0.2‰)$ was obtained by Druffel et al. (2017) for a sample collected near the surface in the North Atlantic Ocean south of Iceland.

The western side of Quebec is dominated by large river systems and hydro-dammed reservoirs surrounded by the boreal forest, leading to higher terrestrial organic inputs into the Hudson Bay compared to the Nachvak and Saglek Fjords. This influx of OC and the dominant surface currents may explain the trend across the Hudson Strait, going from depleted mixed terrestrial/marine organic $\delta^{13}C$ signatures to more enriched signatures as water is transported out to sea from the Hudson Bay across the Hudson Strait (Fig. 2). Previous studies looking at the fate of chromophoric dissolved organic matter (CDOM), another organic matter source indicator, have shown a similar trend in this region (Granskog et al. 2007). Fluorescence analysis of the dissolved organic matter (DOM) from this region, coupled to parallel factorial analysis (PARAFAC), showed that terrestrial organic matter inputs into the Hudson Bay are high and as water is carried from the Hudson Bay through the Hudson Strait there is a loss of terrestrial organic matter biomarkers (Granskog 2012). The $\delta^{13}C$ signature for DOC of $-23.4 \pm 0.4‰$ obtained for the westernmost station included in this study, at the mouth of the Hudson Strait, likely represents a mix of transported terrestrial and freshly produced planktonic organic matter.

Along the southern coast of the Hudson Strait, water flows eastward (Straneo and Saucier 2008) transporting a fraction of the terrestrial inputs from the Hudson Bay through the Hudson Strait, explaining the gradual enrichment in $\delta^{13}C$-DOC signatures going toward the Labrador Sea. The dominant terrestrial characteristics of DOC in the Hudson Bay were not observed within the Hudson Strait in previous studies (Granskog et al. 2007; Guéguen et al. 2011). Here, we show the progressive loss of the terrestrial DOC isotope signature across the Strait, reaching almost entirely marine $\delta^{13}C$-DOC signatures in Canada's northeastern coastal waters.

$\delta^{13}C$-DOC signatures across the St. Lawrence Estuary salinity gradient

The shift in $\delta^{13}C$-DOC signatures toward more enriched values, observed for surface waters moving seaward from Quebec City, coincides with an increase in salinity (Fig. 3a). Water from the freshwater Upper Estuary Sta. 1–4 (salinity < 2.5) flows eastward, where it begins to mix with more saline waters from the Gulf of the St. Lawrence. The seaward change in $\delta^{13}C$-DOC represents differences in organic matter inputs, dilution of terrestrial DOC with endogenously photosynthesized marine DOC, as well as the effect of processes which alter organic matter composition such as photo-oxidation of chromophoric DOM (Xie et al. 2012; Lalonde et al. 2014b).

The trend showing the decreasing terrestrial organic matter contributions in the St. Lawrence Estuary has also been reported in the sediment record, where the relative abundance of terrestrial organic matter biomarkers decreases across the St. Lawrence Estuary to the Gulf (Pocklington and Leonard 1979; Alkhatib et al. 2012). Notably, both the Saguenay and USLE have large terrestrial organic matter inputs from the surrounding mixed temperate and boreal forest delivered by major rivers. The ubiquitous average $\delta^{13}C$-DOC signature for these terrestrial dominated stations, similar to the $\delta^{13}C$-DOC signature of the DOC discharged by the St. Lawrence River (Hélie 2004), suggests that it represents an appropriate terrestrial end-member for $\delta^{13}C$-DOC mixing models. In fact, several freshwater to saline transition zones have $\delta^{13}C$-DOC values similar to the terrestrial organic carbon end-member determined for the Upper St. Lawrence Estuary $(-26.7 \pm 0.4‰)$ including the Baltic Sea, Perdido Estuary in Florida (Coffin and Cifuentes 1999) and the Danube-Black Sea mixing zone (Saliot et al. 2002) as well as for ocean margins near the Mid-Atlantic Blight (Guo et al. 1996).

Additionally, many studies looking at the $\delta^{13}C$-DOC of riverine samples have reported more depleted signatures than the most extreme values reported here (e.g., Spiker and Rubin 1975; Raymond and Bauer 2001b; Guo and Macdonald 2006; Lalonde et al. 2014b). These differences could either be due to methodological artifacts involving some form of discrimination toward a specific fraction of the dissolved organic matter pool when using ultrafiltration or solid-phase extraction to desalt the samples, or to differences in organic matter inputs from the surrounding drainage basin. Only recent analytical advancements (Osburn and St-Jean 2007; Federherr et al. 2014; Lalonde et al. 2014a) have allowed for carbon stable isotope analysis of dissolved organic carbon without fractionating the DOC pool based on molecular weight or chemical composition (reviewed in Raymond and Bauer 2001a). Great care must thus be taken when comparing literature values for $\delta^{13}C$-DOC analysis owing to such methodological differences.

Freshwater to saline transition zones can be found throughout the globe, yet do not always show the same trend between $\delta^{13}C$-DOC and salinity. An interesting case is the Tana Delta in Kenya, where the opposite trend was observed compared to the St. Lawrence Estuary, with less depleted $\delta^{13}C$-DOC signatures observed at the freshwater sampling sites and more depleted signatures at the saline sampling sites (Bouillon et al. 2007). Clearly, the relationship between salinity and the carbon stable isotope signature of DOC is not universal. In the case of the Tana Estuary, the contribution planktonic organic matter to the total DOC pool is very small (Bouillon et al. 2007), yet the measured $\delta^{13}C$-DOC signatures are similar to those observed here for the St. Lawrence Estuary owing to inputs of OM derived from C3 and C4 vegetation in the watershed (Bouillon et al. 2007). This similarity in $\delta^{13}C$-DOC signatures despite the

vastly different sources of DOC further reinforces the need to adequately constrain the end-members used for stable isotope mixing model calculations based on the sources of organic matter inputs.

Based on the combination of the measured δ^{13}C-DOC signatures and ratio of particulate organic carbon to chlorophyll A observed for the Tana estuary, the contribution of a marine planktonic δ^{13}C-DOC member is negligible relative to the total DOC pool (Bouillon et al. 2007). This has the benefit of increasing the discrimination power of isotope mass balance calculations owing to the large difference in δ^{13}C-DOC signatures between the two main end-members. In systems like the St. Lawrence Estuary where the contribution from marine organic matter is significant, establishing the marine end-member for these isotope mixing model calculations can be challenging, with values varying between about $-18‰$ to $-24‰$ being used across different studies (e.g., Bauer et al. 2002; Osburn and Stedmon 2011; Lalonde et al. 2014*b*). The potential artefacts linked to the desalting of DOC using ultrafiltration or solid-phase extraction in preparation for δ^{13}C-DOC analysis are exacerbated for saline samples, with DOC recoveries of less than 50% and as little as 20–30% of the total DOC pool (Raymond and Bauer 2001*a*). Such chemical or size fractionation of dissolved organic compounds with different δ^{13}C signatures most often leads to differences between the δ^{13}C signatures of the desalted and total DOC pools. Based on our results for a system such as the St. Lawrence Estuary where the drainage basin is dominated by boreal forest plants that act as a source of ^{13}C-depleted carbon, an appropriate marine end-member would be similar to our most enriched values of $-20.3 \pm 0.7‰$ (Supporting Information Table S3), similar to the value reported by Williams and Druffel in 1987.

Changes in δ^{13}C-DOC signatures with depth in the water column

Two sources may explain the trend toward more enriched δ^{13}C-DOC values within the CIL compared to surface waters: (1) marine DOC originating from the surface waters of the Labrador Sea, and (2) photodegraded terrestrial DOC transiting through the estuary surface waters.

First, the ^{13}C-enriched organic matter flowing into the St. Lawrence Gulf from the Labrador Sea and Atlantic Ocean is supported by previous work from Mucci et al. (2011), who suggests that the CIL is fed by cold, marine water flowing into the Gulf through the Strait of Belle Isle from the northeast (Mucci et al. 2011). This creates a net landward flow for the CIL north of Anticosti Island where the CIL is thickest. DOC enriched in ^{13}C produced in marine surface waters in the Labrador Sea is transported into the Gulf of the St. Lawrence, where the cold and salty CIL subducts beneath the warmer and less salty surface waters of the Gulf.

Additionally, the heating of surface waters during the spring and summer causes a stratification between the warmer top 30–45 m of the water column and the CIL (Mucci et al. 2011). Therefore, also at play is the partial (photo)degradation of terrestrial organic compounds during their transit across the St. Lawrence Estuary and Gulf. Recent work involving the artificial irradiation of DOC samples, exclusively of riverine origin, has shown an enrichment of up to 3‰ in δ^{13}C-DOC signatures upon irradiation equivalent to a half-year of UV radiation (Lalonde et al. 2014*b*). Exposure of organic matter to sunlight prior to the formation of the CIL could cause this biochemical fractionation through the preferential removal of photosensitive organic molecules. Complex organic molecules containing conjugated double bond systems, such as those found in chromophoric compounds, are more likely to undergo photochemical reworking when exposed to UV radiation (Blough and Del Vecchio 2002; Xie et al. 2012). Such large aromatic compounds are commonly associated with lignin and lignin degradation products in terrestrial environments, as well as vascular plant cell wall materials (tannins and cutans) which tend to be depleted in ^{13}C relative to the bulk organic matter pool (Goñi and Eglinton 1996). Preferential removal of δ^{13}C depleted DOC causes an enrichment in ^{13}C for the residual measurable DOC pool, which could lead to values such as those observed for the cold intermediate layer in this study. More work is needed to determine the relative importance of these two mechanisms explaining the enriched δ^{13}C-DOC signatures within the CIL. These results also suggest that the DOC pool in this mass of water is more heavily altered, and thus more recalcitrant, than in the surface layer just above.

Comparison with the Baltic-North Sea transition zone

The comparison between the St. Lawrence Estuary and the Baltic-North Sea transition zone is a natural one, having similar sized drainage basins (Perttilä et al. 1980; Bugden 1981) dominated by subartic boreal ecosystems (Stepanauskas et al. 2002; Mundy et al. 2010) and affected by bottom water hypoxia (Gilbert et al. 2005; Conley et al. 2009). Also, both transition zones have highly stratified water columns with sub-surface temperature minima characteristic of a CIL. The previous work of Osburn and Stedmon (2011) coupled several biomarkers including δ^{13}C-DOC, excitation-emission matrix fluorescence and dissolved lignin phenol concentrations in order to better understand organic matter reworking in these types of systems, although with a limited number of sampling stations. Only two of the sampling cruises from that study collected δ^{13}C-DOC data from depths near the local temperature minimum within the Baltic Sea proper, unsurprising for the winter cruise as the CIL is formed from meltwater at the tail-end of the winter season (Gilbert and Pettigrew 1997). Interestingly, there were observable differences in δ^{13}C-DOC between the surface waters and this CIL. Unlike in the present study where the DOC from the CIL was found to be more enriched in ^{13}C relative to the surface waters during both the spring 2015 and fall 2016 sampling
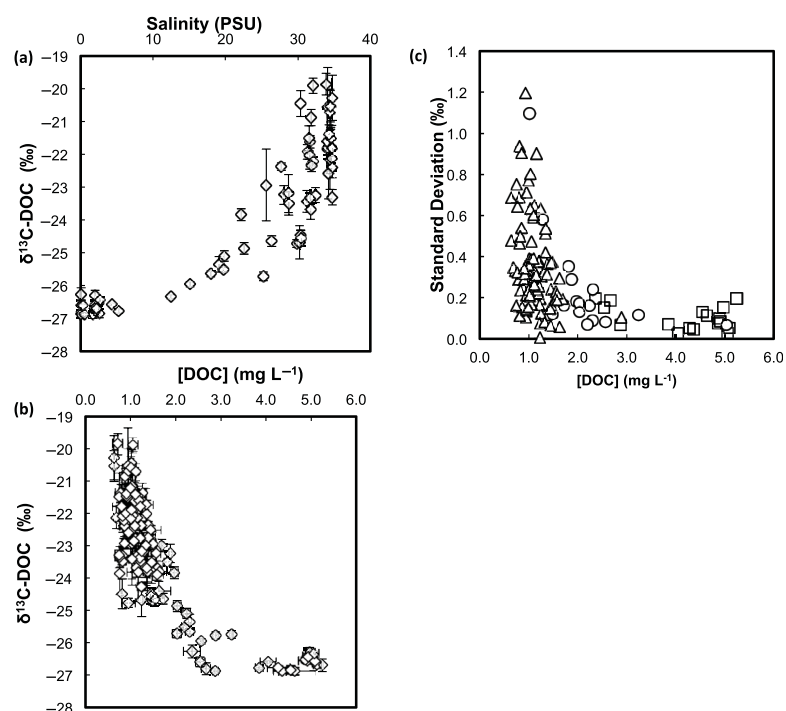
Fig. 5. (**a**) δ^{13}C-DOC signatures across the St. Lawrence Estuary and Gulf as a function of salinity. (**b**) δ^{13}C-DOC as a function of the DOC concentration. The error bars represent the 1σ standard deviation from four replicates for the DOC concentrations (horizontal) and δ^{13}C-DOC signatures (vertical). (**c**) 1σ standard deviations from replicate measurements as a function of DOC concentration for samples with salinities between 0–5 (open squares), 5–30 (open circles), and above 30 (open triangles).

missions, the shifts observed by Osburn and Stedmon (2011) showed an enrichment for the summer cruise (August 2006) while also showing a depletion during the fall (October 2006). More data specifically looking at differences between surface waters and sub-surface temperature minima from the region would be needed in order to compare the cause of these isotopic shifts across both systems.

Conclusion

This study represents the most comprehensive δ^{13}C-DOC dataset for Canada's east coast to date, a step toward building a comprehensive carbon budget for this region. The analytical precision obtained in this study was similar to that of Lalonde et al. (2014*a*), with standard deviations within 0.2‰ being expected for low salt samples with DOC concentrations greater than 2 mg L^{-1}, while those for salty, low DOC

concentration samples, corresponding to the majority of the data, were within 1‰ of the mean (Fig. 5). Terrestrial organic matter inputs can be tracked along fresh to saline water transition zones by exploiting the natural variations in DOC concentrations and δ^{13}C-DOC signatures between terrestrial and marine end-members. However, actual mass balance calculations are innately prone to large errors unless a series of suitable end-members are selected. The selection of the terrestrial end-member from regions where woody trees dominate the drainage basin is trivial, as seen by the high DOC concentrations and the lack of variability in freshwater δ^{13}C-DOC signatures (−26.6 ± 0.4‰ in the Upper St. Lawrence Estuary and Saguenay Fjord; Fig. 5a,b). The marine end-member is more difficult to constrain, with DOC concentrations varying between 0.6 mg L^{-1} and 1.0 mg L^{-1}, and δ^{13}C-DOC signatures varying between about −20‰ and −23‰ for samples with salinities of $\sim$ 35 (Fig. 5a). The larger isotopic

analytical uncertainty associated to the troublesome low DOC, high salt concentration samples ($\pm$ 0.5–1.2‰; Fig. 5c), combined to the higher natural variability found for their δ^{13}C-DOC signatures ($\pm$ 3.3‰; Fig. 5a), lower the discrimination power of isotope mass balance calculations. While mass balance calculations using the DOC concentration for the two end-members suggest largely conservative mixing along the river-estuary continuum (except for a few data points; data not shown), the δ^{13}C-DOC signatures tell a different story, with values that are lower than the conservative mixing line (Fig. 5a), suggesting preferential removal of DOC bearing a marine signature along the continuum. Such conclusions are however largely affected by the uncertainty attributable to the low analytical precision for the measured marine end-member signature, and by its natural variability. As an example of the effect of these two sources of uncertainty/variability on the discrimination power of simple isotopic mixing models, the relative standard deviation obtained when calculating the contribution of marine DOC to total DOC using the measured δ^{13}C-DOC signature is as high as 37.5% (12.5–37.5% for a marine contribution ranging between 20% and 80%) when factoring in the analytical precision of the marine end-member signature ($\pm$ 0.7‰), and it reaches 125% (81–125%, same contribution range) when its natural variability ($\pm$ 3.3‰) is taken into account. Furthermore, organic matter re-working further decreases the discriminating power of isotope mass balance calculations, where the terrestrial organic matter signature can be altered owing to the preferential photo-degradation of specific organic functionalities, as shown by Lalonde et al. (2014*b*). Isotopic mass balance calculations must thus be used with care, particularly in surface waters with a low suspended solid content and high exposure time to sunlight. Future studies targeting the aromatic DOC content, such as fluorescence measurements with PARAFAC analysis, of waters from the CIL could be used to determine if the enrichment in δ^{13}C-DOC signatures observed here are due to photo-oxidation or differences in DOC inputs from the northeast of the St. Lawrence.

References

Aiken, G. R. 1992. Chloride interference in the analysis of dissolved organic carbon by the wet oxidation method. Environ. Sci. Technol. **26**: 2435–2439. doi:10.1021/es00036a015

Alkhatib, M., C. J. Schubert, P. A. del Giorgio, Y. Gelinas, and M. F. Lehmann. 2012. Organic matter reactivity indicators in sediments of the St. Lawrence Estuary. Estuar. Coast. Shelf Sci. **102**: 36–47. doi:10.1016/j.ecss.2012.03.002

Bauer, J. E. 2002. Carbon isotopic composition of DOM, p. 405–453. *In* D. A. Hansell and D. E. Canfield [eds.], Biogeochemisty of marine dissolved organic matter. Elsevier.

Bauer, J. E., and E. R. M. Druffel. 1998. Ocean margins as a significant source of organic matter to the deep open ocean. Nature **392**: 482–485. doi:10.1038/33122

Bauer, J. E., E. R. Druffel, D. M. Wolgast, and S. Griffin. 2002. Temporal and regional variability in sources and cycling of DOC and POC in the northwest Atlantic continental shelf and slope. Deep-Sea Res. Part II Top. Stud. Oceanogr. **49**: 4387–4419. doi:10.1016/S0967-0645(02)00123-6

Bentley, S. J., and E. Kahlmeyer. 2012. Patterns and mechanisms of fluvial sediment flux and accumulation in two subarctic fjords: Nachvak and Saglek Fjords, Nunatsiavut, Canada. Can. J. Earth Sci. **49**: 1200–1215. doi:10.1139/e2012-052

Blough, N., and R. Del Vecchio. 2002. Chromophoric DOM in the coastal environment. *In* D. A. Hansell and D. E. Canfield [eds.], Biogeochemistry of marine dissolved organic matter. Elsevier.

Bouillon, S., M. Korntheuer, W. Baeyens, and F. Dehairs. 2006. A new automated setup for stable isotope analysis of dissolved organic carbon. Limnol. Oceanogr.: Methods **4**: 216–226. doi:10.4319/lom.2006.4.216

Bouillon, S., F. Dehairs, L.-S. Schiettecatte, and A. Vieira Borges. 2007. Biogeochemistry of the Tana estuary and delta (northern Kenya). Limnol. Oceanogr. **52**: 46–59. doi:10.4319/lo.2007.52.1.0046

Bouillon, S., A. Yambélé, R. G. M. Spencer, D. P. Gillikin, P. J. Hernes, J. Six, R. Merckx, and A. Borges. 2012. Organic matter sources, fluxes and greenhouse gas exchange in the Oubangui River (Congo River basin). Biogeosciences **9**: 2045–2062. doi:10.5194/bg-9-2045-2012

Bourgault, D., P. S. Galbraith, and G. Winkler. 2012. Exploratory observations of winter oceanographic conditions in the Saguenay Fjord. Atmos. Ocean **50**: 17–30. doi:10.1080/07055900.2012.659844

Brand, W. A. 2004. Mass spectrometer hardware for analyzing stable isotope ratios, p. 835–856. *In* P. A. de Groot [Ed.], Handbook of stable isotope analytical techniques, Elsevier, v. **1**.

Bugden, G. L. 1981. Salt and heat budgets for the Gulf of St. Lawrence. Can. J. Fish. Aquat. Sci. **38**: 1153–1167. doi:10.1139/f81-155

Cai, W.-J. 2011. Estuarine and coastal ocean carbon paradox: CO_2 sinks or sites of terrestrial carbon incineration? Ann. Rev. Mar. Sci. **3**: 123–145. doi:10.1146/annurev-marine-120709-142723

Coffin, R. B., and L. A. Cifuentes. 1999. Stable isotope analysis of carbon cycling in the Perdido Estuary, Florida. Estuaries Coast. **22**: 917–926. doi:10.2307/1353071

Conley, D. J., and others. 2009. Hypoxia-related processes in the Baltic Sea. Environ. Sci. Technol. **43**: 3412–3420. doi:10.1021/es802762a

Déry, S. J., M. Stieglitz, E. C. McKenna, and E. F. Wood. 2005. Characteristics and trends of river discharge into Hudson, James, and Ungava Bays, 1964–2000. J. Clim. **18**: 2540–2557. doi:10.1175/JCLI3440.1

Druffel, E. R., and P. M. Williams. 1992. Importance of isotope measurements in marine organic geochemistry. Mar. Chem. **39**: 209–215. doi:10.1016/0304-4203(92)90102-G

Druffel, E. R. M., S. Griffin, C. S. Glynn, R. Benner, and B. D. Walker. 2017. Radiocarbon in dissolved organic and inorganic carbon of the Arctic Ocean. Geophys. Res. Lett. **44**: 2369–2376. doi:10.1002/2016GL072138

Elliott, D. L., and S. K. Short. 1979. The northern limit of trees in Labrador: A discussion. Arctic **32**: 201–206. doi:10.14430/arctic2620

El-Sabh, M. I., and N. Silverberg. 2012. Oceanography of a large-scale estuarine system: The St. Lawrence. Springer New York.

Farquhar, G. D., J. R. Ehleringer, and K. T. Hubick. 1989. Carbon isotope discrimination and photosynthesis. Annu. Rev. Plant Biol. **40**: 503–537. doi:10.1146/annurev.pp.40.060189.002443

Federherr, E., C. Cerli, F. Kirkels, K. Kalbitz, H. J. Kupka, R. Dunsbach, L. Lange, and T. C. Schmidt. 2014. A novel high-temperature combustion based system for stable isotope analysis of dissolved organic carbon in aqueous samples. I: Development and validation. Rapid Commun. Mass Spectrom. **28**: 2559–2573. doi:10.1002/rcm.7052

Fry, B., W. Brand, F. Mersch, K. Tholke, and R. Garitt. 1992. Automated analysis system for coupled δ^{13}C and δ^{15}N measurements. Anal. Chem. **64**: 288–291. doi:10.1021/ac00027a009

Gilbert, D., and B. Pettigrew. 1997. Interannual variability (1948 1994) of the CIL core temperature in the Gulf of St. Lawrence. Can. J. Fish. Aquat. Sci. **54**: 57–67. doi:10.1139/cjfas-54-S1-57

Gilbert, D., B. Sundby, C. Gobeil, A. Mucci, and G.-H. Tremblay. 2005. A seventy-two-year record of diminishing deep-water oxygen in the St. Lawrence estuary: The northwest Atlantic connection. Limnol. Oceanogr. **50**: 1654–1666. doi:10.4319/lo.2005.50.5.1654

Goñi, M. A., and T. I. Eglinton. 1996. Stable carbon isotopic analyses of lignin-derived CuO oxidation products by isotope ratio monitoring-gas chromatography-mass spectrometry (irm-GC-MS). Org. Geochem. **24**: 601–615. doi:10.1016/0146-6380(96)00052-6

Granskog, M. A. 2012. Changes in spectral slopes of colored dissolved organic matter absorption with mixing and removal in a terrestrially dominated marine system (Hudson Bay, Canada). Mar. Chem. **134**: 10–17. doi:10.1016/j.marchem.2012.02.008

Granskog, M. A., R. W. Macdonald, C.-J. Mundy, and D. G. Barber. 2007. Distribution, characteristics and potential impacts of chromophoric dissolved organic matter (CDOM) in Hudson Strait and Hudson Bay, Canada. Cont. Shelf Res. **27**: 2032–2050. doi:10.1016/j.csr.2007.05.001

Guéguen, C., M. A. Granskog, G. McCullough, and D. G. Barber. 2011. Characterisation of colored dissolved organic matter in Hudson Bay and Hudson Strait using parallel factor analysis. J. Mar. Syst. **88**: 423–433. doi:10.1016/j.jmarsys.2010.12.001

Guo, L., P. H. Santschi, L. A. Cifuentes, S. E. Trumbore, and J. Southon. 1996. Cycling of high-molecular-weight dissolved organic matter in the Middle Atlantic Bight as revealed by carbon isotopic (^{13}C and ^{14}C) signatures. Limnol. Oceanogr. **41**: 1242–1252. doi:10.4319/lo.1996.41.6.1242

Guo, L., and R. W. Macdonald. 2006. Source and transport of terrigenous organic matter in the upper Yukon River: Evidence from isotope (δ^{13}C, Δ^{14}C, and δ^{15}N) composition of dissolved, colloidal, and particulate phases. Global Biogeochem. Cycles **20**: GB2011. doi:10.1029/2005GB002593

Guy, R. D., M. L. Fogel, and J. A. Berry. 1993. Photosynthetic fractionation of the stable isotopes of oxygen and carbon. Plant Physiol. **101**: 37–47. doi:10.1104/pp.101.1.37

Hedges, J. I., R. G. Keil, and R. Benner. 1997. What happens to terrestrial organic matter in the ocean? Org. Geochem. **27**: 195–212. doi:10.1016/S0146-6380(97)00066-1

Hélie, J.-F. 2004. Geochemistry and fluxes of organic and inorganic carbon in aquatic systems of Eastern Canada: Examples of the St. Lawrence River and Robert-Bourassa Reservoir: Isotopic approach. Ph.D. thesis. Univ. du Québec à Montréal.

Lalonde, K., P. Middlestead, and Y. Gélinas. 2014*a*. Automation of ^{13}C/^{12}C ratio measurement for freshwater and seawater DOC using high temperature combustion. Limnol. Oceanogr.: Methods **12**: 816–829. doi:10.4319/lom.2014.12.816

Lalonde, K., A. V. Vähätalo, and Y. Gélinas. 2014*b*. Revisiting the disappearance of terrestrial dissolved organic matter in the ocean: A δ^{13}C study. Biogeosciences **11**: 3707–3719. doi:10.5194/bg-11-3707-2014

Laruelle, G. G., R. Lauerwald, J. Rotschi, P. A. Raymond, J. Hartmann, and P. Regnier. 2015. Seasonal response of air-water CO_2 exchange along the land-ocean aquatic continuum of the northeast North American coast. Biogeosciences **12**: 1447–1454. doi:10.5194/bg-12-1447-2015

Locat, J., and C. Levesque. 2009. Le fjord du Saguenay: une physiographie et un registre exceptionnels. Rev. Sci. Eau J. Water Sci. **22**: 135–157. doi:10.7202/037479ar

Louchouarn, P., M. Lucotte, R. Canuel, J.-P. Gagné, and L.-F. Richard. 1997. Sources and early diagenesis of lignin and bulk organic matter in the sediments of the Lower St. Lawrence Estuary and the Saguenay Fjord. Mar. Chem. **58**: 3–26. doi:10.1016/S0304-4203(97)00022-4

Louchouarn, P., and M. Lucotte. 1998. A historical reconstruction of organic and inorganic contamination events in the Saguenay Fjord/St. Lawrence system from preindustrial times to the present. Sci. Total Environ. **213**: 139–150. doi:10.1016/S0048-9697(98)00085-0

Mucci, A., M. Starr, D. Gilbert, and B. Sundby. 2011. Acidification of lower St. Lawrence Estuary bottom waters.

Atmos. Ocean **49**: 206–218. doi:10.1080/07055900.2011.599265

Mundy, C. J., M. Gosselin, M. Starr, and C. Michelc. 2010. Riverine export and the effects of circulation on dissolved organic carbon in the Hudson Bay system, Canada. Limnol. Oceanogr. **55**: 315–323. doi:10.4319/lo.2010.55.1.0315

Osburn, C. L., and C. A. Stedmon. 2011. Linking the chemical and optical properties of dissolved organic matter in the Baltic-Noth Sea transition zone to differentiate three allochthonous inputs. Mar. Chem. **126**: 281–294. doi:10.1016/j.marchem.2011.06.007

Osburn, C. L., and G. St-Jean. 2007. The use of wet chemical oxidation with high-amplification isotope ratio mass spectrometry (WCO-IRMS) to measure stable isotope values of dissolved organic carbon in seawater. Limnol. Oceanogr.: Methods **5**: 296–308. doi:10.4319/lom.2007.5.296

Panetta, R. J., M. Ibrahim, and Y. Gélinas. 2008. Coupling a high-temperature catalytic oxidation total organic carbon analyzer to an isotope ratio mass spectrometer to measure natural-abundance δ^{13}C-dissolved organic carbon in marine and freshwater samples. Anal. Chem. **80**: 5232–5239. doi:10.1021/ac702641z

Perttilä, M., P. Tulkki, and S. Pietikäinen. 1980. Mean values and trends of hydrographical and chemical properties in the Gulf of Finland 1962–1978. Finn. Mar. Res. **247**: 38–50.

Peterson, B. J., and B. Fry. 1987. Stable isotopes in ecosystem studies. Annu. Rev. Ecol. Syst. **18**: 293–320. doi:10.1146/annurev.es.18.110187.001453

Peyton, G. R. 1993. The free-radical chemistry of persulfate-based total organic carbon analyzers. Mar. Chem. **41**: 91–103. doi:10.1016/0304-4203(93)90108-Z

Pocklington, R., and J. D. Leonard. 1979. Terrigenous organic matter in sediments of the St. Lawrence Estuary and the Saguenay Fjord. J. Fish. Board Can. **36**: 1250–1255. doi:10.1139/f79-179

Raymond, P. A., and J. E. Bauer. 2001*a*. Use of ^{14}C and ^{13}C natural abundances for evaluating riverine, estuarine, and coastal DOC and POC sources and cycling: A review and synthesis. Org. Geochem. **32**: 469–485.

Raymond, P. A., and J. E. Bauer. 2001*b*. Riverine export of aged terrestrial organic matter to the North Atlantic Ocean. Nature **409**: 497–500. doi:10.1038/35054034

Saliot, A., and others. 2002. Winter and spring characterization of particulate and dissolved organic matter in the Danube–Black Sea mixing zone. Estuar. Coast. Shelf Sci. **54**: 355–367. doi:10.1006/ecss.2000.0652

Schafer, C. T., J. N. Smith, and R. Côté. 1990. The Saguenay Fjord: A major tributary to the St. Lawrence Estuary, p. 378–420. *In* M. I. El-Sabh and N. Silverberg [eds.], Oceanography of a large-scale estuarine system. Springer New York.

Shaffer, G., J. Bendtsen, and O. Ulloa. 1999. Fractionation during remineralization of organic matter in the ocean.

Deep-Sea Res. Part Oceanogr. Res. Pap. **46**: 185–204. doi:10.1016/S0967-0637(98)00061-2

Sharp, J. H. 1997. Marine dissolved organic carbon: Are the older values correct? Mar. Chem. **56**: 265–277. doi:10.1016/S0304-4203(96)00075-8

Sharp, J. H., C. A. Carlson, E. T. Peltzer, D. M. Castle-Ward, K. B. Savidge, and K. R. Rinker. 2002. Final dissolved organic carbon broad community intercalibration and preliminary use of DOC reference materials. Mar. Chem. **77**: 239–253. doi:10.1016/S0304-4203(02)00002-6

Smith, J. N., and A. Walton. 1980. Sediment accumulation rates and geochronologies measured in the Saguenay Fjord using the Pb-210 dating method. Geochim. Cosmochim. Acta **44**: 225–240. doi:10.1016/0016-7037(80)90134-9

Spiker, E. C., and M. Rubin. 1975. Petroleum pollutants in surface and groundwater as indicated by the carbon-14 activity of dissolved organic carbon. Science **187**: 61–64. doi:10.1126/science.187.4171.61

Stepanauskas, R., N. O. JØrgensen, O. R. Eigaard, A. Žvikas, L. J. Tranvik, and L. Leonardson. 2002. Summer inputs of riverine nutrients to the Baltic Sea: Bioavailability and eutrophication relevance. Ecol. Monogr. **72**: 579–597. doi:10.1890/0012–9615(2002)072[0579:SIORNT]2.0.CO;2]

St-Onge, G., and C. Hillaire-Marcel. 2001. Isotopic constraints of sedimentary inputs and organic carbon burial rates in the Saguenay Fjord, Quebec. Mar. Geol. **176**: 1–22. doi:10.1016/S0025-3227(01)00150-5

Straneo, F., and F. Saucier. 2008. The outflow from Hudson Strait and its contribution to the Labrador Current. Deep-Sea Res. Part Oceanogr. Res. Pap. **55**: 926–946. doi:10.1016/j.dsr.2008.03.012

Telang, S. A., R. Pocklington, A. S. Naidu, E. A. Romankevich, I. I. Gitelson, and M. I. Gladyshev. 1991. Carbon and mineral transport in major North American, Russian arctic, and Siberian rivers: The St. Lawrence, the Mackenzie, the Yukon, the arctic Alaskan rivers, the arctic basin rivers in the Soviet Union, and the Yenisei, p. 75–104. *In* E. T. Degens, S. Kempe, and J. E. Richey [Eds.], Biogeochemistry of major world rivers, Chichester: John Wiley, v. **42**.

Tremblay, L., and J.-P. Gagné. 2009. Organic matter distribution and reactivity in the waters of a large estuarine system. Mar. Chem. **116**: 1–12. doi:10.1016/j.marchem.2009.09.006

Wang, X.-C., and E. R. M. Druffel. 2001. Radiocarbon and stable carbon isotope compositions of organic compound classes in sediments from the NE Pacific and Southern Oceans. Mar. Chem. **73**: 65–81. doi:10.1016/S0304-4203(00)00090-6

Ward, N. D., T. S. Bianchi, P. M. Medeiros, M. Seidel, J. E. Richey, R. G. Keil, and H. O. Sawakuchi. 2017. Where carbon goes when water flows: Carbon cycling across the aquatic continuum. Front. Mar. Sci. **4**: 7. doi:10.3389/fmars.2017.00007

Williams, P. M., and E. R. Druffel. 1987. Radiocarbon in dissolved organic matter in the central North Pacific Ocean. Nature **330**: 246–248. doi:10.1038/330246a0

Wilton, D. H. 1996. Metallogenic overview of the Nain Province, northern Labrador. CIM Bull. **89**: 43–52.

Xie, H., C. Aubry, S. Bélanger, and G. Song. 2012. The dynamics of absorption coefficients of CDOM and particles in the St. Lawrence estuarine system: Biogeochemical and physical implications. Mar. Chem. **128**: 44–56. doi:10.1016/j.marchem.2011.10.001

Yamashita, Y., S. L. McCallister, B. P. Koch, M. Gonsior, and R. Jaffé. 2015. Dynamics of dissolved organic matter in fjord ecosystems: Contributions of terrestrial dissolved organic matter in the deep layer. Estuar. Coast. Shelf Sci. **159**: 37–49. doi:10.1016/j.ecss.2015.03.024

Yeats, P. A., and J. M. Bewers. 1976. Trace metals in the waters of the Saguenay fjord. Can. J. Earth Sci. **13**: 1319–1327. doi:10.1139/e76-133

Zhang, Y., and H. Xie. 2015. Photomineralization and photomethanification of dissolved organic matter in Saguenay River surface water. Biogeosciences **12**: 6823–6836. doi:10.5194/bg-12-6823-2015

Conflict of Interest

None declared.

RÉFÉRENCES BIBLIOGRAPHIQUES

Aiken, G., 2002. Organic Matter in Ground Water. U . S . Geol. Surv. Artif. Recharg. Work. April 2-4, 2002, Sacramento , Calif. 21–22.

Anschutz, P., Smith, T., Mouret, A., Deborde, J., Bujan, S., Poirier, D., Lecroart, P., 2009. Tidal sands as biogeochemical reactors. Estuar. Coast. Shelf Sci. 84, 84–90. doi:10.1016/j.ecss.2009.06.015

Aravena, R., Wassenaar, L.I., 1993. Dissolved organic carbon and methane in a regional confined aquifer , Southern Ontario , Canada : Carbon isotope evidence for associated subsurface sources. Appl. Geochemistry 8, 483–493. doi:10.1016/0883-2927(93)90077-T

Aravena, R., Wassenaar, L.I., Spiker, E.C., 2004. Chemical and carbon isotopic composition of dissolved organic carbon in a regional confined methanogenic aquifer. Isotopes Environ. Health Stud. 40, 103–14. doi:10.1080/10256010410001671050

Avery, G.B., Kieber, R.J., Taylor, K.J., Dixon, J.L., 2012. Dissolved organic carbon release from surface sand of a high energy beach along the Southeastern Coast of North Carolina, USA. Mar. Chem. 132–133, 23–27. doi:10.1016/j.marchem.2012.01.006

Barber, A., Brandes, J., Leri, A., Lalonde, K., Balind, K., Wirick, S., Wang, J., Gélinas, Y., 2017a. Preservation of organic matter in marine sediments by inner-sphere interactions with reactive iron. Sci. Rep. 7, 366. doi:10.1038/s41598-017-00494-0

Barber, A., Sirois, M., Chaillou, G., Gélinas, Y., 2017b. Stable Isotope Analysis of Dissolved Organic Carbon in Canada's Eastern Coastal Waters. Limnol. Oceanogr. doi:10.1002/lno.10666

Bauer, J.E., 2002. Carbon Isotopic Composition of DOM, Biogeochemistry of Marine Dissolved Organic Matter. doi:10.1016/B978-012323841-2/50010-5

Bauer, J.E., Cai, W.-J., Raymond, P. a, Bianchi, T.S., Hopkinson, C.S., Regnier, P. a G., 2013. The changing carbon cycle of the coastal ocean. Nature 504, 61–70. doi:10.1038/nature12857

Beck, A.J., Tsukamoto, Y., Tovar-Sanchez, A., Huerta-Diaz, M., Bokuniewicz, H.J., Sañudo-Wilhelmy, S. a., 2007. Importance of geochemical transformations in determining submarine groundwater discharge-derived trace metal and nutrient fluxes.

Appl. Geochemistry 22, 477–490. doi:10.1016/j.apgeochem.2006.10.005

Beck, M., Reckhardt, A., Amelsberg, J., Bartholomä, A., Brumsack, H.J., Cypionka, H., Dittmar, T., Engelen, B., Greskowiak, J., Hillebrand, H., Holtappels, M., Neuholz, R., Köster, J., Kuypers, M.M.M., Massmann, G., Meier, D., Niggemann, J., Paffrath, R., Pahnke, K., Rovo, S., Striebel, M., Vandieken, V., Wehrmann, A., Zielinski, O., 2017. The drivers of biogeochemistry in beach ecosystems: A cross-shore transect from the dunes to the low-water line. Mar. Chem. 190, 35–50. doi:10.1016/j.marchem.2017.01.001

Benner, R., Louchouarn, P., Amon, R.M.W., 2005. Terrigenous dissolved organic matter in the Arctic Ocean and its transport to surface and deep waters of the North Atlantic. Global Biogeochem. Cycles 19, 1–11. doi:10.1029/2004GB002398

Bianchi, T.S., 2011. The role of terrestrially derived organic carbon in the coastal ocean: A changing paradigm and the priming effect. Proc. Natl. Acad. Sci. 108, 19473–19481. doi:10.1073/pnas.1017982108

Boudreau, B.P., Huettel, M., Forster, S., Jahnke, R.A., McLachlan, A., Middelburg, J.J., Nielsen, P., Sansone, F., Taghon, G., Van Raaphorst, W., Webster, I., Weslawski, J.M., Wiberg, P., Sundby, B., 2001. Permeable marine sediments: Overturning an old paradigm. Eos (Washington. DC). 82, 133–136. doi:10.1029/EO082i011p00133-01

Bouillon, S., Yambélé, A., Spencer, R.G.M., Gillikin, D.P., Hernes, P.J., Six, J., Merckx, R., Borges, A. V., 2012. Organic matter sources, fluxes and greenhouse gas exchange in the Oubangui River (Congo River basin). Biogeosciences 9, 2045–2062. doi:10.5194/bg-9-2045-2012

Boyle, E.A., Edmond, J.M., Sholkovitz, E.R., 1977. The mechanism of iron removal in estuaries. Geochim. Cosmochim. Acta 41, 1313–1324. doi:10.1016/0016-7037(77)90075-8

Brisebois, D., 1981. Lithostratigraphie des strates permo-car- bonifères, de l'archipel des Îles-de-la-Madeleine. Ministère de l'Énergie et des Ressources Direction Générale des Energies Conventionnelles, Service de l'Exploration, Québec, Canada, Rep. DPV-796, 1981.

Burban, P.-Y., Lick, W., Lick, J., 1989. The flocculation of fine-grained sediments in estuarine waters. J. Geophys. Res. 94, 8323–8330. doi:10.1029/JC094iC06p08323

Burdige, D.J., 2005. Burial of terrestrial organic matter in marine sediments: A re-assessment. Global Biogeochem. Cycles 19, 1–7. doi:10.1029/2004GB002368

Burnett, W.C., Aggarwal, P.K., Aureli, A., Bokuniewicz, H., Cable, J.E., Charette, M.A., Kontar, E., Krupa, S., Kulkarni, K.M., Loveless, A., Moore, W.S., Oberdorfer, J.A., Oliveira, J., Ozyurt, N., Povinec, P., Privitera, A.M.G., Rajar, R., Ramessur, R.T.,

Scholten, J., Stieglitz, T., Taniguchi, M., Turner, J. V., 2006. Quantifying submarine groundwater discharge in the coastal zone via multiple methods. Sci. Total Environ. 367, 498–543. doi:10.1016/j.scitotenv.2006.05.009

Cai, W.-J., 2011. Estuarine and coastal ocean carbon paradox: CO2 sinks or sites of terrestrial carbon incineration? Ann. Rev. Mar. Sci. 3, 123–145. doi:10.1146/annurev-marine-120709-142723

Cai, W.J., Wang, Y., Krest, J., Moore, W.S., 2003. The geochemistry of dissolved inorganic carbon in a surficial groundwater aquifer in North Inlet, South Carolina, and the Carbon fluxes to the coastal ocean. Geochim. Cosmochim. Acta 67, 631–637. doi:10.1016/S0016-7037(02)01167-5

Chaillou, G., Couturier, M., Tommi-morin, G., Rao, A.M., 2014. Total alkalinity and dissolved inorganic carbon production in groundwaters discharging through a sandy beach. Procedia Earth Planet. Sci. 10, 88–99. doi:10.1016/j.proeps.2014.08.017

Chaillou, G., Lemay-Borduas, F., Couturier, M., 2016. Transport and transformations of groundwater-borne carbon discharging through a sandy beach to coastal ocean. Can. Water Resour. J. 38, 809–828. doi:10.1080/07011784.2015.1111775

Chaillou, G., Lemay-Borduas, F., Larocque, M., Couturier, M., Biehler, A., Tommi-Morin, G., 2017. Flow and discharge of groundwater from a sandy beach : Îles-de-la-Madeleine , Quebec (Canada). J. Hydrol. 557, 1–51. doi:10.1016/j.jhydrol.2017.12.010

Charbonnier, C., Anschutz, P., Poirier, D., Bujan, S., Lecroart, P., 2013. Aerobic respiration in a high-energy sandy beach. Mar. Chem. 155, 10–21. doi:10.1016/j.marchem.2013.05.003

Charette, M.A., Sholkovitz, E.R., 2006. Trace element cycling in a subterranean estuary : Part 2. Geochemistry of the pore water. Geochim. Cosmochim. Acta 70, 811–826. doi:10.1016/j.gca.2005.10.019

Charette, M.A., Sholkovitz, E.R., 2002. Oxidative precipitation of groundwater-derived ferrous iron in the subterranean estuary of a coastal bay. Geophys. Res. Lett. 29, 1–4. doi:10.1029/2001GL014512

Charette, M.A., Sholkovitz, E.R., Hansel, C.M., 2005. Trace element cycling in a subterranean estuary : Part 1. Geochemistry of the permeable sediments. Geochim. Cosmochim. Acta 69, 2095–2109. doi:10.1016/j.gca.2004.10.024

Chen, C., Dynes, J.J., Wang, J., Sparks, D.L., 2014. Properties of Fe-Organic Matter Associations via Coprecipitation versus Adsorption. Environ. Sci. Technol. 48, 13751–9. doi:10.1021/es503669u

Chmura, G.L.., Aharon, P., 1995. Stable carbon isotope signatures of sedimentary carbón in

coastal wetlands as indicators of salinity regime. J. Coast. Res. 11, 124–135.

Cho, H.M., Kim, G., 2016. Determining groundwater Ra end-member values for the estimation of the magnitude of submarine groundwater discharge using Ra isotope tracers. Geophys. Res. Lett. 43, 3865–3871. doi:10.1002/2016GL068805

Ciais, P., Sabine, C., Bala, G., Bopp, L., Brovkin, V., Canadell, J., Chhabra, A., DeFries, R., Galloway, J., Heimann, M., Jones, C., Quéré, C. Le, Myneni, R.B., Piao, S., Thornton, P., 2013. Carbon and Other Biogeochemical Cycles. Clim. Chang. 2013 - Phys. Sci. Basis 465–570. doi:10.1017/CBO9781107415324.015

Clark, I., Fritz, P., 1986. Environmental Isotopes in Hydrogeology, Lewis Publ. ed. New York. doi:10.1016/B978-0-444-81546-0.50005-7

Cole, J.J., Prairie, Y.T., Caraco, N.F., McDowell, W.H., Tranvik, L.J., Striegl, R.G., Duarte, C.M., Kortelainen, P., Downing, J.A., Middelburg, J.J., Melack, J., 2007. Plumbing the Global Carbon Cycle: Integratin Inland Waters into the Terrestrial Carbon Budget. Int. Electron. J. Elem. Educ. 10, 171–184. doi:10.1007/s

Couturier, M., Nozais, C., Chaillou, G., 2016. Microtidal subterranean estuaries as a source of fresh terrestrial dissolved organic matter to the coastal ocean. Mar. Chem. 186, 46–57. doi:10.1016/j.marchem.2016.08.001

Couturier, M., Tommi-Morin, G., Sirois, M., Rao, A., Nozais, C., Chaillou, G., 2017. Nitrogen transformations along a shallow subterranean estuary. Biogeosciences 14, 3321–3336. doi:10.5194/bg-2016-535

Defeo, O., McLachlan, A., Schoeman, D.S., Schlacher, T.A., Dugan, J., Jones, A., Lastra, M., Scapini, F., 2009. Threats to sandy beach ecosystems: A review. Estuar. Coast. Shelf Sci. 81, 1–12. doi:10.1016/j.ecss.2008.09.022

Dittmar, T., Koch, B., Hertkorn, N., Kattner, G., 2008. A simple and efficient method for the solid-phase extraction of dissolved organic matter (SPE-DOM) from seawater. Limnol. Oceanogr. Methods 6, 230–235. doi:10.4319/lom.2008.6.230

Dorsett, A., Cherrier, J., Martin, J.B., Cable, J.E., 2011. Assessing hydrologic and biogeochemical controls on pore-water dissolved inorganic carbon cycling in a subterranean estuary: A 14C and 13C mass balance approach. Mar. Chem. 127, 76–89. doi:10.1016/j.marchem.2011.07.007

Douglas, B.C., 1990. Global sea level rise. J. Geophys. Res.

Druffel, E.R.M., Williams, P.M., 1992. Importance of isotope measurements in marine organic geochemistry. Mar. Chem. 38, 209–215. doi:10.1016/j.cognition.2008.05.007

Dugan, J.E., Defeo, O., Jaramillo, E., Jones, A.R., Lastra, M., Nel, R., Peterson, C.H., Scapini, F., Schlacher, T., Schoeman, D.S., 2010. Give beach ecosystems their day in

the sun. Science (80-.). 329, 1146. doi:10.1126/science.329.5996.1146-a

Edzwald, J.K., Upchurch, J.B., O'Melia, C.R., 1974. Coagulation in Estuaries. Environ. Sci. Technol. 8, 58–63. doi:10.1021/es60086a003

Emery, K., 1968. Relict sediments on continental shelves of the world. Am. Assoc. Pet. Geol. Bull. 52, 445–464.

Filip, Z., Smed-Hildmann, R., 1992. Does fossil plant material release humic substances into groundwaters? Sci. Total Environ. 117, 313–317. doi:10.1016/0048-9697(92)90098-D

Froelich, P.N., Klinkhammer, G.P., Bender, M.L., Luedtke, N.A., Heath, G.R., Cullen, D., Dauphin, P., Hammond, D., Hartman, B., Maynard, V., 1979. Early oxidation of organic matter in pelagic sediments of the eastern equatorial Atlantic: suboxic diagensis. Geochim. Cosmochim. Acta 43, 1075–1090. doi:10.1016/0016-7037(79)90095-4

Gehrels, W.R., 1994. Determining relative sea-level change from salt-marsh foraminifera and plant zones on the coast of Maine, USA. J. Coast. Res. 10, 990–1009. doi:0749-0208

Gehrels, W.R., Belknap, D.F., Black, S., Newnham, R.M., 2002. Rapid sea-level rise in the Gulf of Maine, USA, since AD 1800. The Holocene 12, 383–389.

Gehrels, W.R., Milne, G.A., Kirby, J.R., Patterson, R.T., Belknap, D.F., 2004. Late Holocene sea-level changes and isostatic crustal movements in Atlantic Canada. Quat. Int. 120, 79–89. doi:10.1016/j.quaint.2004.01.008

Goñi, M.A., Gardner, L.R., 2004. Seasonal Dynamics in Dissolved Organic Carbon Concentrations in a Coastal Water-Table Aquifer at the Forest-Marsh Interface. Aquat. Geochemistry 9, 209–232. doi:10.1023/B:AQUA.0000022955.82700.ed

Goñi, M.A., Hedges, J.I., 1995. Sources and reactivities of marine-derived organic matter in coastal sediments as determined by alkaline CuO oxidation. Geochim. Cosmochim. Acta 59, 2965–2981. doi:10.1016/0016-7037(95)00188-3

Goñi, M.A., Montgomery, S., 2000. Alkaline CuO oxidation with a microwave digestion system: Lignin analyses of geochemical samples. Anal. Chem. 72, 3116–3121. doi:10.1021/ac991316w

Gregory, J., Duan, J., 2001. Hydrolyzing metal salts as coagulants. Pure Appl ied Chem. 73, 2017–2026. doi:10.1351/pac200173122017

Guenet, B., Danger, M., Abbadie, L., Lacroix, G., 2010. Priming effet : bridging the gap between terrestrial and aquatic ecology. Ecology 91, 2850–2861.

Guggenberger, G., Kaiser, K., 2003. Dissolved organic matter in soil: Challenging the paradigm of sorptive preservation. Geoderma 113, 293–310. doi:10.1016/S0016-7061(02)00366-X

Guy, R.D., Fogel, M.L., Berry, J.A., 1993. Photosynthetic Fractionation of the Stable Isotopes of Oxygen and Carbon. Plant Physiol. 101, 37–47. doi:10.1104/pp.101.1.37

Haese, R.R., 2006. The biogeochemistry of iron, 2e édition. ed, Marine Geochemistry. Springer Verlag, Berlin, Heidelberg. doi:10.1007/3-540-32144-6_7

Hastings, R.H., Goñi, M.A., Wheatcroft, R.A., Borgeld, J.C., 2012. A terrestrial organic matter depocenter on a high-energy margin: The Umpqua River system, Oregon. Cont. Shelf Res. 39–40, 78–91. doi:10.1016/j.csr.2012.04.002

Hayes, J.M., 1993. Factors controlling 13C contents of sedimentary organic compounds: Principles and evidence. Mar. Geol. 113, 111–125. doi:10.1016/0025-3227(93)90153-M

Hedges, J.I., Keil, R.G., 1995. Sedimentary organic matter preservation: an assessment and speculative synthesis. Mar. Chem. 49, 137–139. doi:10.1016/0304-4203(95)00013-H

Hedges, J.I., Keil, R.G., Benner, R., 1997. What happens to terrestrial organic matter in the ocean? Org. Geochem. 27, 195–212. doi:10.1016/S0146-6380(97)00066-1

Hedges, J.I., Stern, J.H., 1984. Carbon and nitrogen determinations of carbonate-containing solids. Limnol. Oceanogr. 29, 657–663. doi:10.4319/lo.1984.29.3.0657

Heiss, J.W., Michael, H.A., 2014. Saltwater-freshwatermixing dynamics in a sandy beach aquifer over tidal, spring-neap, and seasonal cycles. J. Hydrol. 6, 6747–6766. doi:10.1002/2012WR013085.Received

Helms, J.R., Stubbins, A., Ritchie, J.D., Minor, E.C., Kieber, D.J., Mopper, K., 2008. Absorption spectral slopes and slope ratios as indicators of molecular weight, source, and photobleaching of chromophoric dissolved organic matter. Limonology Oceanogr. 53, 955–969. doi:10.4319/lo.2008.53.3.0955

Henrichs, S.M., 1995. Sedimentary organic matter preservation: an assessment and speculative synthesis—a comment. Mar. Chem. 49, 127–136.

Heymans, J.J., McLachlan, a, 1996. Carbon budget and network analysis of a high-energy beach/surf-zone ecosystem. Estuar. Coast. Shelf Sci. 43, 485–505. doi:10.1006/ecss.1996.0083

Hinkel, J., Nicholls, R.J., Tol, R.S.J., Wang, Z.B., Hamilton, J.M., Boot, G., Vafeidis, A.T., McFadden, L., Ganopolski, A., Klein, R.J.T., 2013. A global analysis of erosion of sandy beaches and sea-level rise: An application of DIVA. Glob. Planet. Change 111, 150–158. doi:10.1016/j.gloplacha.2013.09.002

Hoefs, J., 2009. Stable Isotope Geochemistry, 6th editio. ed.

Huettel, M., 2017. Estuarine and nearhore sediments : biogeochemical hot spots in the coastal zone. 14th International Estuarine Biogeochemistry Symposium, 4-7 juin 2017, Rimouski (Canada)

Huettel, M., Rusch, A., 2000. Transport and degradation of phytoplankton in permeable sediment. Limnol. Oceanogr. 45, 534–549. doi:10.4319/lo.2000.45.3.0534

Huettel, M., Ziebis, W., Forster, S., 1996. Flow-induced uptake of particulate matter in permeable sediments. Limnol. Oceanogr. 151, 41–52. doi:10.4319/lo.1996.41.2.0309

Huguet, A., Vacher, L., Relexans, S., Saubusse, S., Froidefond, J.M., Parlanti, E., 2009. Properties of fluorescent dissolved organic matter in the Gironde Estuary. Org. Geochem. 40, 706–719. doi:10.1016/j.orggeochem.2009.03.002

Jones, D.L., Edwards, A.C., 1998. Influence of sorption on the biological utilization of two simple carbon substrates. Soil Biol. Biochem. 30, 1895–1902. doi:10.1016/S0038-0717(98)00060-1

Juneau, M.-N., 2012. Pas de texte Hausse récente du niveau marin relatif aux îles de la Madeleine. Université du Québec à Rimouski.

Kaiser, K., Guggenberger, G., 2003. Mineral surfaces and soil organic matter. Eur. J. Soil Sci. 54, 219–236. doi:10.1046/j.1365-2389.2003.00544.x

Kaiser, K., Guggenberger, G., 2000. The role of DOM sorption to mineral surfaces in the preservation of organic matter in soils. Org. Geochem. 31, 711–725. doi:10.1016/S0146-6380(00)00046-2

Kaiser, K., Guggenberger, G., Haumaier, L., 2004. Changes in Dissolved Lignin-Derived Phenols , Neutral Sugars , Uronic Acids , and Amino Sugars with Depth in Forested Haplic Arenosols and Rendzic Leptosols. Biogeochemistry 70, 135–151. doi:10.1023/B:BIOG.0000049340.77963.18

Kaiser, K., Guggenbergre, G., Zech, W., 2001. Isotopic fractionation of dissolved organic carbon in shallow forest soils as affected by sorption. Eur. J. Soil Sci. 52, 585–597. doi:10.1046/j.1365-2389.2001.00407.x

Kalbitz, K., Solinger, S., Park, J.-H., Michalzik, B., Matzner, E., 2000. CONTROLS ON THE DYNAMICS OF DISSOLVED ORGANIC MATTER IN SOILS : A REVIEW. Soil Sci. 165, 277–304.

Keil, R., Montluçon, D., Prahl, F., Hedges, J., 1994. Sorptive preservation of labile organic matter in marine sediments. Nature 370, 549–552. doi:10.1038/370549a0

Keil, R.G., Montlucon, D.B., Prahl, F.R., Hedges, J.I., 1994. Sorptive preservation of labile

organic matter in marine sediments. Nature 370, 549–552.

Kim, J., Kim, G., 2017. Inputs of hymis fluorescent dissolved organic matter via submarine groundwater discharge to coastal waters off a volcanic island (Jeju, Korea). Sci. Rep. 7, 1–9. doi:10.1038/s41598-017-08518-5

Kim, T.-H., Waska, H., Kwon, E., Suryaputra, I.G.N., Kim, G., 2012. Production, degradation, and flux of dissolved organic matter in the subterranean estuary of a large tidal flat. Mar. Chem. 142–144, 1–10. doi:10.1016/j.marchem.2012.08.002

Kim, T.H., Kwon, E., Kim, I., Lee, S.A., Kim, G., 2013. Dissolved organic matter in the subterranean estuary of a volcanic island, Jeju: Importance of dissolved organic nitrogen fluxes to the ocean. J. Sea Res. 78, 18–24. doi:10.1016/j.seares.2012.12.009

Lalonde, K., Middlestead, P., Gélinas, Y., 2014a. Automation of 13C/12C ratio measurement for freshwater and seawater DOC using high temperature combustion. Limnol. Oceanogr. Methods 12, 816–829. doi:10.4319/lom.2014.12.816

Lalonde, K., Mucci, A., Ouellet, A., Gélinas, Y., 2012. Preservation of organic matter in sediments promoted by iron. Nature 483, 198–200. doi:10.1038/nature10855

Lalonde, K., Vähätalo, A. V., Gélinas, Y., 2014b. Revisiting the disappearance of terrestrial dissolved organic matter in the ocean: A δ13C study. Biogeosciences 11, 3707–3719. doi:10.5194/bg-11-3707-2014

Linkhorst, A., Dittmar, T., Waska, H., 2017. Molecular fractionation of dissolved organic matter in a shallow subterranean estuary: the role of the iron curtain. Environ. Sci. Technol. 51, 1312–1320. doi:10.1021/acs.est.6b03608

Madelin'Eau, 2004. Gestion des eaux souterraines aux Îles-de-la-Madeleine un défi de développement durable, Final Report.

Maher, D.T., Santos, I.R., Golsby-Smith, L., Gleeson, J., Eyre, B.D., 2013. Groundwater-derived dissolved inorganic and organic carbon exports from a mangrove tidal creek: The missing mangrove carbon sink? Limnol. Oceanogr. 58, 475–488. doi:10.4319/lo.2013.58.2.0475

Mayorga, E., Aufdenkampe, A.K., Masiello, C.A., Krusche, A. V., Hedges, J.I., Quay, P.D., Richey, J.E., Brown, T.A., 2005. Young organic matter as a source of carbon dioxide outgassing from Amazonian rivers. Nature 436, 538–541. doi:10.1038/nature03880

McCoy, C.A., Corbett, D.R., 2009. Review of submarine groundwater discharge (SGD) in coastal zones of the Southeast and Gulf Coast regions of the United States with management implications. J. Environ. Manage. 90, 644–651. doi:10.1016/j.jenvman.2008.03.002

Mcknight, D.M., Boyer, E.W., Westerhoff, P.K., Doran, P.T., Kulbe, T., Andersen, D.T., 2001. Spectrofluorometric characterization of dissolved organic matter for indication of precursor organic material and aromaticity. Limnol. Ocean. 46, 38–48. doi:10.4319/lo.2001.46.1.0038

McLachlan, A., Brown, A.C., 2006. The Ecology of Sandy Shores, Academic P. ed. Burlington, MA.

Mehra, O.P., Jackson, M.L., 1960. Iron oxide removal from soils and clays by a dithionite-citrate system buffered with sodium bicarbonate. Clays anf Clay Miner. 7, 317–327.

Mikutta, R., Lorenz, D., Guggenberger, G., Haumaier, L., Freund, A., 2014. Properties and reactivity of Fe-organic matter associations formed by coprecipitation versus adsorption: Clues from arsenate batch adsorption. Geochim. Cosmochim. Acta 144, 258–276. doi:10.1016/j.gca.2014.08.026

Moore, W.S., 2010. The Effect of Submarine Groundwater Discharge on the Ocean. Ann. Rev. Mar. Sci. 2, 59–88. doi:10.1146/annurev-marine-120308-081019

Moore, W.S., 1999. The subterranean estuary: A reaction zone of ground water and sea water. Mar. Chem. 65, 111–125. doi:10.1016/S0304-4203(99)00014-6

Moore, W.S., Beck, M., Riedel, T., Rutgers van der Loeff, M., Dellwig, O., Shaw, T.J., Schnetger, B., Brumsack, H.J., 2011. Radium-based pore water fluxes of silica, alkalinity, manganese, DOC, and uranium: A decade of studies in the German Wadden Sea. Geochim. Cosmochim. Acta 75, 6535–6555. doi:10.1016/j.gca.2011.08.037

Nel, R., Campbell, E.E., Harris, L., Hauser, L., Schoeman, D.S., McLachlan, A., du Preez, D.R., Bezuidenhout, K., Schlacher, T.A., 2014. The status of sandy beach science: Past trends, progress, and possible futures. Estuar. Coast. Shelf Sci. 150, 1–10. doi:10.1016/j.ecss.2014.07.016

Nevin, K.P., Lovley, D.R., 2002. Mechanisms for Fe(III) Oxide Reduction in Sedimentary Environments. Geomicrobiol. J. 19, 141–159. doi:10.1080/01490450252864253

Osburn, C.L., Stedmon, C.A., 2011. Linking the chemical and optical properties of dissolved organic matter in the Baltic-North Sea transition zone to differentiate three allochthonous inputs. Mar. Chem. 126, 281–294. doi:10.1016/j.marchem.2011.06.007

Palmer, S.M., Hope, D., Billett, M.F., Dawson, J.J.C., Bryant, C.L., 2011. Sources of Organic and Inorganic Carbon in a Headwater Stream : Evidence from Carbon Isotope Studies. Biogeochemistry 52, 321–338. doi:10.1023/A:1006447706565

Peterson, B.J., Fry, B., 1987. Stable isotopes in ecosystem studies. Annu. Rev. Ecol. Syst. 293–320. doi:10.1146/annurev.es.18.110187.001453

Poulin, B.A., Ryan, J.N., Aiken, G.R., 2014. The effects of Iron on Optical Properties of

Dissolved Organic Matter. Environ. Sci. Technol. 48, 10098–10106. doi:10.1021/es502670r

Raymond, P.A., Bauer, J.E., 2001. Use of 14C and 13C natural abundances for evaluating riverine, estuarine, and coastal DOC and POC sources and cycling: A review and synthesis. Org. Geochem. 32, 469–485. doi:10.1016/S0146-6380(00)00190-X

Riedel, T., Biester, H., Dittmar, T., 2012. Molecular fractionation of dissolved organic matter with metal salts. Environ. Sci. Technol. 46, 4419–4426. doi:10.1021/es203901u

Riedel, T., Zak, D., Biester, H., Dittmar, T., 2013. Iron traps terrestrially derived dissolved organic matter at redox interfaces. Proc. Natl. Acad. Sci. 110, 10101–10105. doi:10.1073/pnas.1221487110

Robinson, C., Li, L., Barry, D. a., 2007. Effect of tidal forcing on a subterranean estuary. Adv. Water Resour. 30, 851–865. doi:10.1016/j.advwatres.2006.07.006

Rocha, C., Ibanhez, J., Leote, C., 2009. Benthic nitrate biogeochemistry affected by tidal modulation of Submarine Groundwater Discharge (SGD) through a sandy beach face, Ria Formosa, Southwestern Iberia. Mar. Chem. 115, 43–58. doi:10.1016/j.marchem.2009.06.003

Roy, M., Martin, J.B., Cable, J.E., Smith, C.G., 2013. Variations of iron flux and organic carbon remineralization in a subterranean estuary caused by inter-annual variations in recharge. Geochim. Cosmochim. Acta 103, 301–315. doi:10.1016/j.gca.2012.10.055

Roy, M., Martin, J.B., Smith, C.G., Cable, J.E., 2011. Reactive-transport modeling of iron diagenesis and associated organic carbon remineralization in a Florida (USA) subterranean estuary. Earth Planet. Sci. Lett. 304, 191–201. doi:10.1016/j.epsl.2011.02.002

Rullkötter, J., 2006. Organic Matter: The Driving Force for Early Diagenesis, 2nd Editio. ed, Marine Geochemistry.

Sanderman, J., Lohse, K.A., Baldock, J.A., Amundson, R., 2009. Linking soils and streams: Sources and chemistry of dissolved organic matter in a small coastal watershed. Water Resour. Res. 45, 1–13. doi:10.1029/2008WR006977

Sanders, C.J., Santos, I.R., Sadat-Noori, M., Maher, D.T., Holloway, C., Schnetger, B., 2017. Uranium export from a sandy beach subterranean estuary in Autralia. Estuar. Coast. Shelf Sci. 1–33. doi:10.1016/j.ecss.2017.09.002

Santos, I.R., Burnett, W.C., Chanton, J., Mwashote, B., Suryaputra, I.G.N. a., Dittmar, T., 2008. Nutrient biogeochemistry in a Gulf of Mexico subterranean estuary and groundwater-derived fluxes to the coastal ocean. Limnol. Oceanogr. 53, 705–718. doi:10.4319/lo.2008.53.2.0705

Santos, I.R., Burnett, W.C., Dittmar, T., Suryaputra, I.G.N. a, Chanton, J., 2009. Tidal pumping drives nutrient and dissolved organic matter dynamics in a Gulf of Mexico subterranean estuary. Geochim. Cosmochim. Acta 73, 1325–1339. doi:10.1016/j.gca.2008.11.029

Santos, I.R., Eyre, B.D., Huettel, M., 2012. The driving forces of porewater and groundwater flow in permeable coastal sediments: A review. Estuar. Coast. Shelf Sci. 98, 1–15. doi:10.1016/j.ecss.2011.10.024

Scott, D.B., Brown, K., Collins, E.S., Medioli, F.S., 1995a. A new sea-level curve from Nova Scotia: evidence for a rapid acceleration of sea-level rise in the late mid-Holocene. Can. J. Earth Sci. 32, 2071–2080. doi:10.1139/e95-160

Scott, D.B., Gayes, P.T., Collins, E.S., 1995b. Mid-Holocene Precedent for a Future Rise in Sea-Level Along the Atlantic Coast of North America. J. Coast. Res. 11, 615–622. doi:4298366

Seidel, M., Beck, M., Greskowiak, J., Riedel, T., Waska, H., Suryaputra, I.G.N.A., Schnetger, B., Niggemann, J., Simon, M., Dittmar, T., 2015. Benthic-pelagic coupling of nutrients and dissolved organic matter composition in an intertidal sandy beach. Mar. Chem. 176, 150–163. doi:10.1016/j.marchem.2015.08.011

Seidel, M., Beck, M., Riedel, T., Waska, H., Suryaputra, I.G.N.A., Schnetger, B., Niggemann, J., Simon, M., Dittmar, T., 2014. Biogeochemistry of dissolved organic matter in an anoxic intertidal creek bank. Geochim. Cosmochim. Acta 140, 418–434. doi:10.1016/j.gca.2014.05.038

Shen, Y., Chapelle, F.H., Strom, E.W., Benner, R., 2015. Origins and bioavailability of dissolved organic matter in groundwater. Biogeochemistry 122, 61–78. doi:10.1007/s10533-014-0029-4

Shields, M.R., Bianchi, T.S., Gélinas, Y., Allison, M.A., Twilley, R.R., 2016. Enhanced Terrestrial Carbon Preservation Promoted by Reactive Iron in Deltaic Sediments. Geophys. Res. Lett. 1–25. doi:10.1002/2015GL067388

Sholkovitz, E.R., 1976. Flocculation of dissolved organic and inorganic matter during the mixing of river water and seawater. Geochim. Cosmochim. Acta 40, 831–845. doi:10.1016/0016-7037(76)90035-1

Stedmon, C.A., Markager, S., Bro, R., 2003. Tracing dissolved organic matter in aquatic environments using a new approach to fluorescence spectroscopy. Mar. Chem. 82, 239–254. doi:10.1016/S0304-4203(03)00072-0

Stedmon, C.A., Markager, S., Kaas, H., 2000. Optical properties and signatures of chromophoric dissolved organic matter (CDOM) in Danish coastal waters. Estuar. Coast. Shelf Sci. 51, 267–278. doi:10.1006/ecss.2000.0645

Taniguchi, M., Burnett, W.C., Cable, J.E., Turner, J. V., 2002. Investigation of submarine groundwater discharge. Hydrol. Process. 16, 2115–2129. doi:10.1002/hyp.1145

Tesi, T., Semiletov, I., Hugelius, G., Dudarev, O., Kuhry, P., Gustafsson, Ö., 2014. Composition and fate of terrigenous organic matter along the Arctic land-ocean continuum in East Siberia: Insights from biomarkers and carbon isotopes. Geochim. Cosmochim. Acta 133, 235–256. doi:10.1016/j.gca.2014.02.045

Wada, S., Aoki, M.N., Tsuchiya, Y., Sato, T., Shinagawa, H., Hama, T., 2007. Quantitative and qualitative analyses of dissolved organic matter released from Ecklonia cava Kjellman, in Oura Bay, Shimoda, Izu Peninsula, Japan. J. Exp. Mar. Bio. Ecol. 349, 344–358. doi:10.1016/j.jembe.2007.05.024

Wagai, R., Mayer, L.M., 2007. Sorptive stabilization of organic matter in soils by hydrous iron oxides. Geochim. Cosmochim. Acta 71, 25–35. doi:10.1016/j.gca.2006.08.047

Ward, N.D., Bianchi, T.S., Medeiros, P.M., Seidel, M., Richey, J.E., Keil, R.G., Sawakuchi, H.O., 2017. Where Carbon Goes When Water Flows: Carbon Cycling Across the Aquatic Continuum. Front. Mar. Sci. 4, 1–27. doi:10.3389/fmars.2017.00007

Webster, I.T., Norquay, S.J., Ross, F.C., Wooding, R.A., 1996. Solute exchange by convection within estuarine sediments. Estuar. Coast. Shelf Sci. 42, 171–183. doi:10.1006/ecss.1996.0013

Weishaar, J., Aiken, G., Bergamaschi, B., Fram, M., Fujii, R., Mopper, K., 2003. Evaluation of specific ultra-violet absorbance as an indicator of the chemical content of dissolved organic carbon. Environ. Sci. Technol. 37, 4702–4708. doi:10.1021/es030360x

Williams, P.M., Gordon, L.I., 1970. Carbon-13: carbon-12 ratios in dissolved and particulate organic matter in the sea. Deep. Res. Oceanogr. Abstr. 17, 19–27. doi:10.1016/0011-7471(70)90085-9

Wurl, O., Tsai, M., 2009. Analysis of Dissolved and Particulate Organic Carbon with the HTCO Technique, In: Wurl,O. ed.

Yamashita, Y., McCallister, S.L., Koch, B.P., Gonsior, M., Jaffé, R., 2015. Dynamics of dissolved organic matter in fjord ecosystems: Contributions of terrestrial dissolved organic matter in the deep layer. Estuar. Coast. Shelf Sci. 159, 37–49. doi:10.1016/j.ecss.2015.03.024

Zeebe, R.E., Wolf-Gladrow, D., 2001. Stable Isotope Fractionation. CO2 Seawater Equilibrium, Kinet. Isot. 141–250.